Inaugural dissertation

for

obtaining the doctoral degree

of the

Combined Faculties of Mathematics, Engineering and Natural Sciences

of the

Ruperto-Karls-University

Heidelberg

Presented by

M.Sc. Yuhang Hong

born in Yibin, Sichuan, People's Republic of China

Oral examination: 03.06.2024

Evolution and regulation of the transcriptional response to oxidative stress in vertebrates

Referees: Prof. Dr. Nicholas S. Foulkes

Prof. Dr. Uwe Strähle

Acknowledgements

As time goes by, after four years my doctoral study is finally coming to an end. Here, I want to express my greatest gratitude to all those people who enlightened me when I was in darkness and helped me to complete this important period during my life.

First and foremost, I would like to thank my supervisor Prof. Dr. Nicholas Foulkes, who gave me this precious opportunity to do my PhD in his laboratory with an intriguing project. He is like an elder friend who always supported me, inspired me, encouraged me, and talked with me. I thank him for his wealth of knowledge which guided me toward the correct direction, for his epitome of expertise which inspired me to explore an unknown area, and for his fount of wisdom which encouraged me to overcome all kinds of difficulties. His mentorship has not only enriched my academic growth but also instilled in me a profound passion for the pursuit of knowledge.

I would also like to thank Dr. Daniela Vallone. She was always ready to give me advice and technical support in the lab. Additionally, I am grateful to Dr. Olivier Kassel and Dr. Ravindra Peravali for their kind help in my project.

I extend my thanks to all my former and current lab members. I would like to thank Dr. Hongxiang Li, who firstly helped me to adapt to the lab work and being a truthful friend. I would like to thank Dr. Rima Siauciunaite and Alessandra Boiti, for their kind support in my work which provided me with the promise to keep moving forward, as well as their friendship which brought me company and happiness. I also appreciate Patrizia Birner, Leni Wagner, Hanna Weber, Carina Scheitle and Lea Harrer, for their helpful support in the lab. I would like to especially thank Nathalie Geyer for her valuable advice and continuous assistance in my experiments. I would like to thank Yi Bi, who assisted me with a lot of lab works and was always willing to lend a warmful hand when I needed it. Besides, I would like to thank Dr. Sebastian Gornik from Heidelberg University for help of my RNA-seq data processing.

I am immensely grateful to my thesis advisory committee (TAC), my supervisor Prof.

Dr. Nicholas Foulkes, Prof. Dr. Andrew Cato, Dr. Carsten Weiss and Prof. Dr. Lennart Hilbert, whose invaluable insight and critical feedback have significantly contributed to the refinement and depth of this work.

I am also thankful for my PhD examiners Prof. Dr. Nicholas Foulkes, Prof. Dr. Uwe Strähle, Prof. Dr. Ingrid Lohmann and Prof. Dr. Suat Özbek for their precious time on reading my thesis and attending my defense.

I would like to thank the China Scholarship Council (CSC) and my beloved mother land China for financial support for my PhD study overseas.

Last but not least, I want to thank my family for their unwavering love in every second. My wife Yi Huang, thank you for your understanding, patience and selfless support throughout my study. Your voice is always a pleasure and comfort during challenging times, and a bright star shining on my path whenever I felt lost.

“All the past is but prologue.” Thank everyone who has been part of my past and is witnessing my new beginning.

Table of Contents

Publications

Hong, Y.; Boiti, A.; Vallone, D.; Foulkes, N.S. Reactive Oxygen Species Signaling and Oxidative Stress: Transcriptional Regulation and Evolution. Antioxidants 2024, 13, 312.

Abstract

As byproducts of aerobic respiration, reactive oxygen species (ROS) play dual roles in many important biological processes by acting as both a potential source of damage as well as signal molecules in multiple signaling networks. The mechanisms whereby ROS direct transcriptional regulation have been documented, however, how evolution has shaped these mechanisms in diverse species which may experience very different levels of ROS is poorly understood. To explore this issue, I conducted a comparative study investigating the transcriptional response to ROS in cell lines derived from a range of vertebrate models, including zebrafish, mouse, turtle and frog. Additionally, I also examined a unique fish model, the Somalian cavefish *Phreatichthys andruzzii*, which has evolved in a completely dark environment for over 3 million years and where many light-dependent functions such as photoreactivation DNA repair and photoentrainment of the circadian clock have been lost.

Using RNA-seq, I revealed diverse transcriptional profiles under H_2O_2 exposure among zebrafish, cavefish and mouse cell lines, notably involving the group of DNA repair genes. I then focused on the key nucleotide excision repair gene *xpc* which is transcriptionally induced by H_2O_2 in all the selected vertebrate cell lines with the exception of the cavefish. In the case of the zebrafish *xpc* gene, I identified a ROS inducible, D-box enhancer-driven expression mechanism. In contrast, in mouse cells no D-box was encountered in the *xpc* promoter and furthermore, transcription regulated by the D-box enhancer does not respond to ROS exposure, indicating a distinct regulatory mechanism targeting the mouse *xpc* promoter. Meanwhile, conserved D-box elements were identified in the cavefish *xpc* gene which still mediated ROS-induced transcription in zebrafish cells. However, ROS induced, D-box driven transcription was absent in the cavefish cells.

I then demonstrated that the bZIP PAR factor TEF1 serves as a principal activator of D-box-mediated transcription in response to ROS. I identified several putative MAP Kinase phosphorylation sites in the N-terminal portion of the zebrafish TEF1 protein.

Mutations of these MAPK phosphorylation sites to match the corresponding sequences observed in the cavefish TEF1 protein led to much weaker activation and ROS sensitivity, which is consistent with the significant loss of ROS induced *xpc* gene expression in this cavefish species. Furthermore, I revealed that changes in intracellular ROS levels also affect the nuclear translocation of TEF1 proteins in zebrafish but not in cavefish cells. Differences in the MAPK-regulated nuclear localization of TEF1 may at least in part explain the species-specific differences in how the D-box responds to ROS.

I have therefore revealed that vertebrates have evolved diverse ROS-induced DNA repair gene transcription mechanisms to adapt to varying aerobic environments. In addition, it is tempting to speculate that the loss of D-box mediated expression and differential PAR factor regulation observed in both the cavefish *P. andruzzii* and mouse may point to these species having shared similar selective pressures during their evolution. In summary, my results highlight plasticity in the ROS-induced transcriptional response over the course of vertebrate evolution.

Zusammenfassung

Reaktive Sauerstoffspezies (ROS), die als Nebenprodukte der aeroben Atmung entstehen, spielen in vielen wichtigen biologischen Prozessen eine doppelte Rolle, indem sie sowohl als Schadensquelle als auch als Signalmoleküle in mehreren Signalnetzwerken wirken. Die Mechanismen, durch die ROS die Transkriptionsregulation steuern, sind dokumentiert worden, jedoch ist wenig darüber bekannt, wie die Evolution diese Mechanismen in verschiedenen Arten geformt hat, die sehr unterschiedliche ROS-Werte aufweisen. Um dieses Problem zu untersuchen, habe ich eine vergleichende Studie durchgeführt, in der die Transkriptionsreaktion auf ROS in Zelllinien aus einer Reihe von Wirbeltiermodellen untersucht wurde, darunter Zebrafisch, Maus, Schildkröte und Frosch. Darüber hinaus habe ich auch ein einzigartiges Fischmodell untersucht, den somalischen Höhlenfisch *Phreatichthys andruzzii*, der sich in einer völligen Dunkelheitsumgebung seit über 3 Millionen Jahren entwickelt hat, und bei den vielen lichtabhängigen Funktionen wie die DNA-Reparatur durch Photoreaktivierung und das Photoentrainment der zirkadianen Uhr verloren gegangen sind.

Mithilfe von RNA-seq habe ich unterschiedliche Transkriptionsprofile unter H_2O_2-Belastung bei Zebrafisch-, Höhlenfisch- und Mauszelllinien aufgedeckt, wobei vor allem die Gruppe der DNA-Reparaturgene betroffen war. Anschließend konzentrierte ich mich auf das Schlüsselgen für die Nukleotid-Exzisionsreparatur, *xpc*, das in allen ausgewählten Wirbeltierzelllinien, mit Ausnahme des Höhlenfischs, durch H_2O_2 transkriptionell induziert wird. Im Fall des Zebrafisch-*xpc*-Gens identifizierte ich einen ROS-induzierten Ausdrucksmechanismus, der von einem D-Box-Enhancer-Element gesteuert wird. Im Gegensatz dazu wurde in Mauszellen keine D-Box im *xpc*-Promotor gefunden, und die durch den D-Box-Enhancer regulierte Transkription reagierte nicht auf ROS-Exposition, was auf einen unterschiedlichen Regulationsmechanismus hinweist, der auf den Maus-*xpc*-Promotor abzielt. Unterdessen wurden konservierte D-Box-Elemente im Höhlenfisch-*xpc*-Gen identifiziert, die immer noch die ROS-

induzierte Transkription in Zebrafischzellen vermittelten. Die ROS-induzierte, D-Box-gesteuerte Transkription fehlte jedoch in den Höhlenfischzellen.

Anschließend habe ich gezeigt, dass der bZIP PAR-Faktor TEF1 als Hauptaktivator der D-Box-vermittelten Transkription in Reaktion auf ROS fungiert. Ich habe mehrere mutmaßliche MAP-Kinase-Phosphorylierungsstellen im N-terminalen Bereich des Zebrafisch-TEF1-Proteins identifiziert. Mutationen dieser Phosphorylierungsstellen, die im Höhlenfisch-TEF1-Protein beobachtet wurden, führten zu einer viel schwächeren Aktivierung und ROS-Empfindlichkeit, was mit dem signifikanten Verlust der ROS-induzierten *xpc*-Genexpression in dieser Art übereinstimmt. Darüber hinaus habe ich gezeigt, dass Veränderungen in den intrazellulären ROS-Levels auch die nukleäre Translokation der TEF1-Proteine im Zebrafisch beeinflusst, aber nicht in den Höhlenfischzellen. Unterschiede in der MAPK-regulierten nukleären Lokalisierung von TEF1 können zumindest teilweise die artenspezifischen Unterschiede in der Reaktion der D-Box auf ROS erklären.

Daher vermute ich, dass Wirbeltiere vielfältige ROS-induzierte Transkriptionsmechanismen für die DNA-Reparaturgene entwickelt haben, um sich an unterschiedliche aerobe Umgebungen anzupassen. Insbesondere der Verlust der D-Box-vermittelten Expression und die gestörte PAR-Faktor-Regulation sowohl beim Höhlenfisch *P. andruzzii* als auch bei der Maus deuten auf einen möglicherweise gemeinsamen Selektionsdruck während ihrer Evolution hin. Zusammenfassend verdeutlichen meine Ergebnisse die Plastizität der ROS-induzierten Transkriptionsreaktion im Verlauf der Evolution der Wirbeltiere.

Abbreviations

6-4 phr	6-4 photolyase
AA	amino acids
ANOVA	analysis of variance
AP-1	activator protein 1
ATF-1	activating transcription factor 1
ATP	adenosine triphosphate
ASK1	apoptosis signal-regulating kinase 1
BER	base excision repair
BMAL	brain and muscle ARNT-like
BSA	bovine serum albumin
bZIP	basic leucine zipper
bp	base pair
CAT	catalase
CCG	clock-controlled gene
cDNA	complementary DNA
CLOCK	circadian locomotor output cycles kaput
CPD	cyclobutane pyrimidine dimer
CPD phr	CPD photolyase
cps	counts per second
CREB	cAMP response element-binding protein
CRY	cryptochrome
DAPI	4',6-diamidin-2-fenilindolo
DASH	(Drosophila, Arabidopsis, Synechocystis, Human)-type
D-box	D-box enhancer element
DBP	albumin D-site-binding protein
DDB2	damage-specific DNA binding protein 2
DNA	deoxyribonucleic acid

DSBs	double-strand breaks
DTT	dithiothreitol
E4BP4	E4 binding protein 4
E-box	E-box enhancer element
ECL	enhanced chemiluminescence
EDTA	ethylenediaminetetraacetic acid
ERK	extracellular signal-regulated kinase
HLF	hepatic leukemia factor
HR	homologous recombination
IgG	immunoglobulin G
JNK	c-Jun NH2-terminal kinase
jun-b	jun B proto-oncogene
kb	kilobase
Luc	luciferase
m^2	square metre
MAPK	mitogen-activated protein kinase
min	minute
ml	milliliter
mM	millimolar
MMR	mismatch repair
mRNA	messenger RNA
MTT	3-(4,5-dimethylthiazol-2-yl)-2,5-diphenyltetrazolium bromide
mut	mutagenized
NADPH	nicotinamide adenine dinucleotide phosphate
NER	nucleotide excision repair
NFIL	nuclear factor, interleukin 3 regulated
ng	nanogram
NHEJ	non-homologous end joining
p38	p38 mitogen-activated protein kinase
PAR	proline and acidic amino-acid-residue rich

PBS	phosphate buffered saline
PCR	polymerase chain reaction
PER	period
qRT-PCR	quantitative RT-PCR
RACE	rapid amplification of cDNA ends
RNA	ribonucleic acid
ROS	reactive oxygen species
RT	reverse transcriptase / reverse transcription
SD	standard deviation
SDS	sodium dodecyl sulphate
sec	second
TEF	thyrotroph embryonic factor
Tris	Tris(hydroxymethyl)-aminomethane
TSS	transcription start site
UTR	untranslated region
UV	ultra-violet light
WT	wild type
XPC	xeroderma pigmentosum group C
µg	microgram
µl	microliter

1. Introduction

1.1 Reactive Oxygen Species (ROS) and the cellular origins of oxidative stress

A key event during the early stages of evolution was the establishment of aerobic respiration. This process greatly enhanced the capacity of cells to harness energy from the breakdown of complex macromolecules, notably glucose, by enabling their more complete oxidation to form carbon dioxide and water. However, as electrons transfer through the electron transport chain which drives aerobic respiration in mitochondria, they can prematurely interact with molecular oxygen. This results in the formation of reactive oxygen species (ROS) including superoxide anions (O_2•-), hydrogen peroxide (H_2O_2), and hydroxyl radicals (HO•) [1-4]. Due to their high degree of chemical reactivity, ROS in turn can interact with and thereby covalently modify many classes of macromolecule and so cause cellular damage. Indeed, ROS represent key players in diverse pathological processes in almost all aerobes [5]. It is therefore vital that cells possess mechanisms which can counteract and detoxify the ROS that are continuously generated by mitochondria as part of their normal function (Fig. 1). Any imbalance between the activity of aerobic respiration in mitochondria and the mechanisms which detoxify ROS ultimately results in oxidative stress [6] which in turn can lead to cellular damage, inflammation, tissue damage and organ dysfunction as well as more complex pathologies such as cancer, and the process of aging and senescence.

Mitochondria are not the only organelles which produce ROS (Fig. 1.2). The peroxisomes are sites of enzymes which catalyze ROS formation [7] and also the accumulation of misfolded proteins in the endoplasmic reticulum results in “ER stress” which is associated with increases in ROS levels [8]. In addition, various metabolic enzymes, for example the NADPH oxidases (NOXs) as well as enzymes involved in oxygen metabolism have the capacity to generate ROS [4, 9].

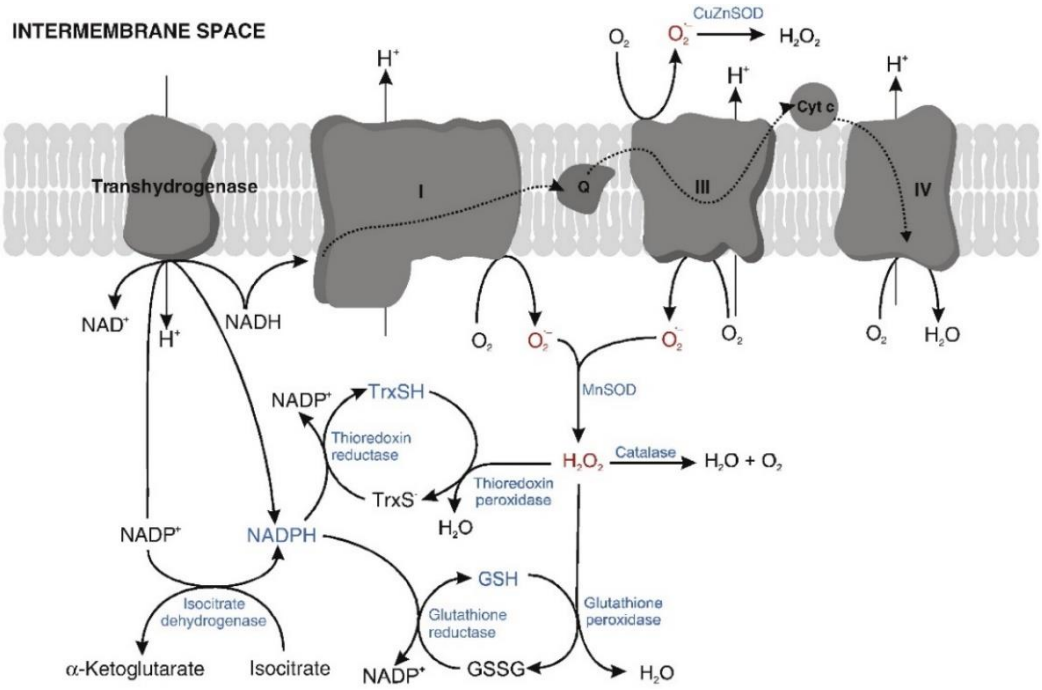

Fig 1.1 ROS production and metabolism in the electron chain in mitochondria. The roman numbers indicate transmembrane oxidoreductase complexes [3].

ROS is not only generated by intracellular, metabolic processes. The interaction of cells with a wide range of environmental stressors including ultra violet (UV) light and xenobiotics can all induce oxidative stress [10]. Therefore, understanding how cells generate and manage ROS represents an important goal for biomedicine and toxicology [11, 12].

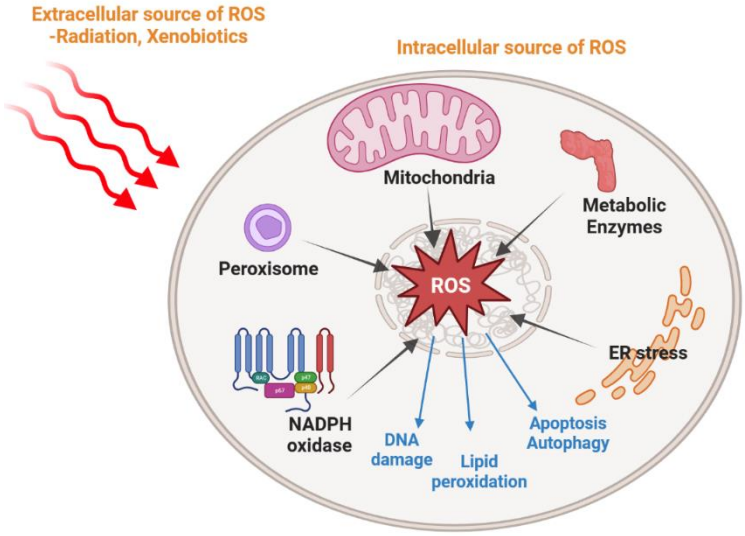

Fig 1.2. Schematic representation of oxidative stress induced by intracellular and extracellular stimuli. Within cells, ROS primarily originates from mitochondria, but it's also produced in other cellular structures such as peroxisomes, the endoplasmic reticulum, and by certain enzymes located in the cytoplasm. External sources of ROS encompass environmental elements like radiation and xenobiotics. An overabundance of ROS can result in cellular apoptosis, autophagy, the peroxidation of lipids, and damage to DNA [13].

1.2 Intracellular ROS balance and antioxidant systems

Cells effectively buffer intracellular increases in oxidative stress via the action of a complex network of metabolic pathways. These include both enzymatic and non-enzymatic detoxification systems (Fig 1.3) [14]. One important example is the enzyme superoxide dismutase (SOD), that catalyzes the conversion of superoxide anions into hydrogen peroxide. To avoid the build-up of harmful levels of hydrogen peroxide, two additional enzymes, namely catalase (CAT) and glutathione peroxidase (GPx), further detoxify this reactive chemical species by converting it into water [15, 16]. Additional mechanisms which include proteolytic and DNA repair enzymes also indirectly contribute to antioxidant defence systems and thereby play an important role in stabilizing the cellular redox state [17, 18].

Other antioxidant systems are not based on enzymatic function. For example, classes of small molecules which include vitamins C and E, glutathione, and various phytochemicals [19], directly react with and thereby neutralize ROS. The precise mechanisms whereby these molecules interact with ROS varies but for example, the vitamin C molecule (ascorbic acid) can serve as an electron donor to interrupt the oxidative chain reactions that are triggered by ROS [19]. Furthermore, ascorbic acid can rejuvenate other antioxidants, for example by reducing the vitamin E radicals that are formed when vitamin E scavenges ROS [20]. One important potential source of ROS is iron. While representing a key component of a multitude of proteins which rely on redox changes for their function, iron can also generate highly reactive hydroxyl radicals from hydrogen peroxide via the so-called Fenton reaction [21]. Therefore, another important class of proteins with antioxidant properties includes metal binding proteins such as ferritin which can sequester iron and thereby limit its capacity to increase oxidative stress. An important feature of many antioxidant proteins is that their expression levels are dynamic and are adjusted to match the redox status on the cell. This reflects the need for many of these homeostatic mechanisms to maintain a delicate balance between minimizing ROS production and at the same time ensuring that related metabolic processes that are critical for normal cellular function are maintained.

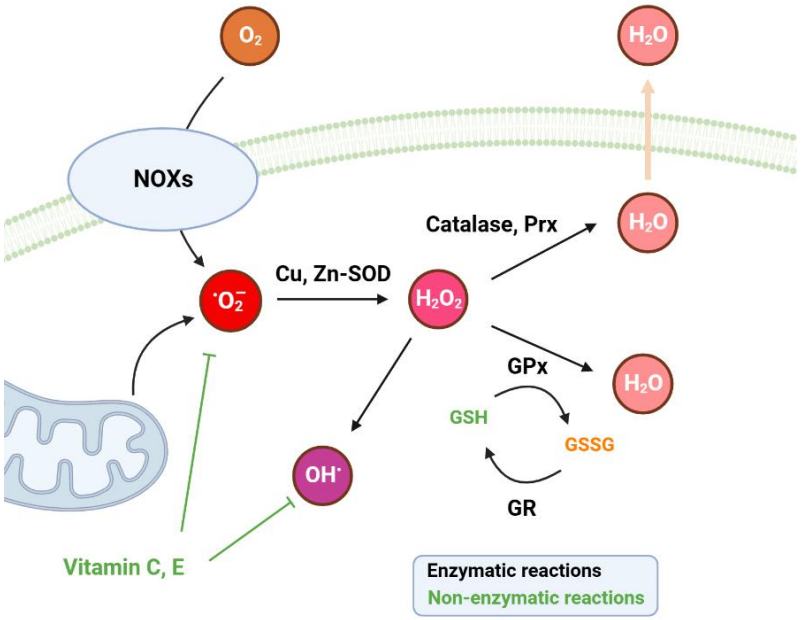

Fig 1.3. Diagram illustrating antioxidant mechanisms featuring both enzymatic and non-enzymatic antioxidants. Black arrows show enzymatic processes, while green arrows represent non-enzymatic processes. Key components include NOXs (NADPH oxidase Nox family), SOD (superoxide dismutase), Prx (peroxiredoxins), GPx (glutathione peroxidase), and GR (glutathione reductase) [13].

1.3 ROS role in cellular signalling systems

While ROS is commonly regarded as playing a disruptive role in cellular and physiological function, one of the most surprising discoveries of the past few decades has been that paradoxically ROS also serve as essential signalling molecules [22]. Many signalling pathways and transcription factors that respond to ROS have now been described [4, 22, 23]. In turn, ROS has been implicated as playing central roles in diverse processes such as cellular proliferation, differentiation and programmed cell death as well as mediating various physiological and cellular responses to environmental stimuli (Fig 1.4) [24]. These important functions rely on the chemical reactivity as well as the intracellular levels of ROS and enable cells to sense the levels of oxidative stress and thereby trigger appropriate cellular responses. Here I survey some of the principal transcription factors and signal transduction pathways where ROS has been documented to play a key regulatory role.

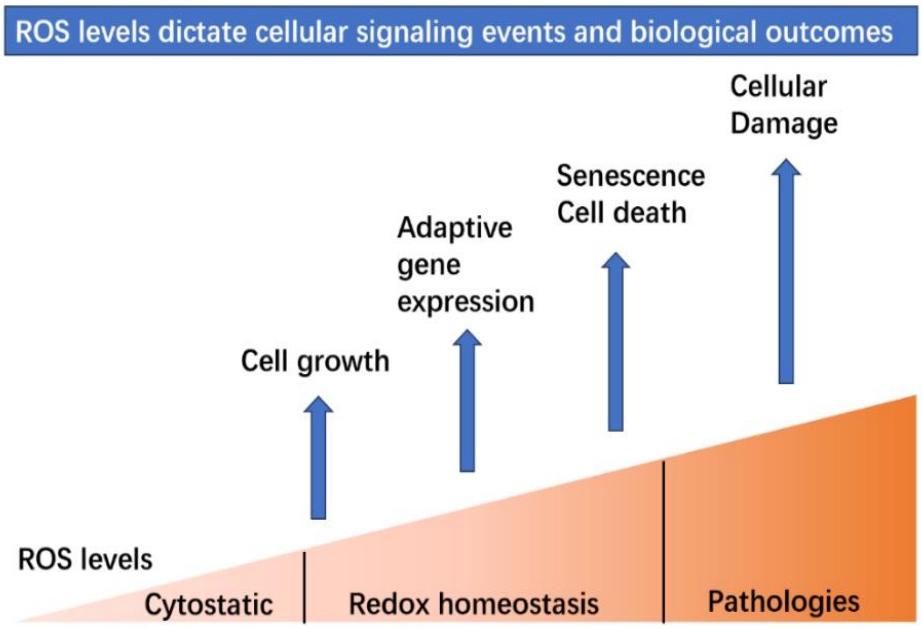

Fig 1.4. Different biological response is determined by intracellular ROS levels. Within normal physiological confines, ROS are integral to various critical cellular functions, aiding in the preservation of redox balance. At minimal concentrations, they encourage cell growth through mechanisms of proliferation and differentiation. An increase in ROS levels triggers a cellular adaptive response, marked by the enhanced expression of genes associated with antioxidant defense. Subsequently, when cells are subjected to elevated ROS concentrations, processes leading to cellular aging or apoptosis are activated [13].

1.3.1 The Mitogen Activated Protein Kinase (MAPK) Signaling Pathway and ROS

In many ways, the Mitogen Activated Protein Kinase (MAPK) signaling pathway sits at the crossroads of the cellular response to a multitude of extracellular and intracellular signals. It enables cells to respond to multiple extracellular signals, amplify and integrate this complex information and then to direct an appropriate cellular response including changes in transcription of sets of genes as well as modifying the properties and function of existing proteins. Thereby MAPK signaling represents a key mechanism coordinating cellular growth and apoptosis [22, 25] and ROS serves as an

important regulator of this pathway allowing it to respond to both the intra- and extracellular environment (Fig 1.5) [26, 27].

The MAPK pathway in vertebrates is constituted by three major families of kinase, the extracellular signal-regulated kinases (ERKs) [28], the c-Jun N-terminal kinases (JNKs) [29], and the p38 kinases [30]. These differentially respond to a variety of stressors, environmental changes, and mitogenic signals and ROS appears to act to specifically modulate the degree of this response [22]. This modulation process involves several mechanisms. Thus, the chemical reactivity of ROS can serve to directly oxidize amino acid residues which form part of the kinase domains structure of the MAPKs themselves or upstream activators within the MAPK signaling cascade such as the MAPKKKs. These covalent modifications cause conformational modifications that result in an overall enhancement of kinase activity [27]. This in turn precipitates a cascade of phosphorylation events that ultimately targets specific sets of transcription factors which then regulate the expression of networks of genes involved in cell survival, proliferation and key processes such as inflammation [31]. ROS also appears to influence the level of MAPK signalling by inhibiting the activity of the MAPK phosphatases (MKPs) [32]. These MAPK pathway components normally dephosphorylate and thereby inactivate MAPKs. Therefore, ROS-induced reduction in MKP function serves to drive sustained MAPK activation and an overall increase in the level of phosphorylation driven by the MAPK pathway. These long-term effects of ROS are important for determining the balance between cell survival and apoptosis and are dependent on the precise levels and context of the ROS signal [33]. Interestingly, the activity of the MAPKs can indirectly affect ROS levels. Consequently, stimulating p38 and ERK MAPKs may boost the expression of genes responsible for enzymes that generate ROS, effectively establishing a positive feedback mechanism [34, 35].

Thus, while too much ROS is clearly detrimental for normal cellular function, physiologically controlled levels of ROS are essential for normal MAPK signaling and adaptation. Given these effects of ROS on the dynamic properties of the MAPK signaling cascade, it is clear that the precise level and nature of oxidative stress is

critical information for determining the precise outcome of this key signaling pathway. Therefore, therapeutic strategies aimed at modulating the effects of ROS on MAPKs and MKPs, offer potential benefits for the treatment of diseases which involve aberrant MAPK activation.

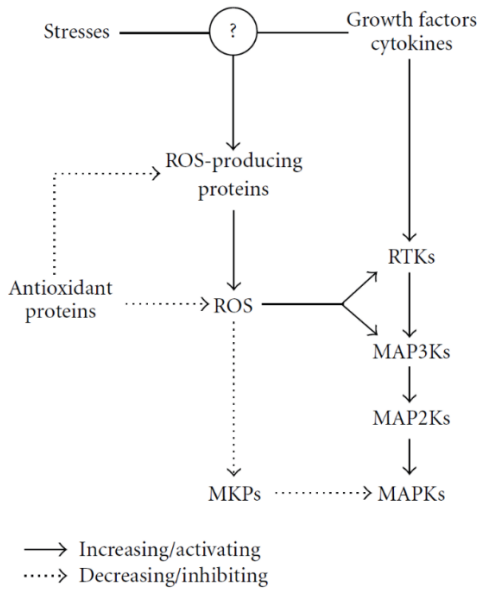

Fig 1.5. Regulation of MAPK pathways by ROS. ROS are induced by various environmental stresses or growth factors and removed by the antioxidative system such as antioxidant proteins. Meanwhile, the residual ROS stimulate the oxidative alteration of MAPK proteins (such as RTKs or MAP3Ks), ultimately resulting in the activation of the MAPK pathway [36].

1.3.2 ROS and transcriptional control by the NF-kB pathway

The transcription factor nuclear factor-kappa B (NF-kB) plays a key role in regulating gene expression in the context of both the innate and adaptive immune responses, specifically being involved in regulating inflammation, and cell survival [13]. This transcription factor possesses a Rel homology domain in its N-terminal region and thereby heterodimerizes with Rel B to form a sequence-specific DNA binding complex. However, prior to its activation, it is retained in the cytoplasm in an inactive form by its physical interaction with the protein IkB. Signal transduction pathways which activate NFkB, operate by specifically directing the degradation of IkB. This releases

NF-kB from its cytoplasmic storage sites and allows it to translocate to the nucleus where it can activate gene expression [37]. Amongst the signals which can activate NF-kB are ROS which specifically activate the IkB kinase complex (IKK) causing IkB degradation and thereby triggering the release of NF-kB and enabling it to regulate transcription (Fig 1.6) [38, 39]. Furthermore, ROS has been reported to modify the NF-kB protein itself, affecting its DNA binding properties as well as it interaction with other regulatory proteins [39]. As a result, ROS plays a central role in shaping the transcriptional response directed by NF-kB and so makes an important contribution to immune system function. While increases in ROS and oxidative stress are important indicators of challenges to the immune system such as infection, the regulation of NF-kB function by ROS also represents a risk to immune cell function. Specifically, excess increases in ROS related to metabolic activity could also inappropriately trigger the expression of gene networks that are regulated by NF-kB [40]. This may lead to sustained activation as the result of impaired negative feedback which is normally responsible for shutting down the pathway following a period of stress. Prolonged activation of NF-kB may in turn lead to pathologies which involve chronic inflammation [38].

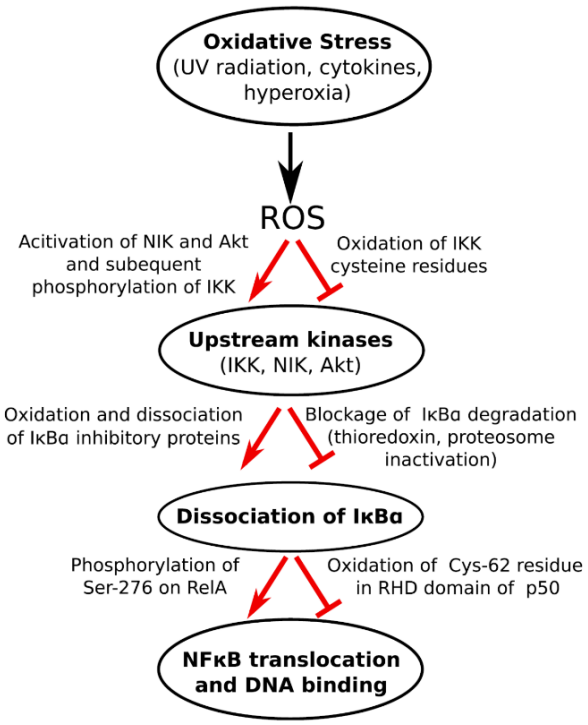

Fig 1.6 Regulation of NF-κB signaling by ROS. Oxidative stress can both activate or inhibit NF-kB signaling by facilitating or inhibiting the degradation of I-kB, a suppressor of NF- kB [38].

1.3.3 p53 and ROS

The p53 protein is one of the most intensively studied regulatory proteins, in large part due to its connection with cancer and tumorigenesis. It has been termed the "Guardian of the genome" based on its function of maintaining genome integrity in response to a range of cellular stressors which include elevated levels of oxidative stress [41]. For this reason, p53 represents an important player in mediating cellular responses to oxidative damage and guiding decisions on cell fate between survival and apoptosis [42]. p53 function is tightly regulated by its interaction with the protein MDM2 and the function of both proteins is affected by the oxidation state of certain cysteine residues. Under normal physiological conditions, p53 is maintained at very low levels as the result of rapid degradation, which is mediated by its partner protein MDM2 that thereby serves as a negative regulator of p53. In the presence of cellular stressors such as oxidative stress, turnover of the p53 protein is reduced and so levels of p53 in the nucleus increase [43]. Here it regulates gene expression leading to cell cycle arrest and increased DNA repair resulting in the enhancement of cell survival or alternatively programmed cell death [44].

p53 also participates in feedback mechanisms which regulate ROS levels. Specifically, p53 activates the transcription of many genes that are involved in antioxidant defenses such as *Sestrins* (*SESN*) and *TP53-induced glycolysis and apoptosis regulator* (*TIGAR*) (Fig 1.7). The function of SESN includes the regeneration of antioxidants such as glutathione and TIGAR serves to direct the course of energy metabolism from glycolysis to the pentose phosphate pathway and so reduces the activity of the electron transport chain [42]. Furthermore, other p53 regulated genes influence mitochondrial integrity and function, including the *cytochrome c oxidase 2* (*SCO2*) gene which encodes an important element of the electron transport chain [45]. Therefore, ROS-

activated p53 indirectly drives a reduction in oxidative stress by activating the expression of genes which serve to decrease ROS production at multiple levels. However, in the case of sustained high levels of ROS, p53 can become chronically activated and this can trigger cellular pathways leading to senescence or apoptosis [42]. Therefore, p53 function is intricately interlinked with ROS levels and it serves as a central relay point for coordinating an appropriate cellular response.

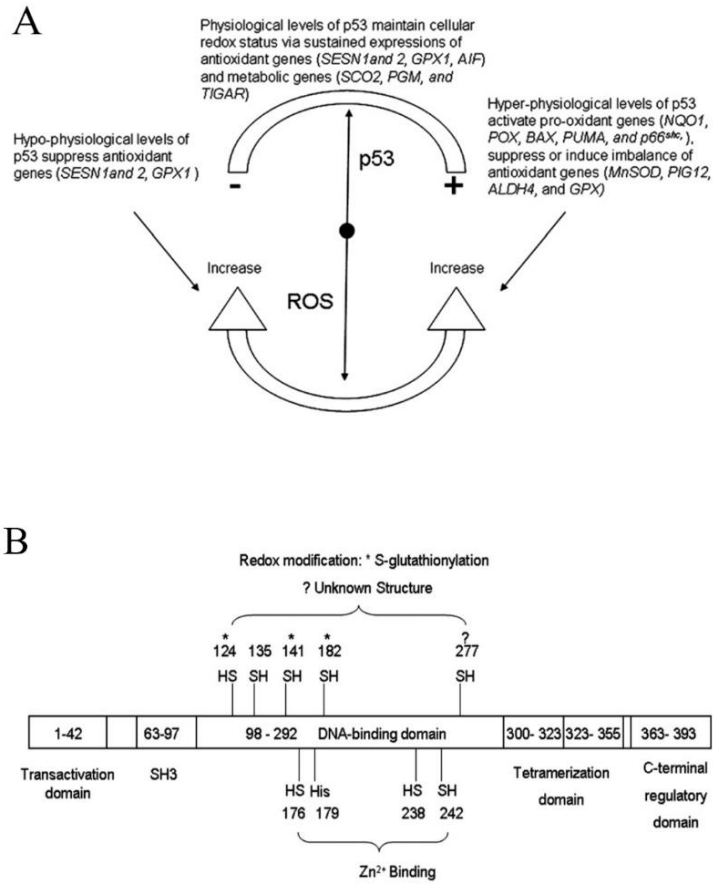

Fig 1.7. Interaction of p53 and cellular ROS. A: Cellular balance of ROS by regulation of p53; B: Redox modification of p53 by ROS [42].

1.3.4 Keap1-Nrf2-ARE signaling and oxidative stress

One signalling pathway that seems to be specifically dedicated to sensing ROS and then coordinating a protective response to oxidative stress is the Keap1-Nrf2-ARE pathway

[46]. The target transcription factor of this pathway is Nuclear Factor Erythroid 2-Related Factor 2 (Nrf2), which belongs to the cap 'n' collar subgroup within the basic leucine zipper (bZip) family of transcription factors. It binds to a DNA sequence termed the antioxidant response element (ARE) which resides in the promoters of genes that are upregulated upon elevation of ROS levels. In a situation reminiscent of NF-kB and IkB, under physiologically normal levels of ROS, Nrf2 is tethered in the cytoplasm via its interaction with its counterpart the Kelch-like ECH-associated protein 1 (Keap1) [47] and is thereby held in an inactive state. Elevation of ROS levels results in modification to Keap1 that triggers release of Nrf2 from its inhibitory cytoplasmic complex which can then translocate to the nucleus. Keap1 can sense and respond to changes in ROS levels as the result of oxidation of critical cysteine residues within its structure which triggers conformational changes which reduce its binding affinity for Nrf2. Once in the nucleus, the liberated Nrf2 factor is able to bind to ARE enhancer elements and thereby coordinate the transcriptional induction of a broad array of genes that share antioxidant and cytoprotective functions (Fig 1.8) [48]. This network of protective genes includes those encoding the enzymes glutathione S-transferase and NAD(P)H quinone dehydrogenase 1 which detoxify ROS and thereby protect cells from elevated oxidative stress. Furthermore, Nrf2 / ARE-induced gene expression also results in an increase in the production of important cellular antioxidants such as glutathione [49]. Therefore, these regulatory mechanisms should counter the negative effects of acute, transient increases in ROS. However, recently, this signalling pathway has also been implicated in the progression of a broad range of serious pathologies including cancer, neurodegenerative and cardiovascular diseases which are all associated with chronically elevated levels of oxidative stress. Indeed, the interaction between Nrf2 and Keap1 as well as regulation of the activity of the Nrf2 protein have become attractive targets for the development of novel small molecules to serve as therapeutic agents [50, 51]. Furthermore, there are many links between ROS, the Keap1-Nrf2-ARE axis and the modulation of inflammatory responses [52]. Therefore, this ROS responsive signalling pathway is of central importance for the progression of many pathological conditions.

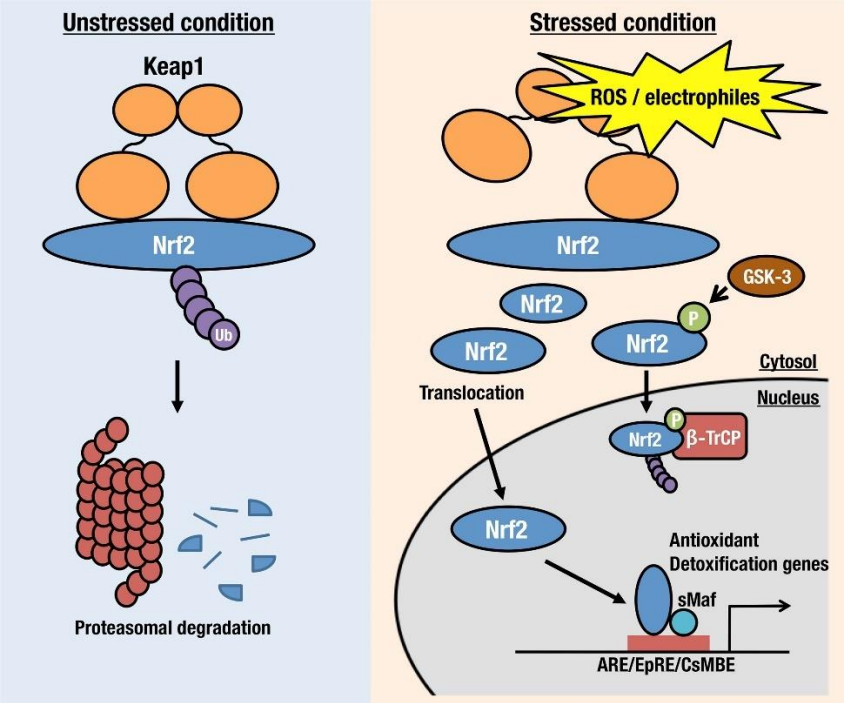

Fig 1.8. Cellular redox regulation by the Keap1-Nrf2-ARE system. In unstressed conditions (left panel), Keap1 interacts with Nrf2, continuously promoting Nrf2 degradation through the ubiquitin (Ub)-proteasome pathway. However, during periods of stress, ROS or electrophiles disrupt Keap1's inhibitory role, allowing newly synthesized Nrf2 to move into the nucleus. There, it partners with sMaf to activate target gene expression [50].

1.3.5 ROS and the circadian timing system

The circadian clock is a widely preserved timing system that allows cells and organisms to predict and adjust to recurring environmental challenges stemming from the day-night cycle's progression. Classically, this biological timing mechanism is recognized as driving characteristic circadian rhythms in the sleep-wake cycle and hormone release [53], however, almost all aspects of physiology and cell biology exhibit some degree of circadian rhythmicity. Several lines of evidence now point to many interactions between ROS and the circadian timing system occuring at two basic levels. 1) ROS has been shown to serve to entrain the circadian clock mechanism. Specifically transient increases in ROS levels can result in shifts in the phase of the clock-generated rhythms that can help synchronize the clock with the day-night cycle of the environment. 2) The

clock has been shown to direct circadian rhythms in the expression of many elements that work on ROS homeostasis [54, 55]. Reflecting the tight linkage between the circadian clock and oxidative stress, the levels of reactive oxygen species (ROS) in cells exhibit daily fluctuations. Indeed, one of the consequences of direct exposure of cells to sunlight is the photochemical generation of ROS. For this reason, it has even been speculated that day-night changes in intracellular levels of ROS may have been one of the factors which led to the evolution of the circadian clock [23, 56, 57].

Which mechanisms link clock function with ROS? The core clock components, the bHLH-PAS domain transcription factors CLOCK and BMAL1, regulate the transcription of several antioxidant genes by binding to E-box enhancer elements within their promoters, thereby driving circadian rhythms in the mechanisms which manage ROS [58]. This results in genes such as superoxide dismutase which plays a critical role in the elimination of superoxide radicals, also being expressed with a circadian rhythm [59]. Concerning the clock entraining properties of ROS, increased oxidative stress results in oxidative modifications to clock proteins as well as influencing signalling pathways that in turn can adjust the phase of the oscillating clock mechanism [60]. By these mechanisms, cells ensure that oxidative damage is minimized while metabolic efficiency is optimized according to the paricular demands of the organism and the time of day [57]. Furthermore, misalignment of the circadian timing system and cycling levels of oxidative stress may well be an important contributing factor to the increased susceptibility to pathologies which have been observed upon regular disruption of the circadian timing system.

1.4 Repairing DNA damage induced by oxidative stress

One of the most disruptive types of macromolecular damage caused by elevated levels of ROS is the introduction of covalent modifications into DNA. This increases the risk of mutations affecting the coding or regulatory sequences of genes and can thereby have a major disruptive effect on normal cell function. Furthermore, it can impact on

genomic stability, and ultimately underlie the development of diseases such as cancer [59]. For this reason, it is essential that cells can efficiently and rapidly recognize and repair a broad spectrum of DNA damage ranging from simple mismatches to complex double-strand breaks [61] [62].

1.4.1 An ancient DNA repair pathway, Photoreactivation

One major environmental source of oxidative damage is exposure to sunlight. UV radiation can directly induce covalent modifications in DNA as well as increasing levels of ROS via a photochemical effect [63]. Therefore it is valuable to consider more generally the repair mechanisms which counter DNA damage induced directly and indirectly by sunlight and UV exposure. Photoreactivation is a conserved DNA repair mechanism that occurs in various organisms, including bacteria, fungi, plants, and most animals [64-66]. It specifically targets certain types of DNA damage induced by ultraviolet (UV) radiation [67]. The primary DNA lesion repaired by photoreactivation are the cyclobutane pyrimidine dimers (CPDs) and pyrimidine (6-4) pyrimidone photoproducts [(6-4) PPs] where UV radiation generates covalent bonds between adjacent pyrimidine bases (thymine or cytosine) in the DNA strand, distorting the DNA helix structure [68, 69] (Fig 1.9).

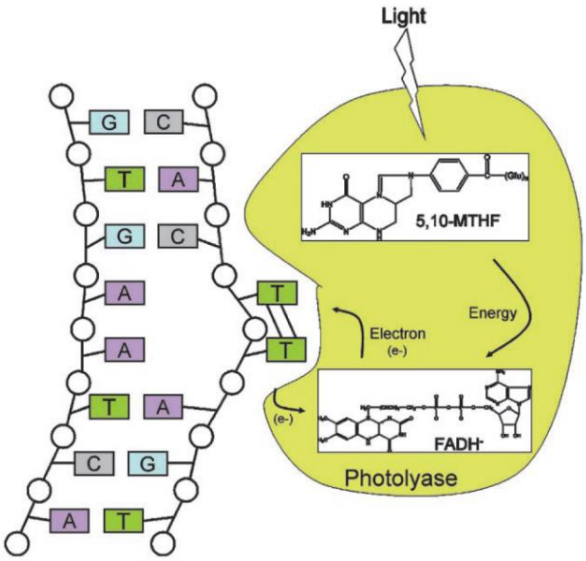

Fig 1.9 Photoreactivation by photolyase. Photolyase binds to DNA lesions consisting of pyrimidine dimers and splits the dimer by a light-dependent reaction. The photoantenna cofactor methenyltetrahydrofolate (5,10-MTHF) captures a photon and conveys the excitation energy to the pyrimidine dimer, breaking the cross-linking bonds. The electron returns to the flavin cofactor to generate $FADH^-$ and results in a dissociation of photolyase from the repaired DNA [69].

Interestingly, the photolyases are not conserved in placental mammals [66]. Only the cryptochromes, which are evolutionary closely related to the photolyase family but serve as circadian clock components, are encountered in the genomes of placental mammals [70]. A 'nocturnal bottleneck' hypothesis has been proposed to account for this curious pattern of photolyase evolution. This hypothesis predicts that early eutherian mammals were exclusively nocturnal animals during the domination of dinosaurs on earth as a strategy to avoid predation by diurnal carnivorous dinosaurs. Due to the lack of regular sunlight exposure for millions of years, this important light-driven DNA repair system was therefore lost in the eutherian mammalian lineage [71, 72].

1.4.2 Dark DNA repair systems in mammals

In addition to the photoreactivation system, there are several DNA repair pathways which operate independently of light include base excision repair (BER), nucleotide excision repair (NER), mismatch repair (MMR), homologous recombination (HR), and non-homologous end joining (NHEJ) [73]. Each of these pathways involves the action of multiprotein complexes and a cascade of protein-protein interactions and enzymatic activities which are orchestrated in a spatially and temporally well defined manner. Together, these mechanisms operate to accurately recognize, excise, and restore damaged DNA to its original sequence.

The BER pathway specifically targets small, non-helix-distorting mutations caused by oxidative damage, spontaneous base loss, or deamination [74]. The first step in the BER repair pathway is the recognition of this damage by a DNA glycosylase which removes

the damaged base molecule but at the same time leaves the sugar-phosphate backbone intact. The name for this enzyme activity relates to the fact that it cleaves a N-glycosidic bond to release the base. The consequence of this function is the generation of an apurinic or apyrimidinic site that is refered to as an AP site. In the next step of BER, an AP endonuclease cleaves the phosphodiester bond which lies just adjacent to the AP site and thereby provides an entry point for repair synthesis by DNA polymerase and DNA ligase. This results in the high fidelity repair of the damage (Fig 1.10 left panel) [74, 75].

NER represents a complementary DNA repair system to photoreactivation and BER. It targets a much wider variety of lesions and bulky adducts as well as UV-induced CPD lesions that all cause significant distortion to the overall structure of the DNA double helix [68]. Similar to BER, NER operates as a multi-step repair mechanism involving the sequential activity of many protein complexes. The first recognition step involves either the XPC complex (for global genome repair, GG-NER) or the RNA polymerase II complex (for transcription-coupled repair, TC-NER) [76]. Following the initial recognition step, other components of the NER machinery unwind the DNA helix around the lesion site and also recruit endonucleases which excise a short, single-stranded DNA segment flanking the damage site. Then, DNA polymerase and DNA ligase perform repair synthesis (Fig 1.10 right panel) [77]. NER thereby plays a central role in the repair of the types of DNA damage that physically interfere with transcription or DNA replication and is therefore vital for cancer prevention as well as the cellular response to environmental mutagens. This important role is reflected in individuals with mutations in the XPC gene, who suffer from Xeroderma Pigmentosum (XP). These patients are unable to target NER function to sites of UV-induced DNA damage. As a consequence, they suffer from a marked susceptibility to skin cancers [78].

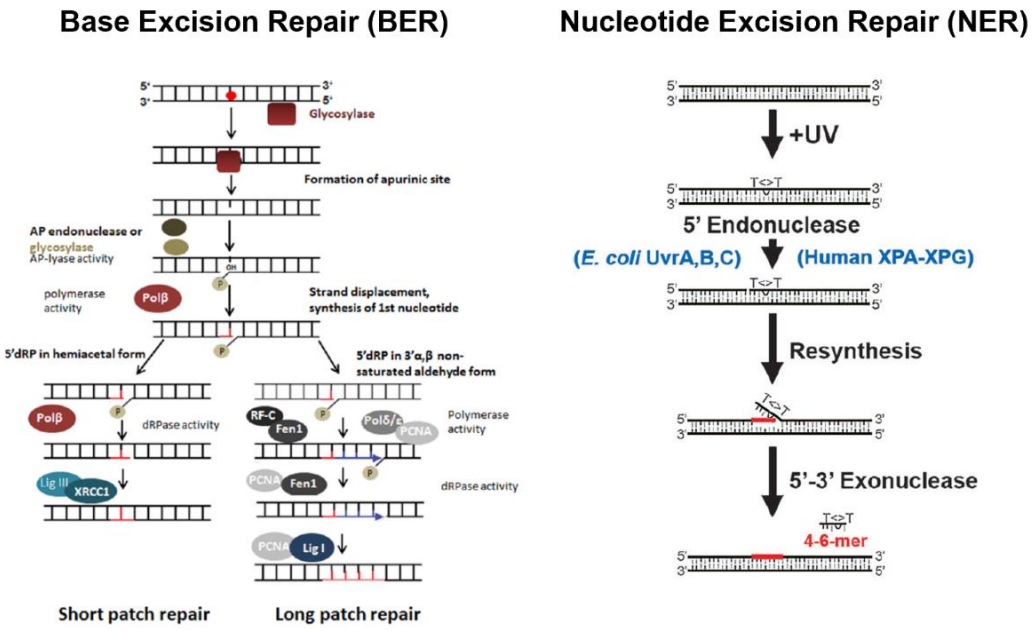

Fig 1.10 Schematic representation of excision repair systems. BER is initiated by DNA glycosylase action and consists of two alternative "patches" depending on the length of the repair region (see left panel) [74]. NER is completed by a series of steps initiated by DNA lesion recognition and repair complex binding, then the gap is finally filled by DNA replication and re-ligation (see right panel) [77].

In contrast to BER and NER, mismatch repair (MMR) is responsible for correcting errors that occur during DNA replication. MMR recognizes and removes mispaired bases which otherwise have a normal covalent structure but are generated during DNA polymerization and have escaped the proofreading activity of DNA polymerases [79]. In MMR, mismatched DNA base pairs are recognized by the Mut protein which then orchestrates the assembly of a complex that performs the final excision and repair synthesis steps [80].

Homologous recombination (HR) operates during the S and G2 phases of the cell cycle and repairs DNA double-strand breaks (DSBs), the most disruptive form of DNA damage. HR involves the search for homologous sequences that then serve as a scaffold for the repair process and subsequently the invasion of DNA strands, a process

coordinated by the RAD51 family of proteins [81]. This then results in the formation of a DNA structure known as the Holiday intermediate, in which the duplex DNA molecules involved in recombination are interconnected through covalent bonds created by single-strand crossovers. Subsequently, specialized enzymes, including MUS81·MMS4, specifically cleave the Holiday intermediate and thereby separate the two duplex DNA molecules involved in the recombination process. [69]. Unlike HR, non-homologous end joining (NHEJ) is an error-prone pathway that directly rejoins the broken DNA ends, often leading to the loss or addition of DNA sequences at the repair site. NHEJ is active throughout the cell cycle and serves as an immediate early response to DSBs [82]. In this repair mechanism, the Ku heterodimer binds to the two exposed ends of a DSB and recruits DNA-PKcs and the ligase4-XRCC4 heterodimer for the subsequent ligation of the two DSB termini.

For all the DNA repair mechanisms that I have described in this section, an important contributor to optimizing and coordinating their repair function is the regulation of the expression and activity of the pathway components in response to environmental and genetic factors. Abnormalities in the control of DNA repair gene expression can contribute to disease susceptibility that is associated with elevated levels of DNA damage. Furthermore, novel therapeutic approaches aimed at correcting these abnormalities can be valuable elements in individualized treatment strategies [83].

1.4.3 ROS-mediated transcriptional control and DNA repair

In order to ensure that repair systems are optimally engaged to counter DNA damage that is induced by elevated oxidative stress, it is vital that cells can initially sense increasing ROS levels at an early stage and then adjust the expression of the various antioxidant systems as well as the components of the DNA repair systems themselves [84]. Therefore, the transcription factors that are regulated by ROS such as Nrf2 and p53 appear to play important coordinating roles in the expression of various elements of the DNA repair machineries [85]. For example, many genes of the BER

repair complex, including those encoding for DNA glycosylases and components of the NER and MMR systems are activated at the transcriptional level by Nrf2 and p53 upon oxidative stress. This results in DNA repair capacity being correspondingly enhanced in order to correct for elevated oxidative DNA damage [86] and thereby to avoid carcinogenesis [87]. ROS mediated upregulation of the expression of DNA repair genes serves not only as a rapid response to acute increases in ROS levels but also clearly plays a role in the adaptive response of cells to chronic oxidative stress. Therefore, studying the basic mechanisms whereby ROS regulates gene expression is important for a better understanding of the regulation of DNA repair systems.

The many basic similarities between the zebrafish and human genomes make the zebrafish an attractive animal model for studying the genetic basis of many human pathologies and genetic control mechansisms. In the case of transcriptional regulation in response to ROS, zebrafish and human cells exhibit comparable gene expression patterns, suggesting a high degree of conservation of this basic process [88]. However, the precise mechanisms involved in ROS-regulated gene-specific expression in the zebrafish have not been explored in detail and so the degree of similarity of the transcription control mechanisms remain poorly understood.

1.5 Fish as animal models

1.5.1 Zebrafish as a model for study ROS physiology

Fish represent by far the largest and most diverse of all vertebrate groups which inhabit almost all aquatic ecosystems and have immense ecological and commercial value. Within this vast group, the zebrafish (*Danio rerio*) has been established as a powerful animal model for biomedical and toxicological research particularly for genetics, molecular biology and developmental studies. One of its most attractive features is its high fecundity and its the rapid development, taking just 24 hours to develop from the single cell zygote stage to a moving, recognizable vertebrate embryo. Furthermore, the

early embryonic stages are optically transparent and there are many genetic tools available to track endogenous gene expression non-invasively using fluorescent and bioluminescent reporter genes, *in vivo* [89]. In addition, the small size of the embryos, their ability to develop in the context of multiwell plates and their suitability for forward and reverse genetic analysis have all contributed to the zebrafish being used as a model for high throughput, high content, forward and chemical genetics screens to study a wide range of biological systems.

The zebrafish has been extensively used as an animal model to study the circadian timing system. Initially this was due to the proven utility of forward genetics as a route to identify the components and organization of the core clock mechanism in other models such as *Drosophila*, *Neurospora* and *Arabidopsis*. However, it subsequently became apparent that the tissues, cells and even cell lines derived from the zebrafish and fish in general, possess a unique property. Specifically direct exposure to light is sufficient to entrain their circadian clocks and induce the transcription of a subset of clock genes [90, 91]. This finding was extended by the discovery that these changes in clock gene expression can be triggered by exposure to the full range of visible light wavelengths as well as ultraviolet light and by treatment with ROS [84, 92]. Characterization of the pathway linking light exposure with transcription control has revealed a diverse group of widely expressed non-visual opsins acting as photoreceptors linked by the MAPK signalling pathway with the D-box enhancer–binding, bZipPAR transcription factors [93-95] (see next section). Furthermore, transcriptomic and gene expression studies have revealed that light and ROS exposure induce D-box dependent transcription of a wider set of genes that also includes DNA repair genes [96].

The zebrafish has also been used as a model to study the impact of ROS on various critical physiological processes. For instance, zebrafish models have played a crucial role in clarifying how reactive oxygen species (ROS) influence angiogenesis, cardiomyocyte proliferation, and tissue regeneration. Consequently, the function of the HECT domain and Ankyrin repeat-containing E3 ubiquitin-protein ligase 1 (hace1) is essential for heart development and operates in a manner influenced by ROS. Loss of

hace1 function leads to elevated ROS levels as well as cardiac abnormalities, thereby revealing the importance of ROS in maintaining normal cardiac function [97].

Zebrafish models have also made important contributions to our general understanding of how ROS affects nervous system function and regeneration. For example, hydrogen peroxide (H_2O_2) treatment has been shown to promote the growth of peripheral sensory axons in the skin, an essential step in the healing of cutaneous injuries [98]. Furthermore, it was revealed that H_2O_2-induced activation of Hedgehog signaling and in particular, upregulation of the sonic hedgehog gene (Shh) plays an important role in the regeneration of the caudal fin post amputation [99].

1.5.2 Role of the bZIP PAR/E4BP4 factors in ROS-mediated transcriptional regulation

Many studies by my group have focused on exploring how direct exposure of fish cells to light results in activation of transcription of many clock and DNA repair genes. This work has identified the D-box enhancer serving as a key light-responsive enhancer element but has also revealed that these effects of light are actually mediated by ROS. Specifically, exposure of fish cells to light triggers progressive increases in ROS levels and also the D-box mediates ROS as well as light-induced transcriptional induction [93]. The D-box represents the canonical binding site for a subclass of bZip transcription factors which are termed the PAR/E4BP4 transcription factors. Therefore, in the zebrafish this class of transcription factors seems to operate in a similar way to Nrf2 and p53 as being nuclear targets of ROS-mediated signalling [100].

The bZip PAR/E4BP4 transcription factors, include three PAR factors, thyrotroph Embryonic Factor (TEF), Hepatic Leukemia Factor (HLF) and D-box Binding Protein (DBP) which serve as activators of transcription and bind to the D-box as homo and heterodimers. D-box binding factors also include NFIL3 (nuclear factor, interleukin 3 regulated), commonly known as E4BP4, which serves as a repressor [101]. In the

zebrafish genome, as for many other genes and gene families, multiple homologs of the bZip PAR/E4BP4 transcription factors have been identified. Therefore, this transcription family in zebrafish is composed of TEF1, TEF2, HLF1, HLF2, DBP1, DPB2 and 6 members of E4BP4 (E4BP4-1 to 6) (Fig 1.11) [101]. My research group has revealed that TEF1 targets the zebrafish *per2* gene promoter by activating the D-box enhancer in a light-responsive manner [92]. Therefore, it is clear that these factors operate within the circadian clock input pathway, relaying environmental timing information to adjust the phase of the core clock oscillator mechanism. Subsequent studies have shown that the transcription driven by the D-box following light exposure is dependent on reactive oxygen species (ROS).

Interestingly, in mammals, the bZip PAR/E4BP4 transcription factors have been extensively studied and have been shown to have a fundamentally different function within the context of the circadian clock. Specifically, PAR factors seem to function within the framework of clock output pathways, as they transmit timing information from the central oscillator to control the transcription of subsequent genes regulated by the clock. In mouse, the CLOCK:BMAL complex drives circadian rhythmic transcription of the DBP gene [102]. By this mechanism the circadian clock directs a circadian expression rhythm in downstream DBP-regulated genes, thereby confering circadian rhythmicity on many physiological functions including certain metabolic pathways and the clearance of xenobiotics [101].

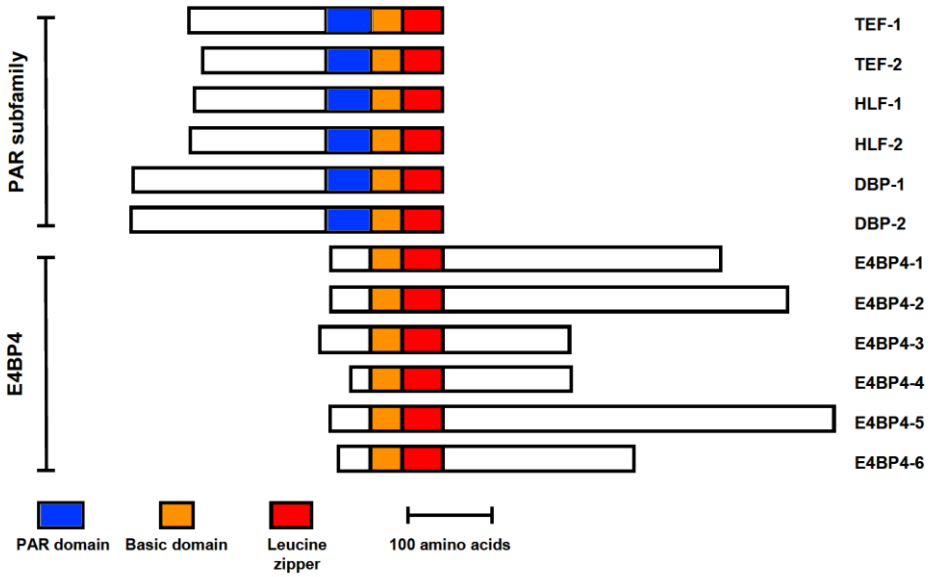

Fig 1.11 Structure of PAR factors and E4BP4s in zebrafish. Conserved PAR-domain, Basic domain and Leucine zipper are highlighted in blue, orange and red, respectively [101].

1.5.3 ROS and evolution: the links between blind cavefish and oxidative stress

The study of how ROS responsive mechanisms have adapted over the course of evolution and the natural selective pressures that have shaped these changes can potentially teach us a lot about the biology of ROS. Animal models that inhabit extreme environments can provide valuable insight for our understanding of many basic biological systems. For example, many unrelated cave-dwelling fish species which have inhabited perpetually dark environments with constant temperatures and scarce food availability, in some cases over the course of millions of years, share many striking adaptations as the result of convergent evolution [103]. These are termed troglomorphisms and include the regression of visual systems, loss of body pigmentation, enhanced tolerance to starvation and extended lifespan, [104-106] as well as increased sensitivity to chemical and mechanical stimuli which enable navigation in the complex cave environment [103, 107].

The mexican tetra (*Astyanax mexicanus*) has become a popular model species to study cavefish biology, genetics and evolution. As well as being relative easy to maintain in a laboratory environment, it exists in a variety of different forms. These include a surface form which lacks troglomorphisms and completely resembles normal surface dwelling fish and a cave adapted form which is exemplified by the Pachón cave population and completely lacks body pigmentation and eyes (Fig 1.12 A). Importantly, although anatomically and physiologically very different from each other, these two forms belong to the same species and so crosses of surface and cave forms produce fertile hybrid offspring which can then be intercrossed over subsequent generations. The pattern of inheritance of the troglomorphic traits can then be followed and used for association genetics studies to explore the genetic basis of these adaptations [108]. Interestingly, despite evolving in a constant dark environment, cave-dwelling populations of *A. mexicanus* have been shown to retain circadian rhythmicity with elevated basal levels of certain light-responsive clock genes, including *per2* [109].

Another extensively studied cavefish species is the Somalian cavefish (*Phreatichthys andruzzii*), which resides in the subterranean waters beneath the central Somalian desert. Having been isolated from surface waters for about 3 million years, *P. andruzzii* shows more extreme troglomorphisms compared to *A. mexicanus*. This includes reduction of the optic tectum in the brain as well as metabolic adaptations for the resistance of starvation (Fig 1.12 B) [110]. However, unlike *A. mexicanus*, there are no surface forms of this species and so it is not possible to perform the type of association genetics studies described for *A. mexicanus*. Interestingly, studies of the circadian clock in this species has revealed the complete loss of light entrainment as a result of loss of function mutations in a subset of the non-visual opsin genes [111]. Furthermore, light, UV as well as ROS induced transcription mediated by the D-box enhancer is completely absent in cells, tissues and even cell lines derived from *P. andruzzii* and also there is a loss of photoreactivation DNA repair resulting from the accumulation of loss of function mutations in the photolyase genes of this species [84].Therefore, evolution in its extreme cave environment has led to many fundamental changes to the way that *P.*

andruzzii cells respond to sunlight and ROS and so make it an interesting model to study these mechanisms in comparison with models such as the zebrafish.

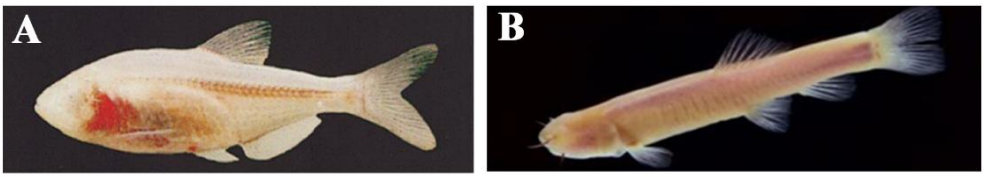

Fig 1.12. Mexican tetra (*Astyanax mexicanus*) (A) and Somalian cavefish (*Phreatichthys andruzzii*) (B). [119, 120]

1.5.4 Evolution of cellular responses to ROS

From a broader perspective, it is tempting to speculate about how the mechanisms which harness oxygen and reactive oxygen species have been subject to evolutionary change. Thus, while life most likely emerged in an anaerobic environment, the oxygen generated by photosynthesis represented a potentially toxic byproduct requiring the establishment of some degree of protection by antioxidant molecules. While the subsequent evolution of oxidative metabolism harnessed oxygen's potential as a source of energy, it represented an additional source of ROS that necessitated the further development of antioxidant mechanisms [112]. This led to the emergence of a sophisticated network of ROS-responsive transcription factors and signaling pathways which were based on the need to detoxify excess ROS as well as using ROS as a signalling molecule. Within this context, the conservation of ROS-regulated transcription factors such as Nrf2 and p53 across evolution is consistent with the fundamental importance of ROS-mediated transcriptional regulation.

However, it is also likely that different species or even individuals within a population of the same species may face very different challenges associated with ROS, depending on the particular environmental stressors they are exposed to. This likely points to ROS sensing, homeostasis and signalling being subject to natural selection and evolutionary changes [1, 113]. Thus, a recent study has implicated evolution of the Keap1 protein, within the Nrf2-Keap1 signaling axis as playing an important role in the evolutionary

transition of vertebrates from aquatic to terrestrial habitats [114]. Specifically, in the zebrafish, more pronounced Keap1 activation leads to reduced Nrf2-driven antioxidative responses compared to those observed in land-dwelling vertebrates. This may represent an adaptation to the fundamental differences in the concentrations of oxygen encountered in terrestrial and aquatic environments.

Furthermore, our own research on the transcriptional response of fish cells to sunlight and associated ROS increases has documented significant species-specific differences. Thus, the D-box enhancer element in zebrafish serves as a robust regulator of clock and DNA repair gene expression in response to light and oxidative stress. However, in the Somalian cavefish *P. andruzzii,* this D-box-mediated mechanism appears to have been severely attenuated (Fig 1.13) [84]. In addition, in mammals the D-box is clock regulated and does not serve as a light or ROS mediated transcriptional regulator. Consequently, exploring how ROS-mediated transcriptional regulation has changed over the course of evolution enriches our understanding of the cellular mechanisms which enable adaptation to a changing environment. It also highlights the delicate balance organisms must maintain in order to minimize the damaging effects of exposure to too much ROS while at the same time maintaining sufficient ROS to enable their normal functions as signalling moelcules.

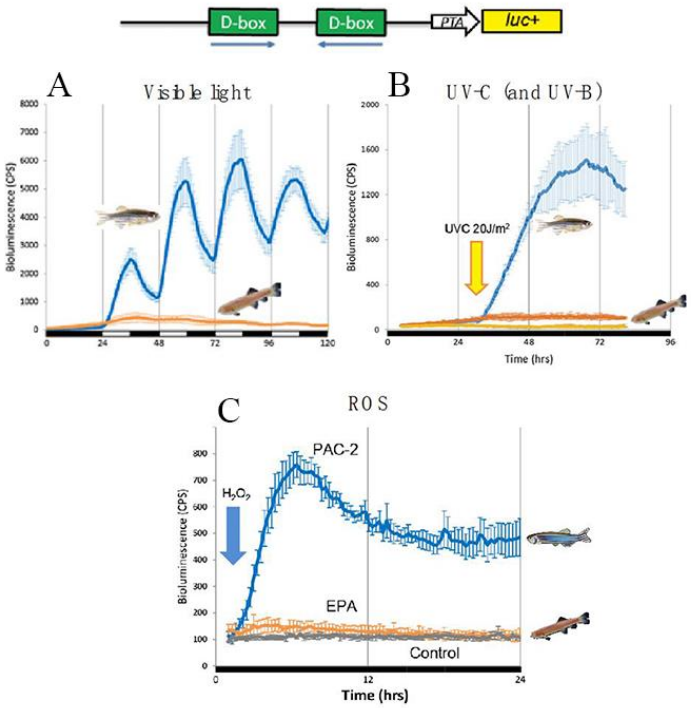

Fig 1.13. Sunlight responsive of the D-box element in zebrafish and cavefish. A luciferase reporter containing two D-box elements from the zebrafish Cry1a promoter was transfected into both zebrafish (Blue trace) and Somalian cavefish (Orange trace) cells. Then cells were exposed to light (A), UV (B) or ROS (C) and a luciferase assay has been conducted by detecting cellular bioluminescence in vivo. The results reveal loss of light, UV and ROS inducibility in cavefish cells [84].

1.6 Experimental aims

The overall goal of this project focuses on exploring how elevated levels of ROS trigger changes in gene expression in fish and how this regulatory circuit has adapted during vertebrate evolution as well as under extreme environmental conditions.

I will aim to answer 3 basic questions that arise from the observation of the striking difference between fish and mammals in terms of how ROS induces gene expression via the D-box enhancer: 1) Is the ROS-dependent activation of certain DNA repair genes via the D-box unique to fish, or is it encountered in other major vertebrate groups?

2) How similar is the ROS regulated transcriptome in zebrafish and mammalian cells? and 3) How is the profile of ROS induced gene expression shaped during evolution in an extreme environment in P.andruzzii cells? To address the above questions, I chose to use different vertebrate cell culture models including the EPA cavefish cell line derived from P. andruzzii and conduct a comparative study to elucidate differences at the molecular level.

2 Materials and Methods

2.1 Cell culture of different vertebrate cells

The PAC-2 zebrafish embryonic cell line [115] was maintained at 26°C in L-15 (Leibovitz) medium (Gibco) enriched with 15% Fetal Calf Serum (FCS) (Biochrom KG). This medium was further fortified with 100 units/ml of Penicillin, 100 µg/ml of Streptomycin, and 0.2% Gentamicin, serving as a fungicide, in a non-humidified cell culture environment devoid of CO2 enhancement. The cavefish (*Phreatichthys andruzzii*) embryonic cell line EPA, established previously in my lab [93], was cultured under the same conditions as the PAC-2 cell line except for the FCS concentration that was 20% . The mouse embryonic cell line NIH-3T3 were kindly provided by Dr. Olivier Kassel (Institute of Biological and Chemical Systems-Biological Information Processing, Karlsruhe Institute of Technology, Germany) and cultured at 37 °C in Dulbecco's Modified Eagle's Medium (DMEM) containing 10% FCS, 2% Penicillin and Streptomycin in a humidified cell culture incubator with a 5% CO_2 supplemented atmosphere. The aquatic turtle, *Trachemys scripta scripta* cell line T1 was a gift from Dr. Marc Thiry (University of Liege) and were originally isolated from liver tissue [116]. T1 cells were incubated at 28 °C in F12K medium (Gibco) supplemented with 12% FCS and 1% of Penicillin and Streptomycin. The frog, *Xenopus tropicalis* cell line 'Speedy' was a gift from Dr. Nicolas Pollet (Institute of Systems and Synthetic Biology, Genopole, CNRS, Universite′ d'Evry Val d'Essonne) and was originally isolated from tadpole hindlimbs [117]. 'Speedy' cells were incubated at 28 °C in 67% (v/v) L-15 medium which was adjusted to amphibian osmolarity by dilution with sterile water. The diluted L15 medium was supplemented with 10% FCS and 1% Pen/Str and cells were cultured in an incubator with constant humidity without enriched CO_2.

These above mentioned cell lines, characterized by their fibroblast-like appearance, thrived best when grown as adherent monolayer cultures on standard tissue culture-treated plastic surfaces (Greiner). Typically, cells were passaged bi-weekly, employing

0.25% trypsin to facilitate cell detachment. Fresh culture medium was added and cells were diluted at ratios of 1: 6 to 1: 10 and then seeded in sterile culture flasks.

2.2 Transient transfection and pharmacological treatments

Vertebrate cells underwent transfection with FugeneHD (Promega) reagent, following the manufacturer's instructions using a 4:1 ratio. They were then incubated under suitable conditions overnight. Culture media were refreshed 24 h after transfection. For H_2O_2 treatment, different concentrations of H_2O_2 were prepared by dilution with sterile water from a 7.97 M stock and directly added to the cell culture medium. Treatment with N-acetylcysteine (NAC) was performed by simply exchanging the culture medium with fresh medium supplemented with a final concentration of 5 mM NAC as previously described [84]. See each figure legend for details of the precise concentrations and times of treatment for each experiment.

2.3 Establishment of stable cell lines

To establish a zebrafish cell line stably overexpressing the catalase protein, PAC-2 cells were transfected with an expression vector for zebrafish catalase in the context of a pcDNA3.1-HA tagged plasmid containing Neomycin resistance (zfCAT-pcDNA-HA). Transfected cells were selected on the basis of acquired resistance to Neomycin G418. Single clones were picked after G418 selection and sub-cultured in individual flasks to generate a confluent monolayer. Then the clones were tested for catalase expression via western-blot by using a HA-tagged antibody and a clone expressing high levels of the recombinant catalase was selected for further experiments.

2.4 Cell viability detection

The MTT (3-(4,5-dimethylthiazol-2-yl)-2,5-diphenyltetrazolium bromide) assay is a

widely used and reliable method to assess cell viability and cell proliferation in a range of cell lines derived from various organisms [118, 119]. This assay consists of the reduction of the yellow tetrazolium dye to form a purple formazan product by metabolically active cells. Vertebrate cell lines were seeded into 96-well plates at a density of 2×10^4 cells per well. After 2 days incubation in darkness, cells were treated with different concentrations of H_2O_2. At different timepoints of incubation with H_2O_2 , the samples were incubated with MTT for 4 hours followed by addition of DMSO to solubilize the formazan product. The absorbance of the colored solution was measured at 490 nm by using a SpectroMax iD3 (Molecular Devices) microplate reader.

Cell viability was determined by comparing the absorbance values of treated samples to those of untreated control samples. The final results were expressed as a percentage, representing the proportion of viable cells compared to the control.

2.5 Transcriptome sequencing

Sample Collection and RNA Extraction: Samples were collected and processed according to the specific experimental protocols. Total RNA from each sample was extracted by using the Trizol reagent according to a standard protocol. The quality and integrity of the extracted RNA were assessed using spectrophotometric methods by NanoDrop (Thermo Scientific) and by agarose gel electrophoresis.

cDNA Synthesis and Library Preparation: Ribosomal RNA (rRNA) was selectively removed from the total RNA using rRNA depletion kits. The remaining RNA was fragmented and converted to complementary DNA (cDNA) using reverse transcription with random primers. The cDNA was then subjected to library preparation. This involved end repair, A-tailing, and adapter ligation. Adapter-ligated cDNA fragments were amplified using polymerase chain reaction (PCR) to generate sequencing-ready libraries.

Sequencing: Transcriptome sequencing was performed commercially by Novogene. Prepared libraries were subjected to high-throughput sequencing using a Novaseq PE150 platform. Sequencing was performed according to the manufacturer's recommendations to generate raw reads. Quality control was conducted using FastQC software. During this process, low-quality bases and adapter sequences were trimmed, and reads that did not meet quality standards were removed.

Alignment and Quantification: In collaboration with Sebastian G. Gornik (COS, Heidelberg), I performed the following bioinformatic analysis in order to analyse the RNAseq data. Filtered reads were aligned to a reference genome (Zebrafish genome ID: GCA_000002035.4; Mouse genome ID: GCF_000001635.27) using HISAT2 software. For the cavefish reads, I conducted a *de novo* assembly by using Trinity software for transcriptome reconstruction.

Differential Expression Analysis: Differential gene expression analysis was performed using statistical software DESeq2. This analysis identified genes with significant expression changes between experimental conditions.

Functional Enrichment and Pathway Analysis: Differentially expressed genes were subjected to functional enrichment analysis using Gene Ontology or KEGG databases. This analysis identified overrepresented biological functions and pathways associated with the gene expression changes, offering insight into the underlying biological significance.

2.6 Gene cloning and coding sequence characterization

Total RNA from different type of cells was extracted by using Trizol Reagent (Invitrogen) according to the manufacturer’s instructions. Reverse transcription was performed using the Transcriptor High Fidelity cDNA Synthesis Kit (Roche). Sequence information of zebrafish catalase was based on the NCBI database, while preliminary sequence information of the cavefish *xpc* and *catalase* genes was acquired from

unpublished cavefish RNA-seq data. High-fidelity Pfu DNA polymerase (Promega) was used to amplify fragments flanking the coding sequence of catalase by PCR reaction as follows: 2 min at 95°C for initial denaturation, then 25 cycles of 95°C 30 sec, 60-65°C 30 sec, 72°C in 2-3 min, with a final extension at 72°C for 5 min. PCR products were purified by Wizard Genomic DNA Purification Kit (Promega) and subcloned into the pCS2-MTK or pcDNA3.1-HA vector for eukaryotic expression using standard molecular cloning methods. For cloning of the full-length cavefish *xpc* gene, a rapid amplification of cDNA ends (RACE) method was adopted by using the SMARTer RACE 5'/3' Kit (TAKARA). For cloning of the promoter region of the cavefish *xpc* gene, a nested PCR-based DNA walking technique was employed, according to the manufacturer's protocols. Firstly, four pools of uncloned, adaptor-ligated genomic DNA fragments have been constructed by blunt-end digestions and following adaptor ligation. These fragment pools were regarded as 'libraries' and nested PCR was performed with gene specific primers and adaptor primers. Resulting constructs were sequenced by a commercial supplier (Microsynth Seq-lab) and analyzed by sequence alignment with the aid of SnapGene 5.2 or DNAMAN 7 software. Primer information is listed below in Table 2.1.

Table 2.1 Primer sequences for zebrafish/cavefish gene cloning

Genes	Oligos	Details
zf cat	F: CGGAATTCAAGGCAGACGACAGAGAAAAGTCG	Catalase coding sequence cloning
	R: CGCTCGAGTCACATCTTAGAAGCTGCAGCCACA	
cf xpc	GATTACGCCAAGCTTAGGGAGCAGAGCTGCGGTTGCCCAACAC	5'RACE primer
	GATTACGCCAAGCTTACCGGCGATCTCTCAGCAGCGGCAGAAT	3'RACE primer 1
	GATTACGCCAAGCTTGCTGCGGTCATTGCGACTCTTCTGTCGG	3'RACE primer 2 for Nested-PCR
	TGCAATCTGCTTCGGTTTCTTTGTGTCGCT	gene specific primer 1

cf xpc promoter	GCCGCTGCTGAGAGATCGCCGGTAGTTTCA	gene specific primer 2 for Nested-PCR
	GTAATACGACTCACTATAGGGC	adaptor primer 1
	ACTATAGGGCACGCGTGGT	adaptor primer 2 for Nested-PCR

2.7 Transient knock down by RNA interference

Transient knockdown of zebrafish *tef1* gene expression in PAC2 cells was performed by using siRNA. In detail, PAC-2 cells were plated at a density of 3×10^5 in 6-well plates and transfected with zfTEF1-siRNA at a concentration of 20 nM using the Lipofectamine RNAiMAX transfection reagent (ThermoFisher Scientific). This siRNA together with a negative control was synthesized and provided by ThermoFisher Scientific. The negative siRNA control was designed to lack homology with any vertebrate transcriptome sequences. The siRNA sequences were as follows: siTEF1 sense: 5'-CGCUGAAACUUCGGCUGCAUUUCCA-3'; siTEF1 anti-sense: 5'-CGCAACAUUGCCGGUACUUUGUCCA-3'.

2.8 Gene expression assay

2.8.1 RNA extraction and reverse transcription

Cultured cell monolayers underwent two washes with PBS. Total RNA extraction was carried out by directly lysing the cells in Trizol Reagent (Gibco, BRL) following the manufacturer's instructions. The total RNA extracted was dissolved in nuclease-free water and stored at -80°C until use.

For the reverse transcription process, 1 µg of the extracted total RNA served as the template for cDNA synthesis using M-MLV reverse transcriptase (Thermo Scientific), adhering to the protocol provided by the manufacturer. The resulting cDNA products were then diluted at a ratio of 1:10 in nuclease-free water and preserved at -20°C for future use.

2.8.2 Quantitative realtime-PCR (qRT-PCR)

Quantitative real-time PCR (qRT-PCR) analysis utilized previously synthesized cDNA as a template, employing the SYBR-green-Primer-Mastermix (Promega). The reaction mixture was composed of 4 µl of diluted cDNA, 10 µl of SYBR-green-Primer-Mastermix, 2 µl of 10 µM primer mix (both forward and reverse primers), and 4 µl of nuclease-free water. qRT-PCR was conducted on either an ABI StepOnePlus or an ABI QuantStudio3 Real-Time RT-PCR machine (Applied Biosystems), following a optimized temperature cycling program tested by our lab. Relative mRNA levels of target genes were assessed using the $2^{-\Delta\Delta CT}$ method, where CT denotes the cycle threshold at which fluorescence surpasses the background level. Expression levels were normalized against *β-actin* mRNA as a reference. Primer sequences for each gene analyzed through qRT-PCR are detailed in Table 2.2.

Table 2.2 Primer sequences for qRT-PCR

Genes	Forward Oligo	Reverse Oligo
zf xpc	GCCAACATCCGTCTCAGAAT	GAACGGTTGGAAAAACCAAG
zf ddb2	TCGGTCTTGCTCTTGGTCTT	GAGGCAGAGCTGGAGGTTC
zf hsp70	CAACGGCAGAGAACTGAACAA	GTCGGAGTAGGTGGTGAAGG
zf fosb	GTCGGAGTAGGTGGTGAAGG	TCCTGGCTTGTGGTGATGG
zf soul5	GCCACTATGATGCTGCCAAG	ATACACTGACGACTGCCACAT
zf β-actin	GATGAGGAAATCGCTGCCCT	GTCCTTCTGTCCCATGCCAA
cf xpc	GTGGACTCGACTGAACTAGC	CAGGTCAGACTCACAGCAC

cf ddb2	AGGGCTCAGACAGATTCCTCT	CCTCCAATCCATTTGACACTTGC
cf atf3	TCTCACCTCACGCTTCATTACA	CACTCACGCTGGACGACTT
cf fosb	GGTTCTGCTGGATGATCTGTC	GGTATTCCTGCGGAGAGTGA
cf ppm1k	CCTGACCGACGCTATTCCA	GATGTATGGCAACGCTTCTCT
cf β-actin	GATGAGGAAATCGCTGCCCT	GTCCTTCTGTCCCATGCCAA
m xpc	CATGCACAAGGTTCACCTGC	TGGCACCTTGGTAAAGCGAA
m ddb2	TTAAAGGGATTGGAGCTGGAG	GCTCTTGGCAGAAACATCAAG
m junb	TACACCAACCTCAGCAGTTACT	TACGGTCTGCGGTTCCTCT
m gadd45a	TCAGCAAGGCTCGGAGTCA	GCAGGATGTTGATGTCGTTCTC
m hspa5	TCGGACGCACTTGGAATGA	GCCTCAGCAGTCTCCTTCA
m β-actin	GGCTGTATTCCCCTCCATCG	CCAGTTGGTAACAATGCCATGT
turtle xpc	GACACCTGGCTGAAGCAA	GGGAACCCTTCCATCCAC
turtle ddb2	GCAGCATCATCCACTACATCTAC	CTGTTCGGAAGAGGCGGTAT
turtle β-actin	GGACCTGACAGACTACCTCAT	GAACCGCTCGTTGCCAATA
frog xpc	CCTCTGCCAACATCCATCAC	ACTTCTGCCAACCTTACAACTC
frog ddb2	TGTTGATGATGAAGCAGGAGGA	CTGGAATGTGGCAATCTGGAAT
frog β-actin	CCGTAAGGACCTCTATGCCAAT	GAACCGCCAATCCAGACAGA

2.9 Protein analysis

2.9.1 Western blotting (WB) assay

After applying the respective treatments, the culture medium was removed and cells were rinsed twice with ice-cold PBS. Proteins were extracted by adding 200 µl of Laemmli buffer (1×, which includes 6% SDS, 20% glycerol, 125 mM Tris at pH 6.8, 0.01% bromophenol blue, and 100 mM DTT) enhanced with a protease inhibitor mixture from Sigma Aldrich to each culture well. The cells were then harvested using

a sterile scraper, and the protein lysates were heated for 5 minutes to unfold the proteins, prior to being stored at -20°C. Gel electrophoresis was carried out on a Bio-Rad miniprotean3 apparatus, and proteins were subsequently transferred onto a PDVF membrane from Millipore via electrophoretic transfer for analysis. Following transfer, the membranes were blocked for one hour at room temperature using either 5% non-fat dry milk or 5% BSA in a freshly prepared PBST buffer (containing 0.1% Tween-20 in PBS). The process of antibody incubation and subsequent washings adhered to the protocols provided by the manufacturers. Immunoreactive bands were detected using the ECL system (Thermo Scientific). The resulting images were obtained and analyzed with the Image Lab™ system (Bio-Rad). The specific antibodies utilized in this experiment are detailed in Table 2.3.

2.9.2 Immunofluorescence assay (IFA)

The IFA was applied as described previously [84] with some modifications. Transfected cells, plated at a density of 1×10^5 cells per well of a 24-well plate on glass slides and fixed at specific time points or treatments with 4% PFA at room temperature for 20 min. Cells were wash 3× 5 min with 1x PBS and 2× 10 min with 1x PBST (0.1% Tween-20 in PBS) followed by incubation with 0.2% Triton X-100 in 1x PBS for 5 min. After washing again with PBS, cells were pre-incubated in blocking solution (1%BSA in 1x PBST) at room temperature for 1 hour. The primary antibody was applied by incubation in blocking solution at a dilution of 1: 500 overnight at 4 °C. Thereafter, cells were washed with PBS 3 times and then incubated in blocking solution containing a mixture of fluorescently labelled secondary antibody (diluted 1: 500) and DAPI (diluted 1: 10000) for 1 hour at room temperature. Labelled cells were mounting on microscope slides using the VECTASHIELD mounting medium for fluorescence (Vector). Images were acquired using a LSM900 Confocal Microscope and analyzed by Image J or CellProfiler software. Antibodies used in this test are listed below in Table 2.3.

Table 2.3 Antibodies used in the WB and IFA.

Antibody	**Product information**	**Dilution**
Primary Antibody		
Anti-Myc-Tag	Mouse IgG2a, Cell signaling 9B11	IF 1:500
Anti-Phospho-Histone H2AX (Ser139)	Rabbit polyclonal, Cell signaling 9718	IF 1:500
Anti-HA-Tag	Rat IgG1, Roche	WB 1: 1000
Anti-beta-actin	Mouse monoclonal, Sigma-Aldrich A2228	WB 1:1000
Secondary Antibody		
Anti-mouse IgG	Polyclonal Goat HRP, Cell signaling 7076	WB 1: 5000
Anti-rabbit IgG	Polyclonal Goat HRP, Cell signaling 7074S	WB 1: 5000
Anti-rabbit Cy3	Polyclonal Goat anti-rabbit IgG, Jackson ImmunoResearch	IF 1: 500

2.10 Luciferase reporter gene assay

2.10.1 *In vitro* Luciferase assay

Cells were plated in a 24-well plate (CELLSTAR, Greiner) at a density of 1×10^5 cells per well. Once a confluent monolayer was established, cells underwent transfection with 200 ng of a promoter-luciferase-reporter vector and varying amounts of an expression vector using FuGeneHD reagent, as per the guidelines from Promega. In each transfection, 50 ng of a β-galactosidase expression vector (pcDNA3.1/myc-His/lacZ from Invitrogen) was also included to monitor transfection efficiency. The culture medium was replaced 24 hours post-transfection, and the cells were then kept in the dark for an additional 24 hours. Cell lysis was performed using lysis buffer, followed by measurement of firefly luciferase activity using a VICTOR Multilabel Plate Reader (Perkin Elmer) with the Luciferase Assay System kit from Promega,

according to the manufacturer's instructions. Results were standardized for transfection efficiency using the results from the β-galactosidase assay.

2.10.2 In vivo real-time bioluminescence assay and data analysis

Cells were seeded at a density of 2×10^4 cells per well in a 96-well plate (Perkin Elmer) a day prior to the assays. The next day, cells from each well underwent transfection with 100 ng of promoter-luciferase-reporter vectors, with varying doses of transcription factor expression constructs, using FugeneHD transfection reagent (Promega). Twenty-four hours post-transfection, the culture medium was aspirated and replaced with 200 µl of complete medium infused with 0.5 mM beetle luciferin potassium salt solution (Promega). For experiments involving H_2O_2, the plates received H_2O_2 treatment in the dark while containing luciferin to avoid light influence. All plates were covered with an adhesive sealing sheet (Packard) and placed into either an EnVision multilabel counter (Perkin Elmer) or a Topcount NXT automatic scintillation counter (Perkin Elmer) to measure bioluminescence in counts per second (cps) at 15-30 minute intervals. The specific lighting conditions for each experiment are detailed in the figure legends. Data analysis was conducted using Microsoft Excel software and results were graphed using Graphpad Prism 5.0 software.

2.10.3 Luciferase reporter constructs

zfXPC736bp-Luc:

A 736 bp length of genomic DNA fragment from the zebrafish *xpc* promoter was amplified by PCR using Pfu DNA polymerase (NEB) and subcloned into the pGL3-basic vector (Promega). The following primers incorporating a 5' KpnI and 3' XhoI restriction site were used: F: CGCGGTACCTGAACCGCCAACTTATCCAGCAT; R: CGCCTCGAGGCATCACATCACCAGTAGCGACTA.

zfXPC184bp-Luc:

We amplified a 184 bp of genomic DNA fragment from the zebrafish *xpc* promoter internal to the 736 bp region mentioned above by PCR, using GoTaq G2 DNA polymerase (Promega) and subcloned into the pGL3-basic vector (Promega). The following primers incorporating a 5' KpnI and 3' XhoI restriction site were used: F: CGCGGTACCTGACGTTTATTCGCATCTCCTG; R: CGCCTCGAGTTCTCCTTCTTCTGATGTTGCT

cfXPC184bp-Luc:

We amplified the conserved 184 bp promoter region from the cavefish *xpc* by using a Genome Walking PCR Kit (Clontech) and subcloned into the pGL3-basic vector (Promega). The following primers incorporating a 5' KpnI and 3' XhoI restriction site were used: F: CGGAGCTCTGACGTATACGGATCCCCTGCA; R: CGCTCGAGGAGAGATCGCCGGTAGTTTCAG.

zfXPC-2×D-box1-Luc:

This construct harbors two duplicates of the initial D-box element (5'-TTATGAAA-3') from the zebrafish *xpc* gene promoter (position -140 bp relative to the ATG) in the pTAL-pLuc minimal promoter reporter vector (Stratagene). Oligos with a 5' KpnI and 3' XhoI restriction site (F: CGGGTACCGTGTTATGAAAGGTGTGTTATGAAAGGTCTCGAGGC; R: GCCTCGAGACCTTTCATAACACACCTTTCATAACACGGTACCCG) were annealed to form DNA double strand and further subcloned into the reporter vector.

zfXPC-2×D-box2-Luc:

This construct harbors two duplicates of the second D-box element (5'-TTGGGTAA-3') from the zebrafish *xpc* gene promoter (position -114 bp relative to the ATG) in pTAL-pLuc minimal promoter reporter vector (Stratagene). Oligos with a 5' KpnI and 3' XhoI restriction site (F: CGGGTACCGTGTTGGGTAACAGGTGTTGGGTAACAGCTCGAGGC; R:

GCCTCGAGCTGTTACCCAACACCTGTTACCCAACACGGTACCCG) were annealed to form double stranded DNA and thereby subcloned into the reporter vector.

zfXPC-2×D-box3-Luc:

The construct harbors two duplicates of the third D-box element (5'-TTACACAA-3') from the zebrafish *xpc* gene promoter (position -96 bp relative to the ATG) in pTAL-pLuc minimal promoter reporter vector (Stratagene). Oligos with a 5' KpnI and 3' XhoI restriction site (F: TGGGAAGTGAATGTGTTACACAACAGTGTGGTCTTCAGGTTACATTACAC AAGT; R: ACTTGTGTAATGTAACCTGAAGACCACACTGTTGTGTAACACATTCACTTC CCA) were annealed to form double stranded DNA and further subcloned into the reporter vector.

zfXPC-3×D-box-Luc:

The construct contains two duplicates of the third D-box element (5'-TTACACAA-3') from the zebrafish *xpc* gene promoter (position -96 bp relative to the ATG) in pTAL-pLuc minimal promoter reporter vector (Stratagene). Based on the *zfXPC-2×D-box3-Luc* reporter vector, an additional D-box3 was added by using the Q5-site-directed mutagenesis kit with primers: F: ACAAGGTGGGAAGTGAATGTGTTAC; R: GTAACACAGAAAGCATGCACTTTG.

zfXPC-2×D-box1-mut-Luc

The construct contains two copies of the first D-box element mutated from 5'-TTATGAAA-3' to 5'-ATATGAAA-3' and subcloned into the pTAL-pLuc minimal promoter reporter vector (Stratagene) by using mutant sequence oligos but with the same restriction sites described above.

zfXPC-2×D-box2-mut-Luc

The construct contains two copies of the second D-box element mutated from 5'-TTGGGTAA-3' to 5'-ATGGGTAA-3' and subcloned into the pTAL-pLuc minimal

promoter reporter vector (Stratagene) by using mutant sequence oligos but with the same restriction sites described above.

zfXPC-2×D-box3-mut-Luc

The construct contains two copies of the third D-box element mutated from 5'-TTACACAA-3' to 5'-ATACACAA-3' and subcloned into the pTAL-pLuc minimal promoter reporter vector (Stratagene) by using the mutant sequence oligos but with same restriction sites described above.

2×D-boxIns-Luc:

The construct contains one ATF-1/CREB binding site element (5'-TGACGT-3') from the zebrafish *xpc* gene promoter (position -184 bp relative to the ATG) and two copies of the third D-box element (5'-TTACACAA-3') from the zebrafish *xpc* gene promoter (position -96 bp relative to the ATG) in pGL3-basic reporter vector (Promega). Based on the *zfXPC-2×D-box3-Luc* reporter vector, an additional ATF-1/CREB element was incorporated by using the Q5-site-directed mutagenesis kit with primers: F: TGACGTTTATTCGCATCTCCTGCAG; R: GGTACCTATCGATAGAGAAATG

15×D-box$_{cry1a}$-Luc:

The construct was previously prepared by my lab members and contains the multimerized D-box sequence (5'-AAGTTATACAAC-3') from the zebrafish *cry1a* gene promoter (position -331 relative to the ATG) in pLuc-MCS (Stratagene) plasmid as 15 copies in a tandem array.

2.10.4 Deletion and substitution by site-directed mutagenesis

To pinpoint the promoter elements driving ROS-induced transcription from the *xpc* gene promoter, each element was systematically deleted using the Q5 Site-Directed Mutagenesis Kit (NEB) following the instructions provided by the manufacturer.

Information of the construct names, types of mutations, and the primers employed is listed in Table 2.4 below.

Table 2.4. Zebrafish *xpc* promoter deletions and mutations primers

Construct name	**Mutation type**	**Primers**
zfXPC-184bp-Del1	ATF1/CREB binding site (TGACGT) deleted	F: TTATTCGCATCTCCTGCAG R: GGTACCTATCGATAGAGAAATG
zfXPC-184bp-Del2	D-box1 (TTATGAAA) deleted	F: GGTGGGAAGTGAATGTGTTG R: CACAGAAAGCATGCACTTTG
zfXPC-184bp-Del3	D-box2 (TTGGGTAA) deleted	F: CAGTGTGGTCTTCAGGTTAC R: CACATTCACTTCCCACCTTTC
zfXPC-184bp-Del4	D-box3 (TTACACAA) deleted	F: GTTCACGTGTAATGTAAAGATC R: TGTAACCTGAAGACCACAC
zfXPC-184bp-Del5	E-box (CACGTG) deleted	F: TAATGTAAAGATCTGTGTCC R: AACTTGTGTAATGTAACCTG
zfXPC-184bp-Del6	D-box1, 2, 3 all deleted	F: GTTCACGTGTAATGTAAAGATC R: CACAGAAAGCATGCACTTTG
zfXPC-184bp-Del7	D-box1 and 2 deleted	F: CAGTGTGGTCTTCAGGTTAC REV CACATTCACTTCCCACCC
zfXPC-184bp-Del8	D-box1 and 3 deleted	F: CAGTGTGGTCTTCAGGTTAC R: CACATTCACTTCCCACCTTTC
zfXPC-184bp-Del9	D-box2 and 3 deleted	F: CAGTGTGGTCTTCAGGTTAC R: CACATTCACTTCCCACCTTTC
zfXPC-184bp-Del10	ATF1/CREB, D-box1 and D-box2 deleted	F: CAGTGTGGTCTTCAGGTTAC R: CACATTCACTTCCCACCTTTC
zfXPC-184bp-Del11	ATF1/CREB, D-box1, 2 and E-box deleted	F: TAATGTAAAGATCTGTGTCC R: AACTTGTGTAATGTAACCTG

zfXPC-184bp-Del12	D-box1, 2, and E-box deleted	F: TAATGTAAAGATCTGTGTCC R: AACTTGTGTAATGTAACCTG
zfXPC-184bp-Sub1	D-box1 mutated by single-base substitution	F: TAGGTACCTGTCGTTTATTCG R: TCGATAGAGAAATGTTCTG
zfXPC-184bp-Sub2	D-box2 mutated by single-base substitution	F: GCTTTCTGTGATATGAAAGGTGGG R: ATGCACTTTGCCTGCAGG
zfXPC-184bp-Sub3	D-box3 mutated by single-base substitution	F: AGTGAATGTGATGGGTAACAG R: TCCCACCTTTCATAACAC
zfXPC-184bp-Sub4	D-box4 mutated by single-base substitution	F: TCAGGTTACAATACACAAGTTCAC R: AGACCACACTGTTACCCA
zfXPC-184bp-Sub5	D-box5 mutated by single-base substitution	F: ACACAAGTTCTCGTGTAATGTAAAG R: AATGTAACCTGAAGACCAC

2.10.5 Expression constructs and mutation

For transcription factors and catalase co-transfection experiments in both *in vivo* and *in vitro* luciferase assays, expression constructs were prepared by cloning the coding sequences into a pCS2-MTK (Myc-Tagged) or pcDNA3.1 (HA-Tagged) expression vectors to express an epitope-tagged fusion protein. Constructs including zfTEF1-pCS2-MTK, zfTEF2-pCS2-MTK, zfDBP1-pCS2-MTK, zfDBP2-pCS2-MTK, zfHLF1-pCS2-MTK and zfHLF2-pCS2-MTK were prepared previously in our group as stocks. Constructs including cfTEF1-pCS2-MTK, cfTEF2-pCS2-MTK, cfDBP1-pCS2-MTK, cfDPB2-pCS2-MTK, cfHLF1-pCS2-MTK and cfHLF2-pCS2-MTK were prepared by my colleague Alessandra Boiti (IBCS-BIP, KIT). Detailed information of other expression constructs and their mutants generated in my study are listed below in Table 2.5.

Table 2.5. Expression constructs and mutations

Constructs	Details	Primers
zfCAT-pCS2-HA	Expression of zebrafish Catalase with HA-Tag	F: CGGAATTCTAAGGCAGACGACAGAGAAAAGTCGA R: ATCTCGAGTCACATCTTAGAAGCTGCAG
zfTEF1-T28A	Thr28 mutated to Ala in zfTEF1	F: AATAATGGAAGCTCCTCCACCGAATC R: TTCTTTAAAACTACTGGAAATGC
zfTEF1-T64A	Thr64 mutated to Ala in zfTEF1	F: AGCCGCCTTAGCTCCAGCCATCT R: GAAGGTCCCATTTCACTGAC
zfTEF1-T113A	Thr113 mutated to Ala in zfTEF1	F: CATACAGCTGGCAGCCGAGGAAC R: TTTTCCTTCTCACTGCTCTTTTG
zfTEF1-T119A	Thr119 mutated to Ala in zfTEF1	F: GGAACCATCCGCAGCCTCTGC R: TCGGCTGCCAGCTGTATG
zfTEF1-T165A	Thr165 mutated to Ala in zfTEF1	F: GAACCGGATGGCTCCAGATCCCA R: TCTTCTGATTTGTTGTCTGCTG
hyTEF1-pCS2-MTK	a hybrid TEF1 protein between cfTEF1 (N-terminal) and zfTEF1 (C-terminal)	ZF F: CGGATGACACCAGATCCCATTA ZF R: TTACAGCGCTCCGTATTTGG CF F: TTGGACGCAGGCTCTGATATTCC CF R: GGCCTCGTCTGATTTGGTGT
cfTEF1-I31T	Ile31 mutated to Thr in cTEF1	F: AATCATGGAAACCCTGCCACCGAATC R: TTCTTTAAAACTACTGGGAAAG
cfTEF1-TP	Ile31+Leu32 mutated to Thr +Pro in cfTEF1	F: AATCATGGAAACCCCTCCACCGAATCTTCTCG R: TTCTTTAAAACTACTGGGAAAG
mTEF-pCS2-MTK	Expression of mouse Tef with a Myc epitope Tag	F: AGGAATTCACGTCCGACGCGGGCG R: AGCTCTAGATTACAAGGGCCCGTACTTGGTCTCG

2.11 Plasmid DNA preparation

Bacterial liquid cultures were initiated by inoculating LB medium with single bacterial colonies. Plasmid DNA was then isolated from saturated overnight cultures following a standard alkaline lysis protocol. The resulting DNA pellets were reconstituted in nuclease-free water, and their concentration and purity were evaluated using a spectrophotometer and agarose gel visualization.

2.12 Statistical analysis

Statistical analyses were carried out using either SPSS 21.0 or GraphPad Prism 4.0 (http://www.graphpad.com) software. Specifically, one-way or two-way ANOVA, followed by Bonferroni's multiple comparison tests were adopted to assess significant difference between control and treatments. Results are displayed as the mean ± SD derived from three biological replicates. A p-value of less than 0.05 was considered statistically significant. In the graphical displays, p-values of less than 0.05, 0.01, and 0.001 are denoted by *, **, and ***, respectively.

3 Results

3.1 Cell toxicity of H_2O_2 in vetebrate cell lines

3.1.1 H_2O_2 differentially affects cell viability of zebrafish, cavefish and mouse cell lines.

In order to explore the gene expression response whereby cells from various vertebrate groups react to elevated ROS levels, I initially selected a set of fibroblast-like cell lines derived from a range of vertebrate groups specifically, mammalian (mouse, NIH-3T3), fish (zebrafish, PAC-2 and the blind cavefish *P. andruzzii*, EPA), amphibian, (*Xenopus tropicalis*, Speedy) and reptilian (the aquatic turtle, *Trachemys scripta scripta*, T1) cell lines. To induce elevated ROS levels in each cell line, I supplemented the cell culture medium with H_2O_2. However, it was important to first determine which concentration of H_2O_2 to use for each line since very high concentrations are frequently cytotoxic. In order to explore the toxicity of ROS for each of our vertebrate cell lines, I initially performed a MTT assay on zebrafish PAC-2, the cavefish *P. andruzzii* EPA, mouse NIH 3T3, Turtle T1 and Frog 'Speedy' cells following exposure to a range of H_2O_2 concentrations. As shown in Fig. 3.1, cells showed different sensitivities to H_2O_2. For PAC-2 and EPA cells, H_2O_2 ranging from 50 to 1000 μM did not affect the cell viability throughout the test. However, cell viability decreased in 3T3 cells at 600 and 1000 μM in a dose-dependent manner following 6-hours exposure to H_2O_2, indicating that these mammalian cells are more sensitive to ROS. The Turtle T1 and Frog 'Speedy' cells also showed a higher H_2O_2 tolerance than mouse cells with T1 cells showing a significant decrease of cell viability upon exposure to 1000 μM H_2O_2. In order to test the effects of ROS on gene expression, I chose to use 300 μM ROS treatment as a suitable concentration which did not result in excess cell death in any of the cell lines.

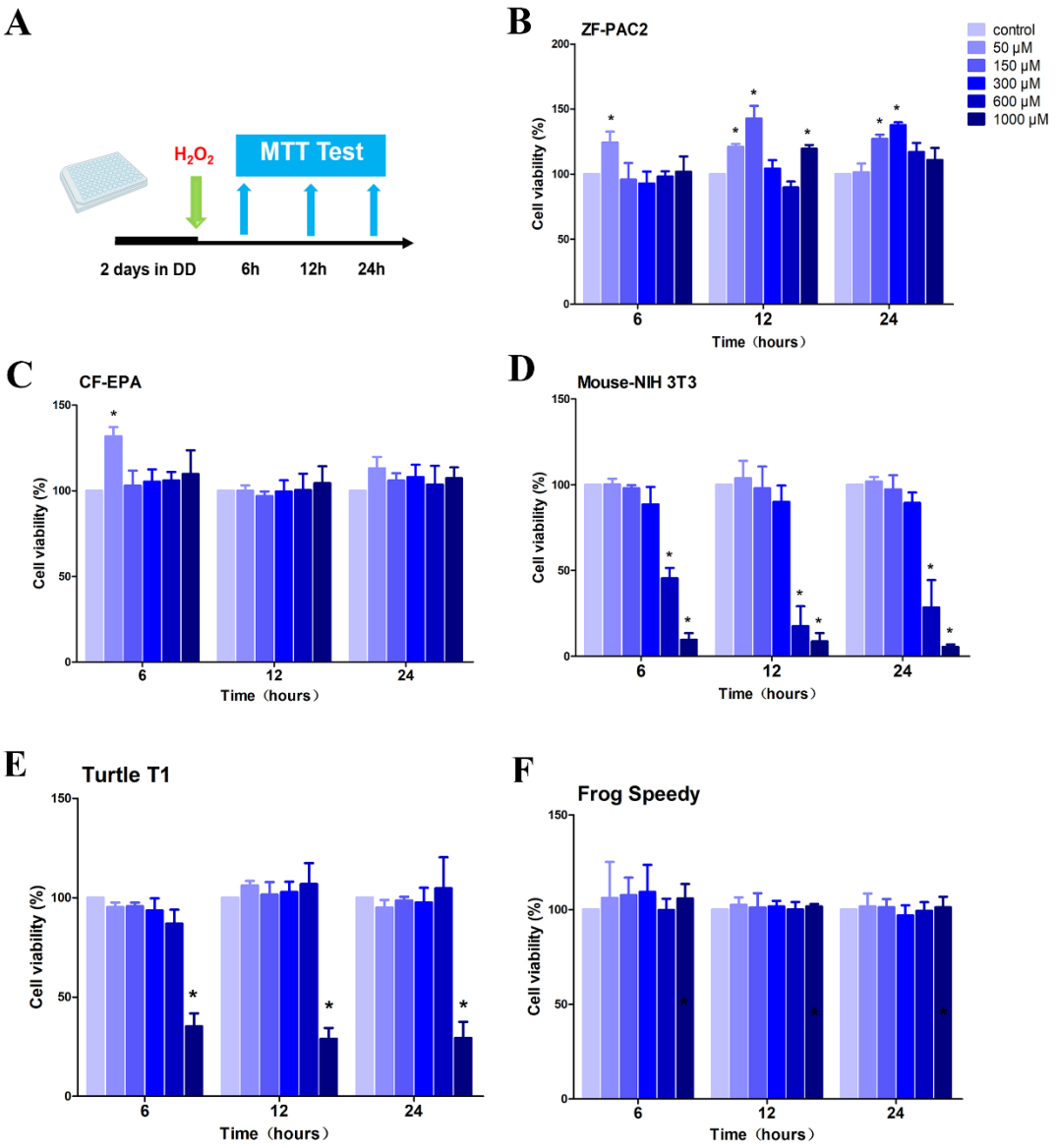

Fig 3.1. MTT assay reveals the effects of H_2O_2 on cell viability in different vertebrate cell lines.

A: Schematic representation of the viability assay. Cells were seeded into 96 well plates and incubated for 2 days in darkness. Then cells were exposed to different concentrations of H_2O_2 and incubated again for 24h. Cells were sampled at 6, 12 and 24 h for MTT assay. All procedures were performed in darkness; B: zebrafish PAC-2 cells; C: cavefish EPA cells; D: mouse NIH 3T3 cells; E: turtle T1 cells; F: Frog 'Speedy' cells. Results are expressed as mean ± SEM (n=3) and the asterisk above the columns represent significant difference between treatment and control (p <0.05).

3.1.2 DNA damage induced by H_2O_2 in different cell types

I next chose to focus on comparing the cellular response of the mouse and fish cell lines to elevated ROS levels in more detail. One important consequence of the exposure of cells to elevated levels of ROS is an increase in DNA damage. Induced levels of phosphorylation of Histone H2AX at Ser 139 (also called γ-H2AX) are a commonly used biomarker for DNA damage. Upon exposure to genotoxic agents, such as ionizing radiation or certain chemotherapeutic drugs, the histone variant H2AX becomes rapidly phosphorylated at serine 139, forming gamma-H2AX foci at the sites of DNA damage. These foci serve as a platform to recruit DNA repair proteins and activate the cellular DNA damage response. In the present study, I exposed the fish and mouse cell lines to 300 μM of H_2O_2 under darkness and then used immunofluorescence staining to quantify levels of γ-H2AX. As shown in Fig 3.2, all PAC-2, EPA and NIH-3T3 cells exhibited elevated γ-H2AX levels under H_2O_2 exposure. Furthermore, 3T3 cells exhibited elevated sensitivity to H_2O_2, as evidenced by a notable increase in γ-H2AX levels after only 1 hour of exposure. Nevertheless, a conspicuous reduction in γ-H2AX levels for all three cell lines after 12 h exposure is consistent with the preservation of DNA integrity through the function of DNA repair systems.

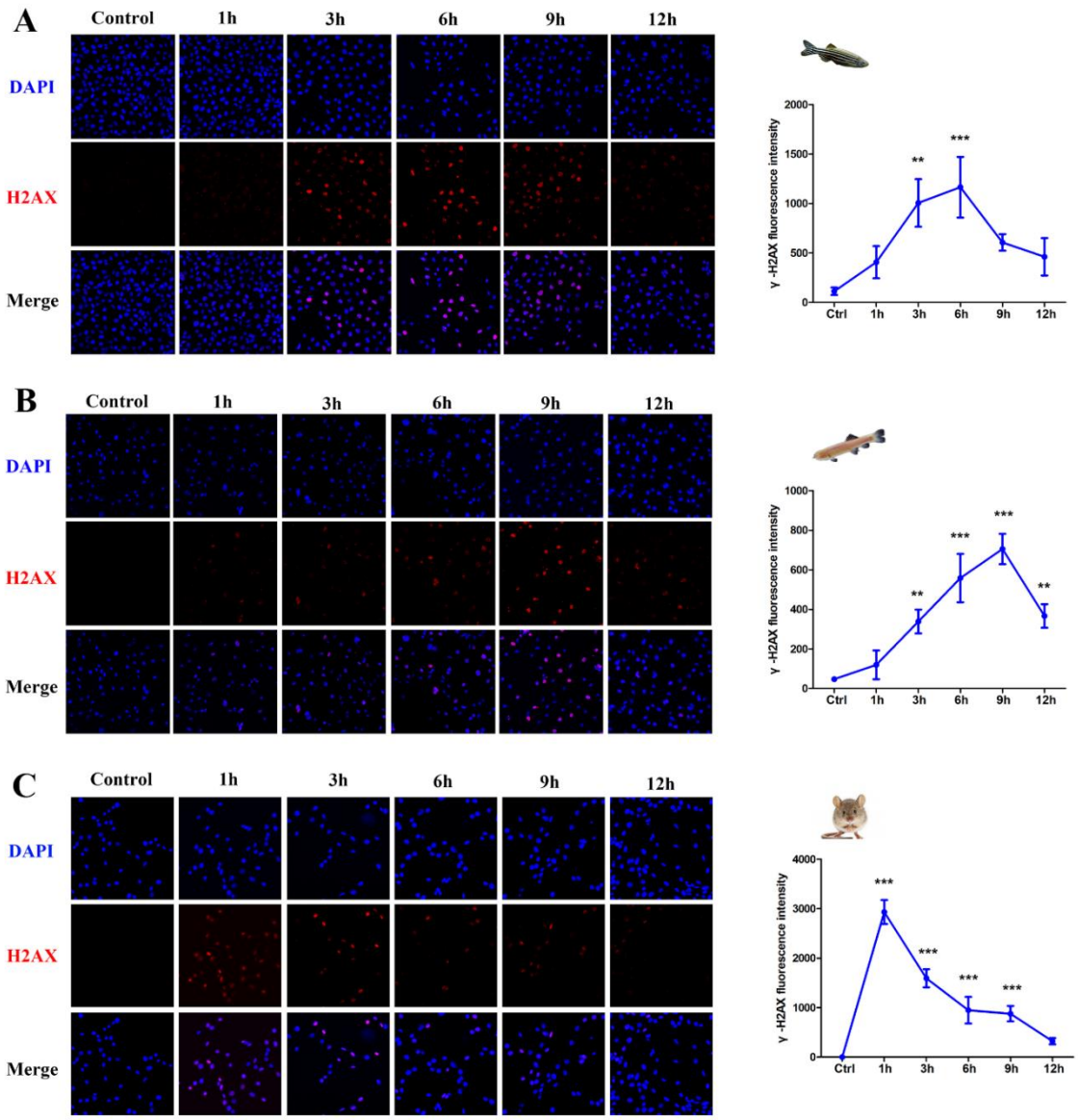

Fig 3.2. Immunofluorescence assay of γ-H2AX reveals DNA damage induced by H_2O_2 in different cell lines from (A) zebrafish, (B) cavefish and (C) mouse. Left panels are representative fluorescence images and right panels are quantification of fluorescence intensity and statistical analysis of that data from the different cell lines. On the x-axes are plotted time and on the y-axes are γ-H2AX fluorescence intensities calculated by Cellprofiler software. Results are expressed as mean ± SEM (n=3 and at least 200 cells per time point were counted). Asterisks represent significant difference between treatment and control (0 h) (*p <0.05, **p<0.01, *** p<0.001).

3.2 Trancriptome analysis reveals differential transcriptional response to ROS in vertebrates

Previous studies have documented several genes where transcription is increased upon exposure to ROS in zebrafish while the same genes are no longer induced by ROS in cavefish, for example, photolyase genes [84]. However, we still lack a global view of how the ROS-regulated transcriptome in zebrafish compares with that in the cavefish *P. andruzzii*, which has evolved in an extreme environment or in mammals. In essence, how conserved is the ROS-regulated transcriptome between different vertebrate groups? To tackle this question, I adopted the RNA-seq technique to examine the transcriptome of PAC-2, EPA and NIH-3T3 cells upon sublethal H_2O_2 exposure (Fig 3.3). After quality control, a mean of 32,660,382, 31,271,782 and 32,972,484 clean reads were obtained from each sample of the PAC-2, EPA and 3T3 cell lines, respectively. Subsequent bioinformatics analysis of this sequence data was performed in collaboration with Sebastian G. Gornik (COS, Heidelberg). Clean reads were mapped to the reference genome of zebrafish (GCA_000002035.4) or mouse (GRCm38/mm10). For cavefish *P. andruzzii* which currently lacks a referenced genome, a *de novo* assembly strategy was applied. From transcriptome analysis, a total of 334 (205 up and 129 down, control vs 1 h) and 515 (336 up and 179 down, control vs 6 h) differentially expressed genes (DEGs) were identified in zebrafish samples (Fig 3.4). GO enrichment analysis indicates that most DEGs are enriched in terms of 'metabolic process', 'cellular process' in Biological Process and 'binding' in 'Molecular Function'. Many more DEGs identified in 3T3 samples both at 1 h and 6 h implies significant differences in the transcriptional response of these mammalian cells to ROS (Fig 3.6). However, there were fewer DEGs at 6 h compared to 1 h in cavefish samples (Fig 3.5). To validate the RNA-seq data, I randomly selected a subset of significantly regulated genes and then assayed their mRNA levels using a qPCR assay. The qPCR data showed a similar trend of gene expression as predicted by the RNA-seq data, thus validating the quantitative results of my RNAseq analysis (Fig 3.7).

By GO analysis, the DEGs of cavefish and mouse were enriched for a 'binding' class of genes, which includes the group of DNA repair genes. Therefore, I compared the expression of DNA repair genes in different species. As shown in Fig 3.8A, most DNA repair genes showed different transcriptional kinetics in response to H_2O_2 in the different cell lines. I subsequently focused on genes involved in Excision DNA repair which are known to play a pivotal role in the repair of various types of oxidative DNA damage under ROS stress. These include in particular the *xpc* and *ddb2* genes which encode the key recognition factors that bind to sites of DNA damage and then recruit other members of the NER repair cascade to repair covalently damaged DNA[120]. Both RNA-seq and the qPCR results confirmed that H_2O_2 robustly induced *xpc* expression in zebrafish cells, the same gene being moderately induced in mammalian cells, but not significantly induced in cavefish cells (Fig 3.8B). Meanwhile, *ddb2* was induced in both zebrafish and cavefish cells but not in mouse cells (Fig 3.8C).

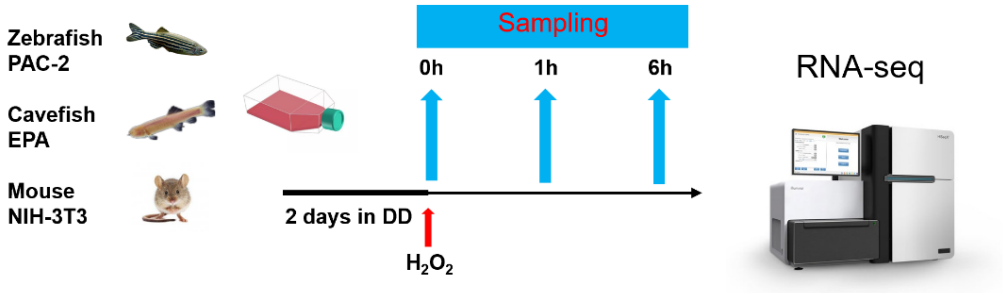

Fig 3.3. Schematic representation of RNA-seq analysis for three vertebrate cells following exposure to 300 μM H_2O_2. Cells were incubated in darkness for 2 days to avoid any direct influence of light or endogenous circadian rhythmicity. Afterwards, cells were sampled at 0 h (as control), 1 h and 6 h and total RNAs were used for RNA-seq analysis at the Novaseq PE150 platform.

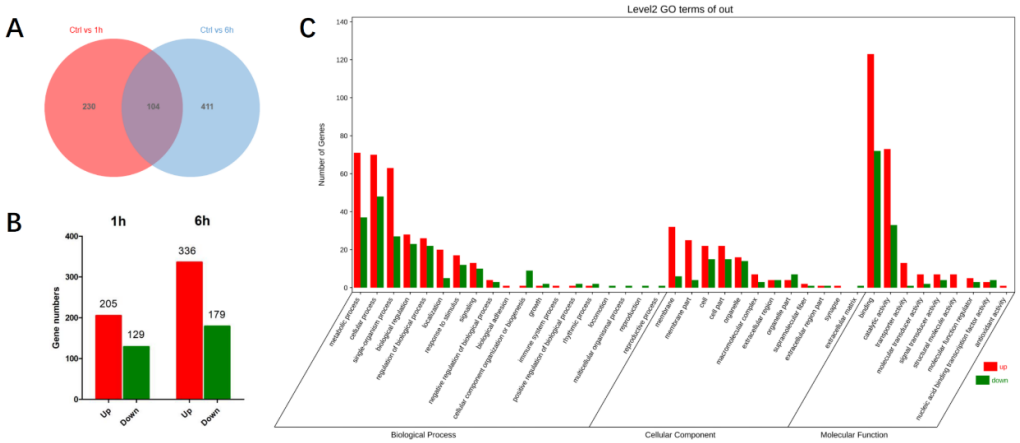

Fig 3.4. Differentially Expressed Gene (DEG) analysis and GO analysis of RNA-seq data from zebrafish PAC-2 cells. A: The venn plot indicates DEGs between control and H_2O_2 treatment (1h and 6h respectively) and the shared DEGs. B: 1 h and 6 h DEGs, up-regulation was indicated in red and down-regulation in green. C: DEGs annotated in different GO terms. The y-axis plots the number of DEGs enriched for each specific function. Up-regulation is indicated in red and down-regulation in green.

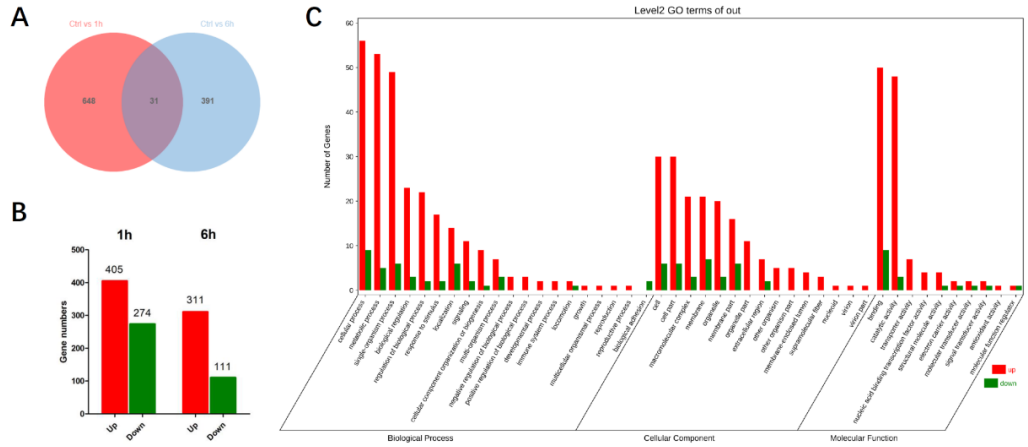

Fig 3.5. DEGs analysis and GO analysis of RNA-seq data from cavefish EPA cells. A: The venn plot indicates DEGs between control and H_2O_2 treatment (1h and 6h respectively) and the shared DEGs. B: 1 h and 6 h DEGs, up-regulation was indicated in red and down-regulation in green. C: DEGs annotated in different GO terms. The y-axis plots the number of DEGs enriched for each specific function. Up-regulation is indicated in red and down-regulation in green.

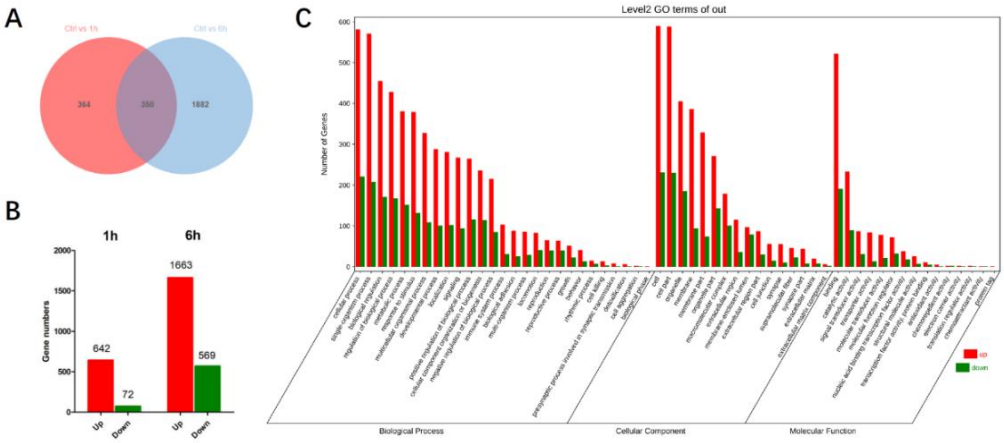

Fig 3.6. DEGs analysis and GO analysis of RNA-seq data from mouse NIH-3T3 cells. A: The venn plot indicates DEGs between control and H_2O_2 treatment (1h and 6h respectively) and the shared DEGs. B: 1 h and 6 h DEGs, up-regulation was indicated in red and down-regulation in green. C: DEGs annotated in different GO terms. The y-axis plots the number of DEGs enriched for each specific function. Up-regulation is indicated in red and down-regulation in green.

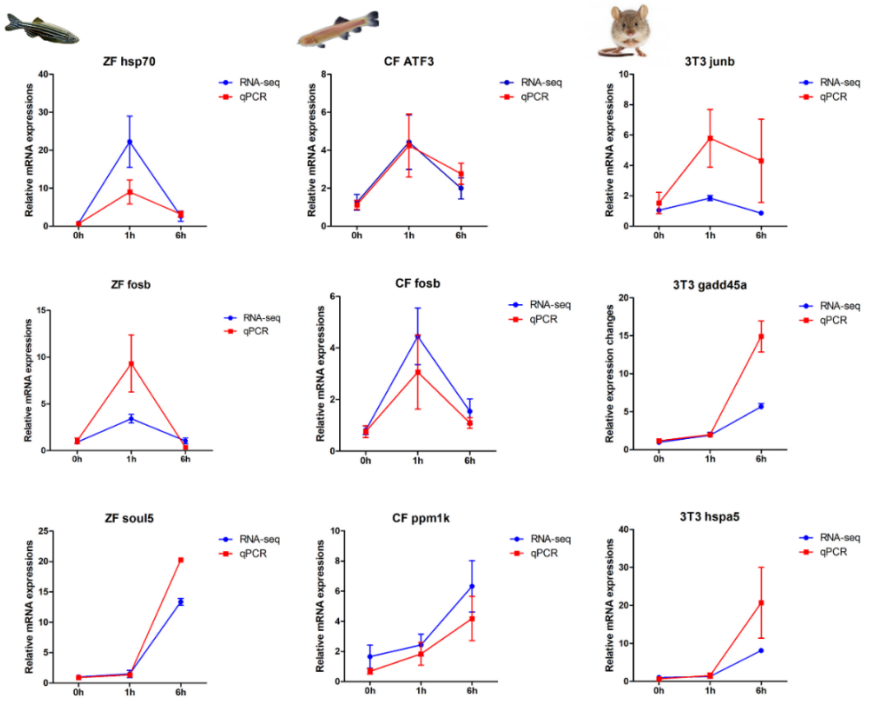

Fig 3.7. Validation of RNA-seq data by qPCR. Left panels: zebrafish; middle panels: cavefish; right panels: mouse. Data were shown as fold change relative to the control at 0 h.

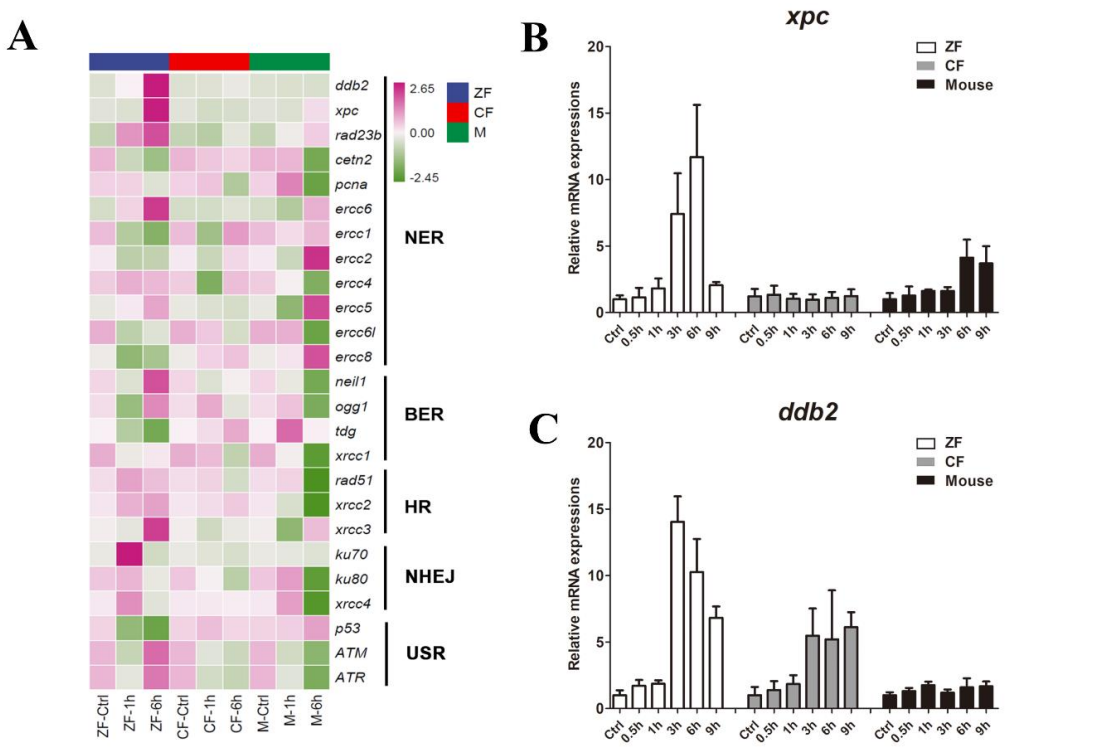

Fig 3.8. Transcriptional profile of induced DNA repair genes in response to H_2O_2. A. Relative expression of DNA repair genes from RNA-seq data. Coloured bar represents the log2-fold induction from up-regulation (dark pink) to down-regulation (green). Each rectangle indicates the mean value from three biological replicates. NER: nucleotide excision repair; BER: base excision repair; HR: homologous recombination; NHEJ: non-homologous end joining; USR: up-stream regulator. B and C. *xpc* and *ddb2* mRNA levels in different cell lines upon 300 µM H_2O_2 treatment, respectively. Relative fold-induction to control group is plotted on the y-axis as mean ± SEM (n=3) and time point is plotted on the x-axis.

3.3 Comparison of the zebrafish and cavefish *xpc* genes

I next decided to focus on one H_2O_2 induced DNA repair gene, the *xpc* gene given its key role in NER repair. My goal was to try to understand the mechanisms regulating this gene in the various cell lines. No induction of *xpc* mRNA levels was observed under H_2O_2 stress in cavefish. This raised the question as to whether there might be any

mutations affecting the cavefish *xpc* gene in a similar fashion to the loss of function mutations that my group previously described for the cavefish photolyase genes? To explore this question, I firstly analysed the primary structure of cavefish *xpc* gene. Based on the partial coding sequence of *xpc* gene obtained from RNA-seq data, I cloned the full length *xpc* cDNA of the *P. andruzzii* cavefish by RACE PCR. Herein I obtained a full-length cDNA of 3060 bp with 107 bp 5'UTR and 295 bp 3'UTR. Sequence alignment revealed a high degree of amino acid sequence identity (91%) compared to its zebrafish homolog (Fig 3.9) with for example, the predicted nuclear localization signal (NLS) being highly conserved in cavefish compared with zebrafish *xpc*. I failed to detect any premature termination mutations or any evidence of unspliced introns or major genomic rearrangements.

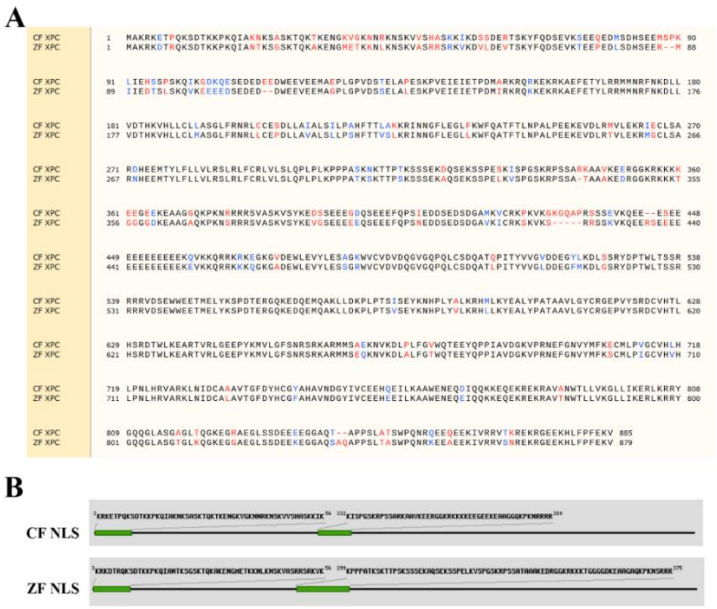

Fig 3.9. Amino acid sequence alignment of the *xpc* gene between zebrafish and cavefish and the nuclear localization signal (NLS) prediction. A. The alignment was performed by Snapgene software and results were presented by colour-coding the amino acid sequences accordingly (identical (black), similar (blue) and not similar (red)). B. The candidate NLS sequences of both *P. andruzzii* and zebrafish *xpc* genes were predicted by using the NLStradamus algorithm (http://www.moseslab.csb.utoronto.ca/NLStradamus/).

3.4 Characterizing the molecular mechanism of ROS-induced *xpc* transcription in vertebrates

3.4.1 Loss of the ROS-induced expression driven by D-box elements in cavefish

Given the lack of evidence for any major changes in the organization of the *xpc* gene between cavefish and zebrafish, I next chose to explore possible major differences between the promoters of the *xpc* genes in these different species as well as in transcriptional control mechanisms. My group had previously demonstrated that the D-box enhancer element seems to play a key role in the regulation of a set of circadian clock and DNA repair genes in response to visible light, UV and ROS in zebrafish [84]. I therefore speculated that other DNA repair genes such as the *xpc* gene may share the same D-box-driven regulation mechanism. Therefore, I amplified a 736 bp putative promoter fragment including the 5'UTR and first exon of the zebrafish *xpc* gene and cloned this into a luciferase reporter vector (zfXPC736bp-Luc). I then transiently transfected zebrafish PAC-2 cells or cavefish EPA cells with this construct and used an *in vivo* bioluminescence assay to monitor expression of this *xpc* promoter reporter construct in real-time immediately following 300 μM H_2O_2 treatment. In PAC-2 cells, H_2O_2 exposure robustly induced bioluminescence levels after 3 h, in contrast, no induction of *xpc* reporter expression was observed in EPA cells (Fig 3.10). This result is consistent with the observed H_2O_2 induced expression time course of endogenous *xpc* mRNA in zebrafish cells and the failure to observe induced *xpc* induction in cavefish cells following H_2O_2 treatment.

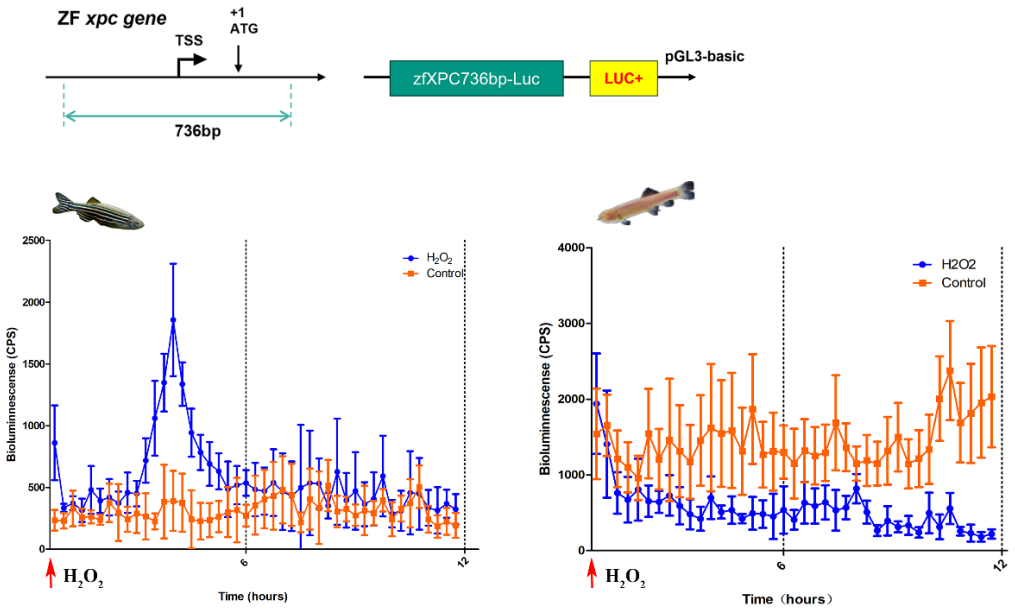

Fig 3.10. Real-time luciferase assay in zebrafish and cavefish cells transfected with zfXPC736bp-Luc reporter vector. Upper panels present the structure of the construct. Transcription starting site (TSS), initial codon (ATG) and luciferase reporter gene (LUC+) are shown. Lower left panel shows the real-time bioluminescence detected in zebrafish PAC-2 cells and lower right panel shows the data in cavefish EPA cells. Blue traces are samples treated with 300 µM H_2O_2 and orange traces are untreated controls. Bioluminescence is expressed as counts per seconds (cps) plotted in y-axes and time points are expressed as hours plotted in x-axes. The data for each time point represents the mean value derived from a minimum of six independently transfected wells, with the standard error of the mean (SEM) indicated.

To pinpoint the essential cis-elements mediating the regulation of ROS-induced expression of *xpc* in this region, I performed a transfection factor binding site prediction analysis by the Genomatix software (Precigen Bioinformatics Germany GmbH, Germany). Within this 736 bp region, I identified a 184 bp fragment containing an activating transcription factor-1/cAMP response element binding protein (ATF-1/CREB) binding site, three D-boxes and one E-box element, which have been previously identified in zebrafish photolyases and *ddb2* promoters as well as in various clock genes [92, 121, 122](Fig 3.11). ATF-1 and CREB belong to the basic leucine

zipper (bZIP) superfamily of transcription factors and are known as prototypical stimulus-inducible transcription factors. The ATF-1/CREB binding site shares a core consensus sequence 'TGACGT', the so-called cAMP responsive element (CRE) and has been demonstrated to participate in light-induced phase shift of the mammalian circadian clock [123, 124]. A D-box with a consensus motif of 'TTAYGTAA' has been identified as a cis-element in the promoter of zebrafish clock genes and DNA repair genes involved in both light and ROS responsiveness [121, 122]. The E-box (CACGTG) plays a central role in the circadian clock regulation in many circadian clock control genes.

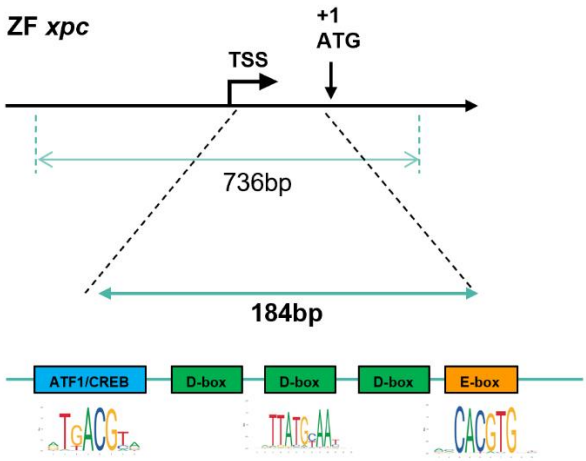

Fig 3.11. Schematic representation of the 184 bp promoter region of the *xpc* promoter region that regulates transcription in response to H_2O_2 stress.

After aligning the sequence of this region from different bony fish species including zebrafish, cavefish, carp, tilapia and rainbow trout, I found it to be highly conserved in fish species. There were only very limited base changes, in particular, changes in the third D-box and the E-box in cavefish sequence compared to zebrafish (Fig 3.12). Next, I cloned a shorter 184 bp fragment of this promoter region which maintained these 5 putative enhancer elements into a luciferase reporter vector (zfXPC184bp-Luc) and tested its regulation of luciferase reporter gene regulation by transient transfection of both PAC-2 and EPA cells and the use of an *in vivo* luciferase assay. My results showed

that this 184 bp region is also sufficient to direct ROS-induced expression in zebrafish cells, but failed to respond to ROS treatment in cavefish cells (Fig 3.13).

Fig 3.12. Alignment of the 184 bp fish *xpc* promoter region. Black boxes represent putative cis-elements identified by Genomatix software. Identical nucleotides among species are highlighted in yellow.

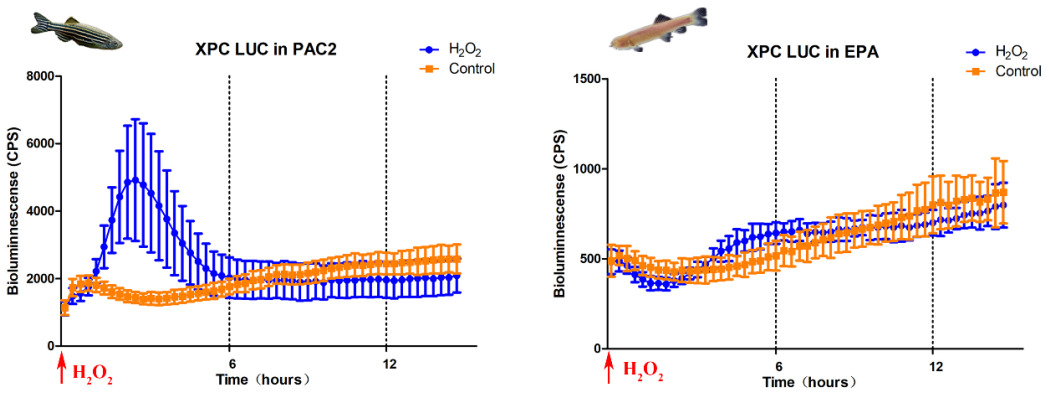

Fig 3.13. Real-time luciferase assay in zebrafish and cavefish cells transfected with zfXPC184bp-Luc reporter vector. Bioluminescence is expressed as counts per seconds (cps) plotted on the y-axes and time points are expressed as hours plotted on the x-axes. The data for each time point represents the mean value derived from a minimum of six independently transfected wells, with the standard error of the mean (SEM) indicated. An arrowhead indicates the moment that H_2O_2 was added to the culture medium.

To explore whether the lack of induction of *xpc* transcription might reflect a reduced sensitivity to ROS levels in cavefish cells, I tested whether the H_2O_2-induced expression of zfXPC184bp-Luc is dose-dependent in transfected PAC-2 and EPA cells by performing an *in vivo* luciferase assay following exposure to different concentrations of H_2O_2. The transfected cells were exposed to a range of H_2O_2 concentrations from 300 to 2000 µM. My results indicate that H_2O_2 -induced expression is dose-dependent in zebrafish but however, in cavefish cells this promoter fails to respond to this full range of H_2O_2 concentrations (Fig 3.14).

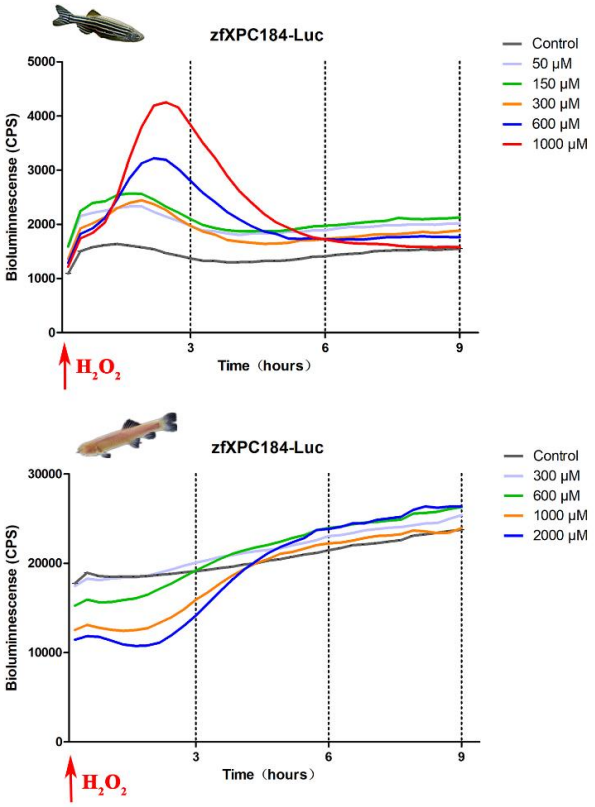

Fig 3.14. ROS-induced expression of zfXPC184bp-Luc is dose-dependent in zebrafish PAC-2 cells (upper panel) but completely absent in cavefish EPA cells (lower panel). Bioluminescence is expressed as counts per seconds (cps) plotted on the y-axes and time points are expressed as hours plotted on the x-axes. The data for each time point represents the mean value derived from a minimum of six independently transfected wells, with the standard error of the mean (SEM) indicated.

Might changes in the cavefish *xpc* promoter contribute to the loss of ROS responsiveness? To answer this question, I also cloned the 184 bp conserved *xpc* promoter region from the cavefish into a reporter vector (cfXPC184bp-Luc) by the Genome-walking technique, and then tested its regulation by H_2O_2 treatment in transfected zebrafish and cavefish cells by real-time bioluminescence assay. The cavefish promoter region is still able to direct ROS-induced expression in zebrafish cells, but not in cavefish cells under H_2O_2 exposure (Fig 3.15). Given that the zebrafish *xpc* promoter is also unable to direct H_2O_2 -induced transcription in cavefish cells, this points to alterations in upstream signaling events rather than changes in the promoter region of the *xpc* gene to be the origin of the absence of ROS inducibility in cavefish.

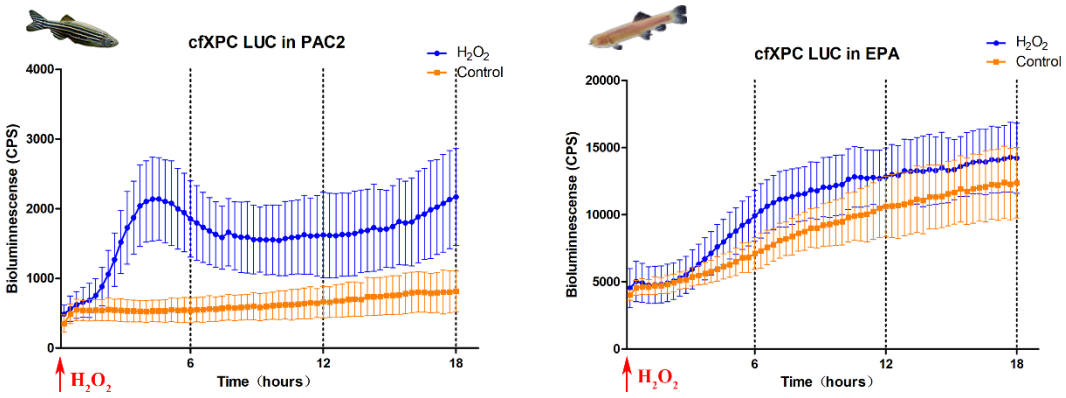

Fig 3.15. Real-time luciferase assay in zebrafish and cavefish cells transfected with cfXPC184bp-Luc reporter vector. Bioluminescence is expressed as counts per seconds (cps) plotted on the y-axes and time points are expressed as hours plotted on the x-axes. The data for each time point represents the mean value derived from a minimum of six independently transfected wells, with the standard error of the mean (SEM) indicated.

To investigate the functional contribution of each element in the *xpc* promoter to ROS responsiveness, I performed a systematic deletion of individual elements in the zebrafish *xpc* promoter within the context of zfXPC184bp-Luc reporter via site-directed mutagenesis. Single deletion of any individual element did not influence the H_2O_2 -

induced expression in PAC-2 cells (Fig 3.16 A-E). However, deletion of all three D-boxes, as well as deletion of any two D-boxes resulted in loss of ROS responsiveness (Fig 3.16 F-L). This reveals that a minimum of two D-boxes is essential for robust ROS-mediated expression in zebrafish. Considering the possibility that the deletion of these individual enhancers might also affect other regulatory elements in this region, I also conducted point mutagenesis of each individual element. Based on their core consensus sequences as well as previously published results [92, 125], I introduced single-base substitutions that would lead to loss or significant reduction of function of the ATF-1/CREB binding site, D-box, and E-box. My results obtained with this point mutation approach closely resemble the results of the deletion tests (Fig 3.17).

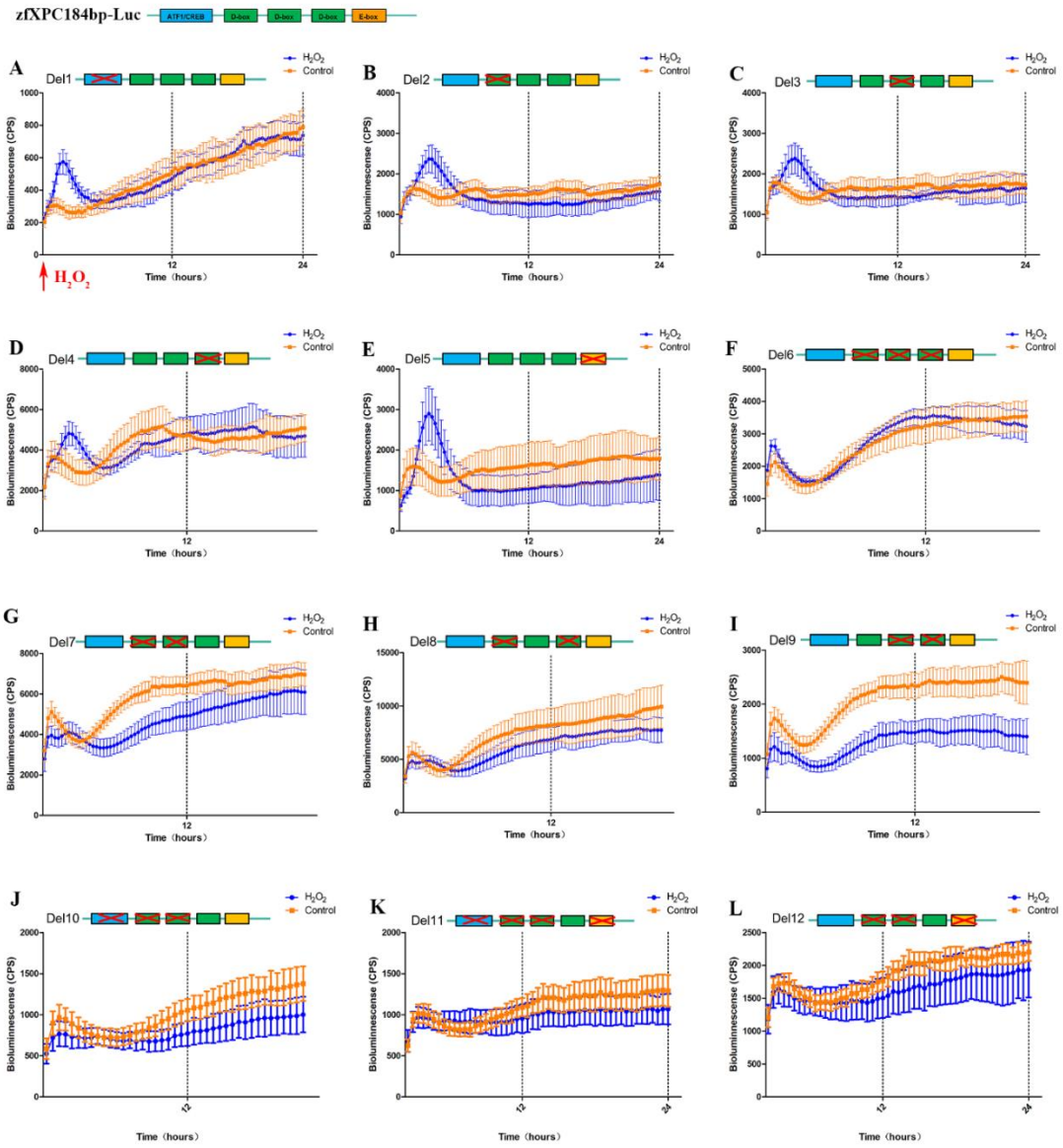

Fig 3.16. Real-time luciferase assays from zebrafish PAC-2 cells transfected with zfXPC184bp-Luc deletion mutants 1-12 (panels A-L, respectively). Cells were exposed to 300 μM H_2O_2 and then kept in darkness for the luciferase assay. In mutants 1-5 (panel A-E), each individual element was deleted by site-directed mutagenesis. In mutants 6 (panel F), all three D-boxes were deleted. In mutants 7-9 (panels G-I), each combination of two D-boxes deletion have been conducted. In mutants 11-12 (panels J-L), only the third D-box was remained with different combination of deletion of other elements. Bioluminescence is expressed as counts per seconds (cps) plotted on the y-axes and time points are expressed as hours plotted on the x-axes. The data for each time point represents the mean value derived from a minimum of six independently transfected wells, with the standard error of the mean (SEM) indicated.

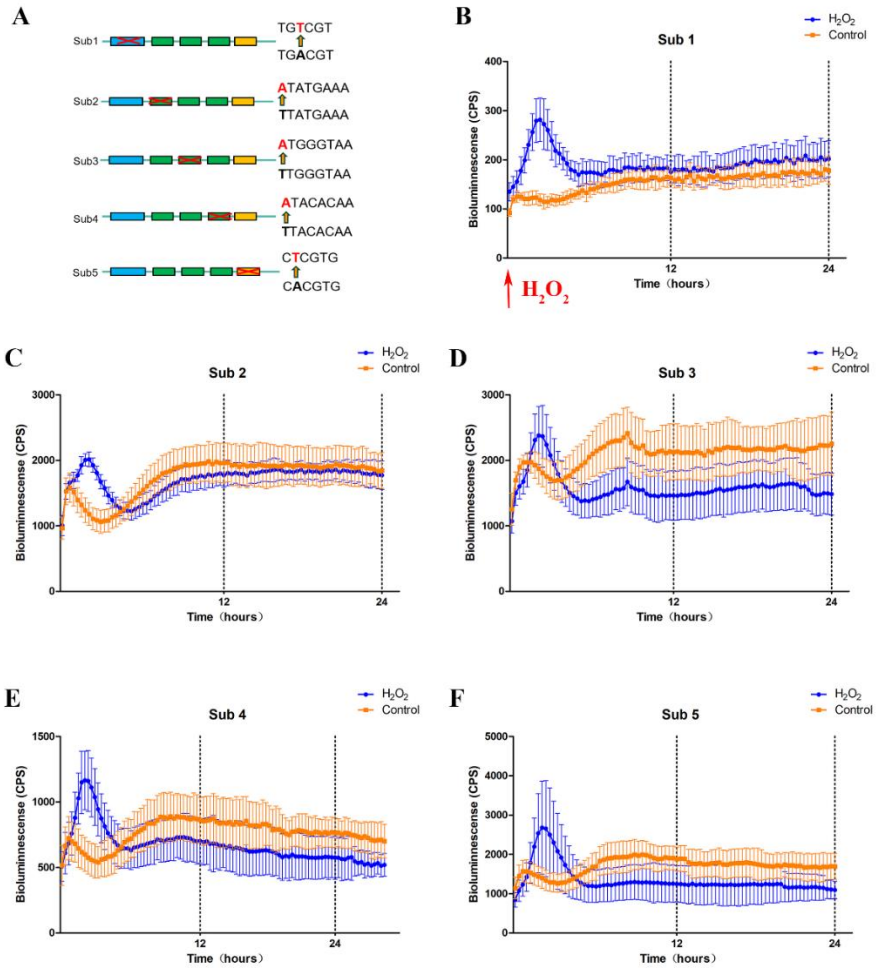

Fig 3.17. Real-time luciferase assays from zebrafish PAC-2 cells transfected with zfXPC184bp-Luc single-base substitution mutants 1-5 (panels B-F, respectively). Panel A is a schematic presentation of the substitution mutations in the case of zfXPC184bp-Luc construct. Bioluminescence is expressed as counts per seconds (cps) plotted on the y-axes and time points are expressed as hours plotted on the x-axes. The data for each time point represents the mean value derived from a minimum of six independently transfected wells, with the standard error of the mean (SEM) indicated.

To further confirm the ROS responsiveness of the D-box elements alone, I subcloned two copies of each D-box element from the zebrafish *xpc* promoter (D-box1, 2 and 3), and in addition, three copies of the third D-box into a minimal promoter-luciferase

reporter pTAL-Luc which contains its own minimal promoter. All heterologous constructs displayed H_2O_2 inducibility (Fig 3.18). Together, my results suggest that a minimum of two copies of any D-box element from the zebrafish *xpc* promoter are necessary and sufficient to confer ROS-induced expression.

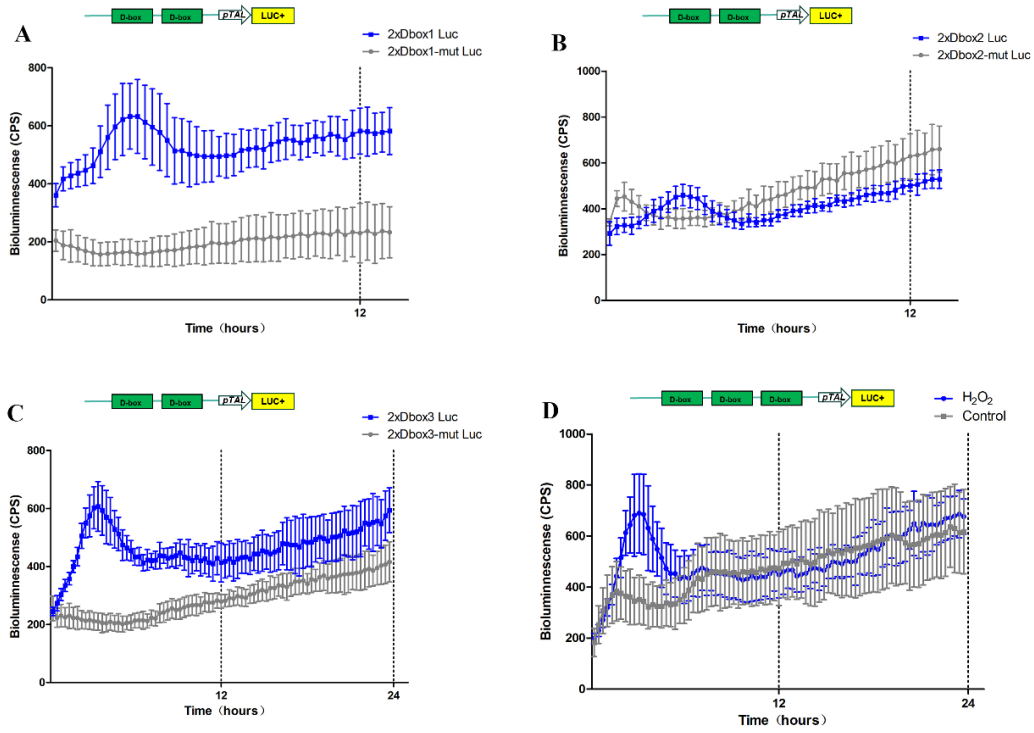

Fig 3.18. Real-time luciferase assays from zebrafish PAC-2 cells transfected with zfXPC-2×D-box-Luc and the single-base mutants. A. 2×D-box1-Luc (blue trace) and the mutant (grey trace); B. 2×D-box2-Luc (blue trace) and the mutant (grey trace); C. 2×D-box3-Luc (blue trace) and the mutant (grey trace); D: 3×D-box3-Luc (blue trace) and the control without H_2O_2 treatment (grey trace). Bioluminescence is expressed as counts per seconds (cps) plotted on the y-axes and time points are expressed as hours plotted on the x-axes. The data for each time point represents the mean value derived from a minimum of six independently transfected wells, with the standard error of the mean (SEM) indicated.

In contrast, I failed to detect any influence of E-box deletion on the H_2O_2-induced

expression of zfXPC184bp-Luc. However, deletion of the ATF-1/CREB binding site resulted in a decreased basal level of bioluminescence expression (see Fig 3.17 B). Therefore, I performed an *in vitro* luciferase assay to explore further the influence of the ATF-1/CREB element in the response to ROS stress by subcloning an additional ATF-1/CREB binding site element into the zfXPC-2×D-box-pGL3-Luc heterologous promoter construct. Consistent with my previous mutagenesis experiments within the context of the *xpc* promoter reporter construct, the presence of the ATF-1/CREB element resulted in significantly higher levels of bioluminescence from the heterologous reporter constructs, indicating the regulatory effect of this element in terms of the basal level of *xpc* expression (Fig 3.19).

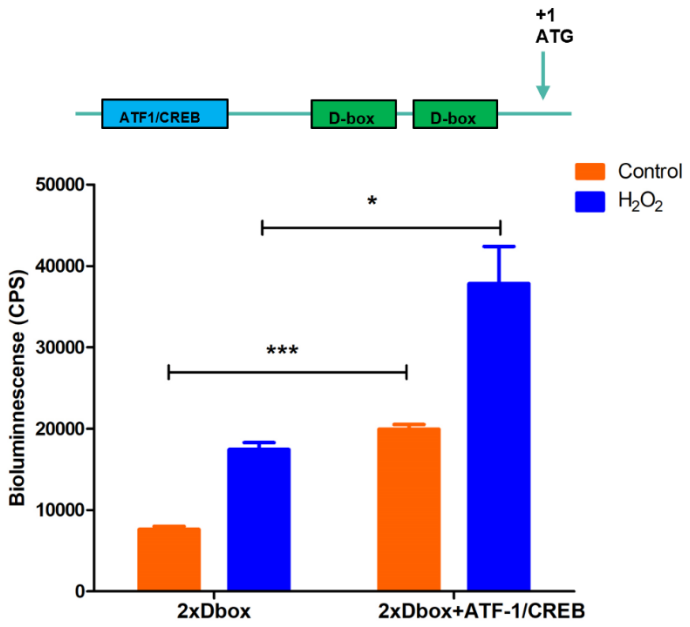

Fig 3.19. In vitro luciferase assay from zebrafish PAC-2 cells transfected with zfXPC-2×D-box-pGL3-Luc with or without an additional upstream ATF1-CREB element. Results are represented as three independent biological replicates ± SEM. Bioluminescence is expressed as counts per seconds (cps) plotted on the y-axes and standardized for transfection efficiency by using β-gal as an internal control.

3.4.2 D-box regulation of ROS-induced *xpc* expression in other vertebrates.

Is the D-box mediated ROS inducibility of DNA repair genes observed in zebrafish cells also conserved in other major vertebrate groups? I addressed this question by initially exploring ROS inducibility in reptilian, amphibian and mouse cell lines. Then, I exposed T1 and 'Speedy' cells to 300 µM H_2O_2 and assayed endogenous mRNA levels of the *xpc* and *ddb2* genes by qPCR. Both turtle and frog cells displayed up-regulation of the *xpc* gene but for *ddb2*, there was no induction in frog cells (Fig 3.20). Combining these results with the *xpc* mRNA expression data from fish and mouse cells, there is a range of transcriptional responses in vertebrate groups under ROS stress.

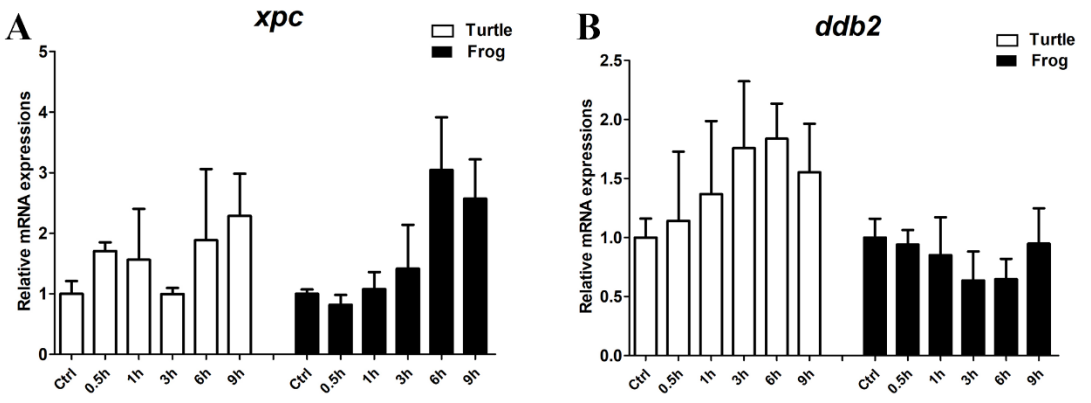

Fig 3.20. mRNA expression of DNA repair genes *xpc* and *ddb2* in Turtle T1 cells and Frog 'speedy' cells. Relative fold-induction to control group is plotted on the y-axis as mean ± SEM (n=3) and time point is plotted on the x-axis.

To explore whether ROS-induced *xpc* expression is also mediated by the D-box in mouse, turtle or frog cells, I transfected the zfXPC-2×D-box-Luc construct into T1, 'Speedy' and 3T3 cells. I also tested the regulation of a reporter construct containing 15 copies of the D-box sequence (5'-AAGTTATACAAC-3') derived from the zebrafish *cry1a* gene promoter which has been used extensively in my lab and displays

a very strong transcriptional response to both light and ROS exposure in zebrafish cells. Neither the expression of the zfXPC-2×D-box-Luc nor the 15×D-box-luc construct were induced by H_2O_2 in mouse, turtle or frog cells (Fig 3.21). Therefore, the D-box regulated ROS inducibility in fish seems not to be conserved in other vertebrate groups and other transcriptional mechanisms may respond to ROS in other vertebrate groups.

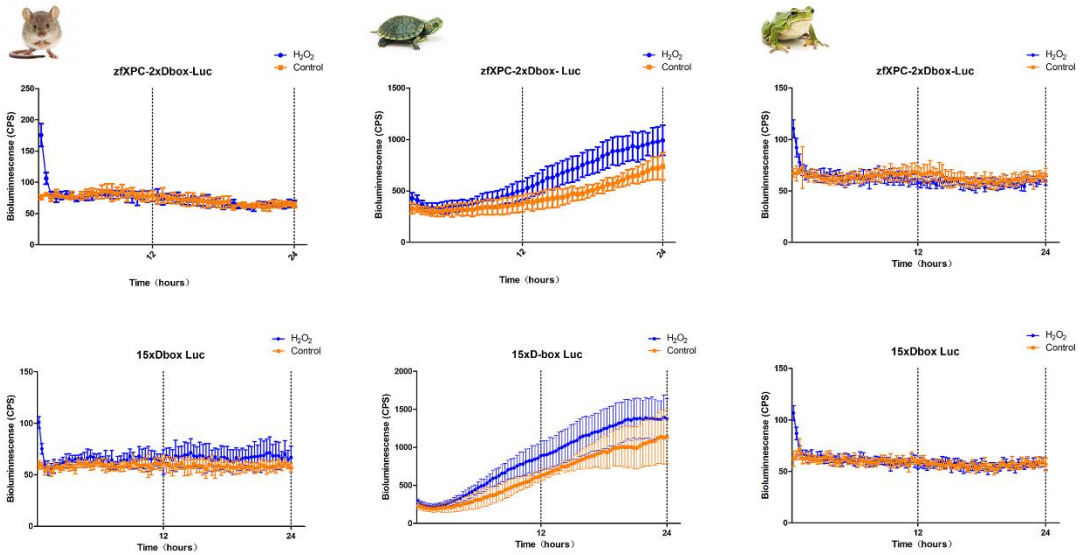

Fig 3.21. Real-time luciferase assays from mouse NIH-3T3 cells (Left panels), turtle T1 cells (middle panels) and frog 'Speedy' cells (right panels) transfected with zfXPC-2×D-box-Luc (upper panels) or 15×D-box-Luc (lower panels). Cells were exposed to 300 μM H_2O_2 and then kept in darkness for the duration of the in vivo luciferase assay. Data at each time point represents the mean value of at least 6 independently transfected wells ± SEM.

3.4.3 Role of PAR factors in D-box-regulated ROS inducibility

My group have previously documented significant complexity in the transcription control mechanisms that target the D-box enhancer. A family of 6 bZip/PAR transcription factors (Thyrotroph Embryonic Factors TEF1/2, Hepatic Leukemia Factors HLF1/2, D-box Binding Proteins DBP1/2) can bind to D-box enhancer elements in different homo and heterodimeric combinations, thereby enhancing

transcriptional activity. How are PAR factors responsible for the D-box enhancer transcriptional activation in response to ROS in DNA repair genes in zebrafish? How does the function of these highly conserved factors differ in other vertebrate groups. The answer to this question might also help understand the loss of D-box-mediated ROS inducibility of DNA repair genes in cavefish and thereby how evolution has shaped this fish conserved mechanism in other vertebrate groups. To initially test the potential contribution of each of the PARbZip factors to D-box regulation of the *xpc* promoter in fish cells, I co-transfected zebrafish PAC-2 or cavefish EPA cells with the zfXPC184bp-Luc reporter vector and an expression vector for each of the 6 PAR factors. The *in vitro* luciferase assay showed that zebrafish TEF1 is the strongest activator of this *xpc* promoter reporter in both zebrafish and cavefish cells (Fig 3.22). In a previous study from my lab, HLF-2 served as the strongest transcriptional activator for the photolyase D-box reporter, while DBP-2 co-expression resulted in the highest level of D-box-mediated expression in clock genes [84]. Therefore, the regulation of D-box elements by PAR factors appears to be very much gene and promoter-dependent.

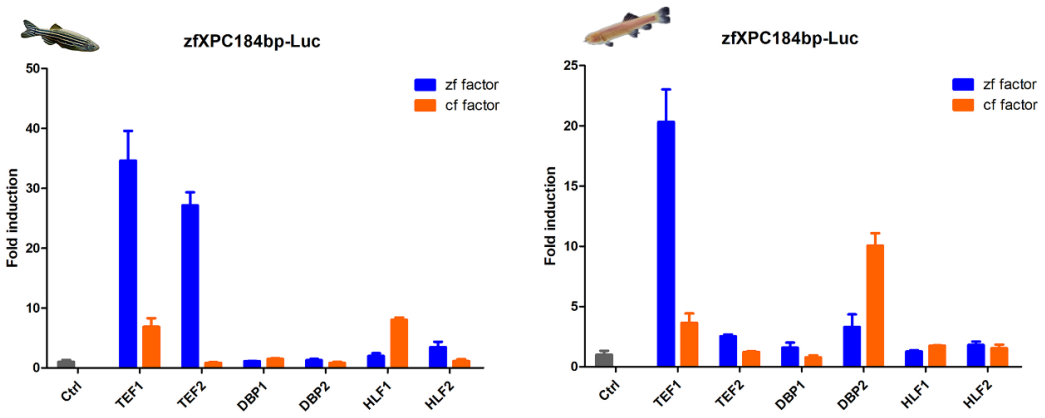

Fig 3.22. In vitro luciferase assay from zebrafish PAC-2 cells (left panel) or cavefish EPA cells (right panel) co-transfected with zfXPC184-Luc reporter vector together with 6 PAR factor expression constructs (1 ng). The expression constructs are indicated below in the x-axis with only the reporter construct alone as a control. Fold induction of relative bioluminescence levels are plotted on the y-axis. Data were standardized for transfection efficiency by using β-gal as an internal control.

A fellow PhD student in my lab, Alessandra Boiti has as part of her project, cloned each of the PAR bZip transcription factors from the cavefish. She has also prepared expression vectors for each of the cavefish factors and allowed me to test these constructs in my own project work. In this analysis I also tested the effect of coexpression of the cavefish factors on the *xpc* promoter reporter construct in both zebrafish and cavefish cell lines. Interestingly, significantly less activation by cavefish TEF1 and TEF2 was observed in both zebrafish and cavefish cells. Is TEF1 the dominant regulator of ROS-induced DNA repair genes expression? Does the attenuated activation of cavefish TEF1 contribute to the loss of ROS inducibility of the *xpc* gene? To address these questions, I initially knocked down the endogenous *tef1* expression by a siRNA method in PAC-2 cells. Knockdown of *tef1* resulted in a significant decrease of both H_2O_2-induced *xpc* and *ddb2* expression, but no reduction in their basal expression levels (Fig 3.23). In an alternative approach, I used a N-terminally truncated zebrafish TEF1 protein which has lost its trans-activation function, so-called dominant-negative TEF1 (dN-TEF1). This has the effect of heterodimerizing with endogenous TEF1 protein and thereby interfering with its transactivation function. In zebrafish PAC-2 cells, ectopic expression of the truncated TEF1 protein abolished the robust H_2O_2-induced expression of artificial *xpc* promoter-derived D-box reporters (Fig 3.24). Therefore, an intact transactivation function of TEF1 is required for D-box activation. Combined with the knockdown result, it is consistent with TEF1 being a crucial transcription factor regulator involving in mediating ROS-induced expression.

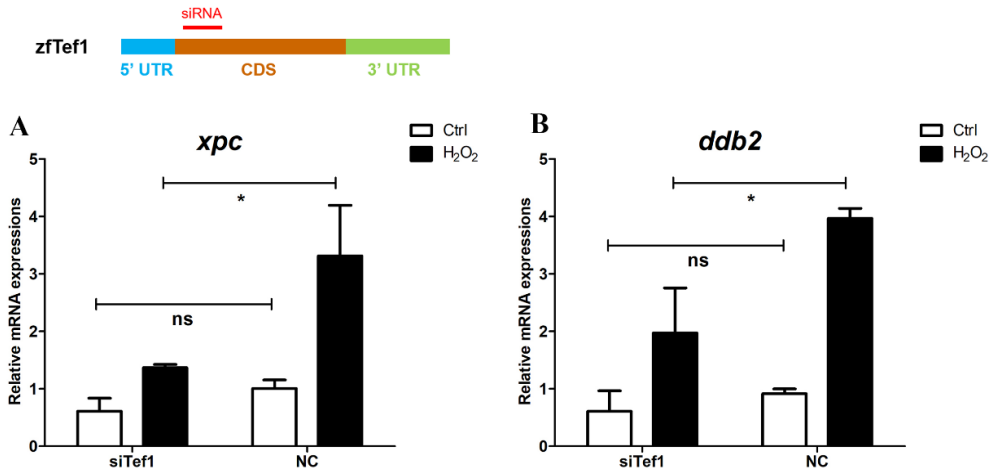

Fig 3.23. mRNA expression of DNA repair genes *xpc* (A) and *ddb2* (B) in *tef1* knockdown zebrafish PAC-2 cells. Results are expressed as mean ± SEM (n=3) and the asterisk above the columns represent significant difference between treatment and control (p <0.05).

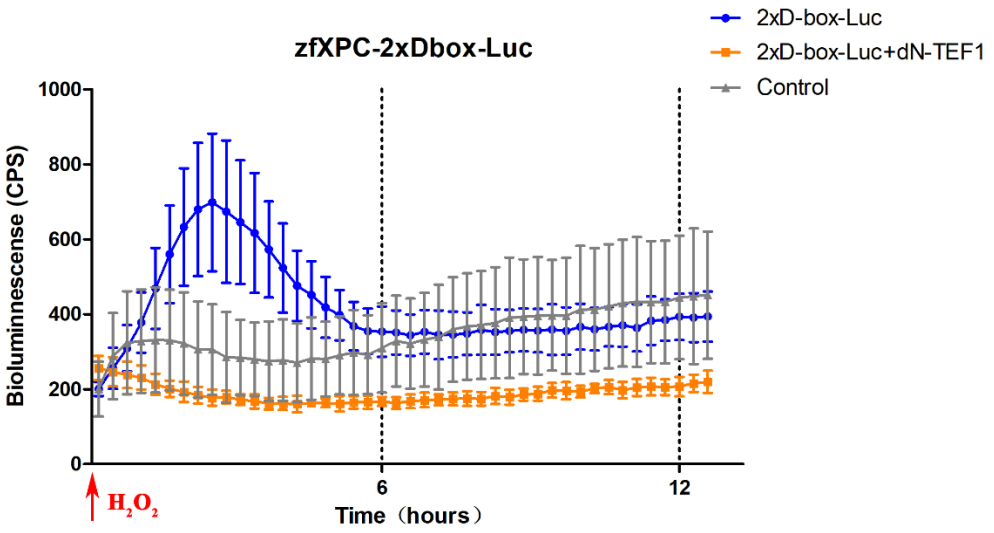

Fig 3.24. Real-time luciferase assays from zebrafish PAC-2 cells transfected with zfXPC-2×D-box-Luc together with or without dN-TEF1 expression vector. Blue and orange traces represent cells treated with 600 μM H_2O_2 and grey traces represent control without H_2O_2 treatment. The data for each time point represents the mean value derived from a minimum of six independently transfected wells, with the standard error of the mean (SEM) indicated

I next wished to understand the mechanism whereby TEF1 is able to respond to ROS and thereby activate transcription via the D-box enhancer. I chose to initially use a comparison of the cavefish and zebrafish TEF1 proteins as a way to pinpoint which domains within the protein might be involved in this ROS sensing function. As a first step I aligned the amino acid sequence of cavefish TEF1 with its zebrafish homolog. The main functional domains which include the PAR domain, DNA binding domain and Leucine zipper domain, are highly conserved between the two fish species. Meanwhile, divergent amino acid sequences were found in the N-terminal region which includes the trans-activation region which was identified in a previous study (Fig 3.25) [47]. In order to identify which region of the cavefish TEF1 protein might account for the reduced transcriptional activation function that I measured in my previous co-transfection assays, I next prepared a hybrid TEF1 protein in the context of pCS2-MTK expression vector which consisted of the N-terminal region of cavefish TEF1 but fused to the C-terminal region of the zebrafish TEF1 protein. This hybrid TEF1 construct (hyTEF1-pCS2-MTK) was co-transfected with either the zebrafish zfXPC184bp-Luc or the cavefish cfXPC184bp-Luc *xpc* promoter reporters into cavefish EPA cells. Like the cavefish TEF1 protein results, the hybrid protein resulted in attenuated *xpc* reporter expression (Fig 3.26). Therefore, the significant differences in amino acid sequence in the N-terminal region, rather than the small number of amino acid sequence differences in the C-terminal region of the cavefish TEF1 protein seem to be the key contributors to the attenuated basal levels of *xpc* activation relative to its zebrafish counterpart.

→ PAR domain
→ Basic domain
→ Leucine zipper
→ NLS

82.1% identity in 301 residues overlap; Score: 1261.0; Gap frequency: 1.0%

```
zfTEF1          3 PISITMDAGAET-SAAFPVVLKKIMETPPPNLLEGDDENDKEKLFESVESGGVSEMGPSA
cfTEF1          5 PVSVTMDAGSDIPSPAFPVVLKKIMEILPPNLLEGDDENDKEKLFEDVDTGGVTEIGPSA
                  * * *****    * ***********  ****************** *  *** * ****

zfTEF1         62 ALTPAIWEKTIPYDGDTFHLEYMDLEEFLMENGIAAAENE--QKSSEKENIQLTAEEPST
cfTEF1         65 ALTPAIWEKTIPYDGETFHLEYMDLEEFLMENGIPATEDEDQQKSLAKESLQLPTEKPSA
                  *************** ****************** * * *  ***  **  **  * **

zfTEF1        120 ASAVKTAPAVTLLPVMALDPCEEEVVTIITTSSSSSADNKSEENRMTPDPINPDEIEVDVN
cfTEF1        125 TSTSKTALAISLMPVMELDQCEEEVVTIITASSPSLTDTKSDEARVTPDPIDPDEIEVEIN
                   *  *** *  * *** ** ********* ** *  * ** * * ***** ******  *

zfTEF1        180 FEPDPTDLVLSSIPGGELFDPRKHRFSEEELKPQPMIKKAKKVFVPEDQKDDKYWQRRKK
cfTEF1        185 FEPDPTDLVLSSIPGGELFNPRKHRFSEEELKPQPMIKKAKKVFVPEEQKDDKYWQRRKK
                  ****************** ************************** ************

zfTEF1        240 NNVAAKRSRDARRLKENQITVRAAFLERENSALRQEVAELRKDFGRCKNTVARYEAKYGA
cfTEF1        245 NNIAAKRSRDARRLKENQITVRAAFLERENSALRQEVAELRKDFGRCKNVVARYETKYGP
                  ** ********************************************* ***** ***

zfTEF1        300 L
cfTEF1        305 L
                  *
```

Fig 3.25. Alignment of zebrafish and cavefish TEF1 amino acid sequences. Identical amino acids between zebrafish and cavefish are presented with an asterisk (*) below. The predicted functional domains are highlighted as light blue (PAR domain), green (basic domain) and red (leucine zipper). A putative nuclear location signal (NLS) sequence is indicated by underlining

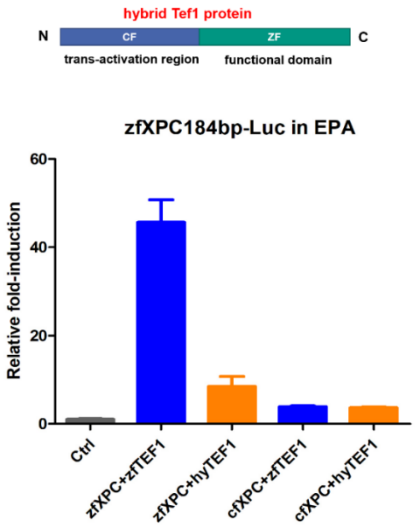

Fig 3.26. In vitro luciferase assay from cavefish EPA cells co-transfected with zfXPC184-Luc or cfXPC184-Luc reporter vector together with the zfTEF1 or hyTEF1 expression construct (1 ng). Fold induction of relative bioluminescence levels are plotted on the y-axis. Data were standardized for transfection efficiency by using β-gal as an internal control.

As a next step, I explored the links between ROS and the activation effects of both zebrafish and cavefish TEF1 proteins on the *xpc* reporter by treating cells with H_2O_2 or alternatively co-transfection with my catalase expression vector. By overexpressing catalase, the effect should be to enzymatically convert endogenous H_2O_2 to H_2O and thereby to reduce ROS levels. Interestingly, H_2O_2 treatment did not lead to stronger activation of zebrafish PAR factors (Fig 3.27). In contrast, removal of endogenous H_2O_2 by catalase overexpression drastically inhibited the activation of all zebrafish and cavefish PAR factors, particularly TEF1 and TEF2 in zebrafish cells. In addition, there were mild inhibitory effects, or even enhancement of the activation by some factors (for example, the zfTef2, cfTef2 and cfDDB1) in cavefish cells (Fig 3.28). These results point to a potent role for ROS levels in determining the transcriptional activation function of the TEF protein as well as other members of the bZip PAR transcription factor family.

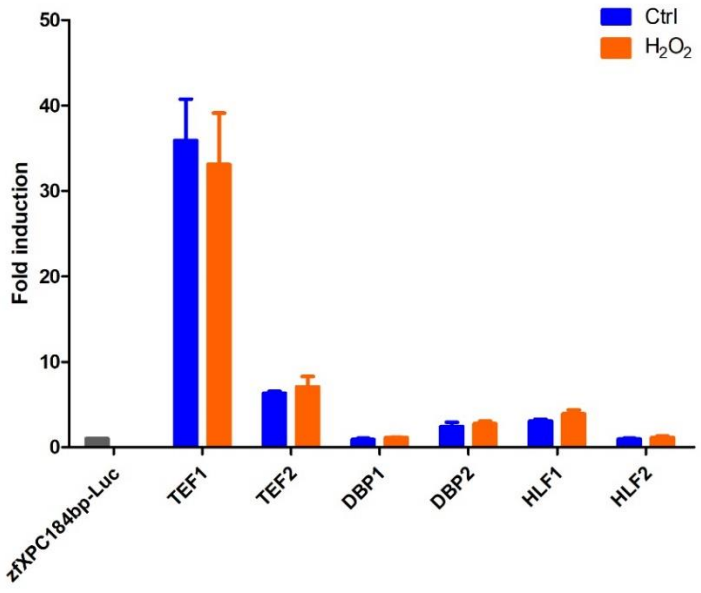

Fig 3.27. Effects of H_2O_2 treatment upon on activation of zfXPC184bp-Luc by PAR factors in zebrafish. PAC-2 cells were co-transfected with the zfXPC184bp-Luc together with a PAR factor expression vector (1 ng). Fold induction of relative bioluminescence levels are plotted on the y-axis. Data were standardized for transfection efficiency by using β-gal as an internal control.

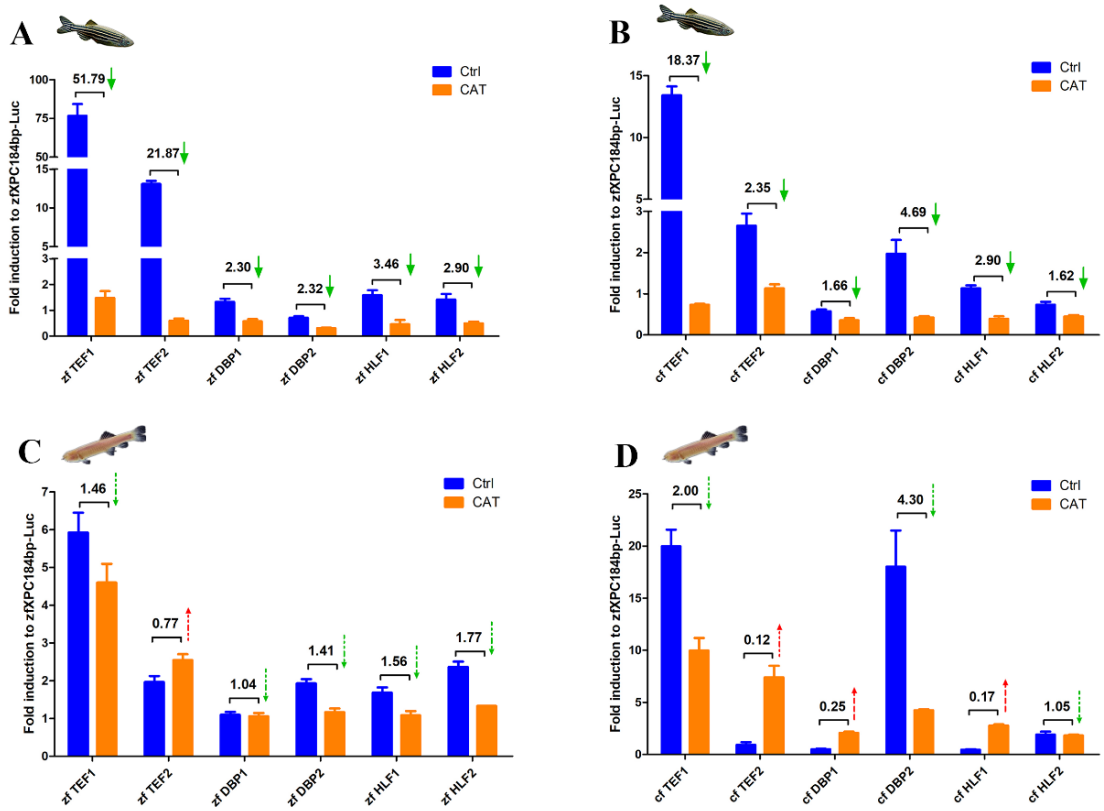

Fig 3.28. Effects of H_2O_2 reduction upon on activation of zfXPC184bp-Luc by PAR factors in zebrafish (A and B) and cavefish cells (C and D). Green arrows indicate down regulation by zfCAT co-expression and red arrows indicate upregulation. Numbers above the column represent fold change compared to controls.

3.4.4 Identification of MAPK phosphorylation targets in fish TEF1

The mitogen-activated protein kinase (MAPK) is reported to serve as a crucial player in signal transduction of cellular stress stimuli including elevated levels of ROS. Studies have demonstrated that direct exposure to ROS or various cellular stimuli that induce ROS production can activate MAPK pathways in multiple cell types [36]. Thereby, particular biological responses are directed by downstream signals that are regulated by MAPKs, such as proliferation and cell cycle arrest, etc [126]. Transcriptional regulation by the MAPK signaling cascade has been well documented in eukaryotic cells with

MAPKs directly control gene expression by phosphorylating transcription factors [127].

A previous study from my group has revealed that H_2O_2 exposure activates p38 and JNK phosphorylation rapidly in zebrafish cells and thereby regulates ROS-induced expression of clock and photolyase genes [93]. Similar activated MAPK signaling cascades in cavefish cells were observed upon H_2O_2 stimulation, indicating an intact input of MAPK signaling in the cavefish but loss of function mutations affecting elements which lie between MAPK targets and their downstream effectors. To test the role of MAPK regulation in *xpc* transcription and its connection with PAR factors, I co-transfected either the zfXPC184bp-Luc or cfXPC184bp-Luc reporter together with the zebrafish/cavefish TEF1 expression vectors with or without dominant-negative p38 (dN-p38), dominant-negative JNK (dN-JNK) or dominant-negative ERK (dN-ERK) expression vectors which encode dominant-negative forms of human p38, JNK and ERK proteins respectively [128]. Trans-activation of the zebrafish *xpc* reporter by zfTEF1 was strongly inhibited upon coexpression of all three dominant forms of MAPKs. Comparable results were obtained in EPA cells with the dominant negative MAPKs attenuating the activation of cfXPC184-Luc by cfTEF1, however, to a lower extent (Fig 3.29). Therefore, the activation of D-box-mediated transcriptional regulation by TEF1 appears to involve MAPK signaling in both zebrafish and cavefish cells.

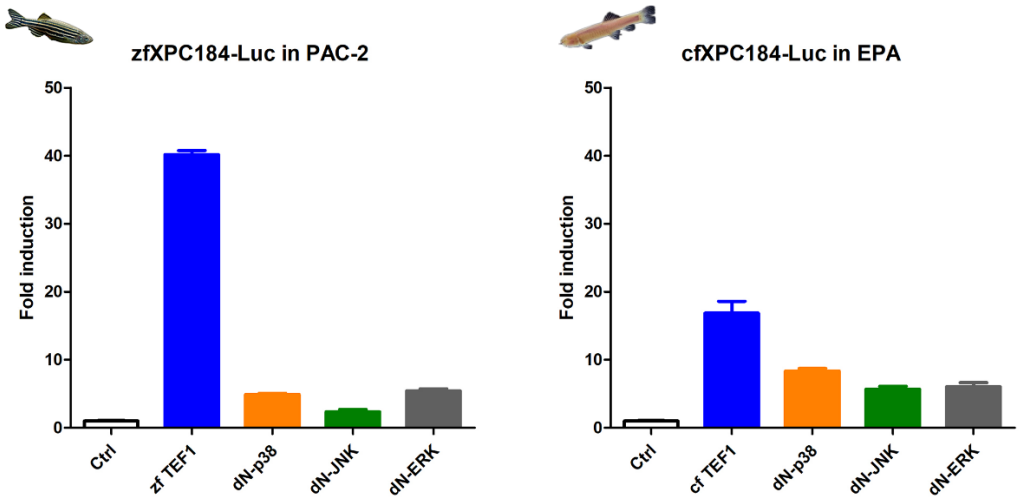

Fig 3.29. In vitro luciferase assay of xpc reporter expression in zebrafish PAC-2 and cavefish EPA cells. PAC-2 cells were co-transfected with zfXPC184-Luc together with zfTEF1 expression construct (1 ng) and also dominant negative p38 (dN-p38), dominant negative JNK (dN-JNK) or dominant negative ERK (dN-ERK) expression vectors (Left panel). EPA cells were co-transfected with cfXPC184-Luc together with cfTEF1 expression construct (1 ng) and also the same dominant negative vectors (right panel). Fold induction of relative bioluminescence levels are plotted on the y-axis. Data were standardized for transfection efficiency by using β-gal as an internal control.

So far, numerous transcription factors including the bZip superfamilies have been identified as targets of different MAPK cascades by direct phosphorylation [127, 129]. However, the PAR bZip factors have only been reported to serve as clock-controlled proteins involved in detoxification and drug metabolism in mammalian cells [130, 131]. Are the PAR factors such as TEF1 regulated by MAPKs via phosphorylation? To this end, I initially identified several putative MAPK phosphorylation sites in the zebrafish TEF1 protein with the aid of GPS 5.0 software. Four top scoring sites were listed as Thr 28 (28T), Thr 64 (64T), Thr 113 (113T) and Thr 119 (119T) in the N-terminal region (Fig 3.30). Interestingly, there are two Thr-Pro sites discovered among them (the Thr28-Pro29 and Thr64-Pro65) which has been demonstrated to serve as the minimal phosphoaccepter motif of MAPKs targets [127, 132, 133]. By aligning the zebrafish TEF1 protein with the cavefish and mouse homologs, these four sites were not conserved except for the 64T position which is only conserved between zebrafish and cavefish TEF1.

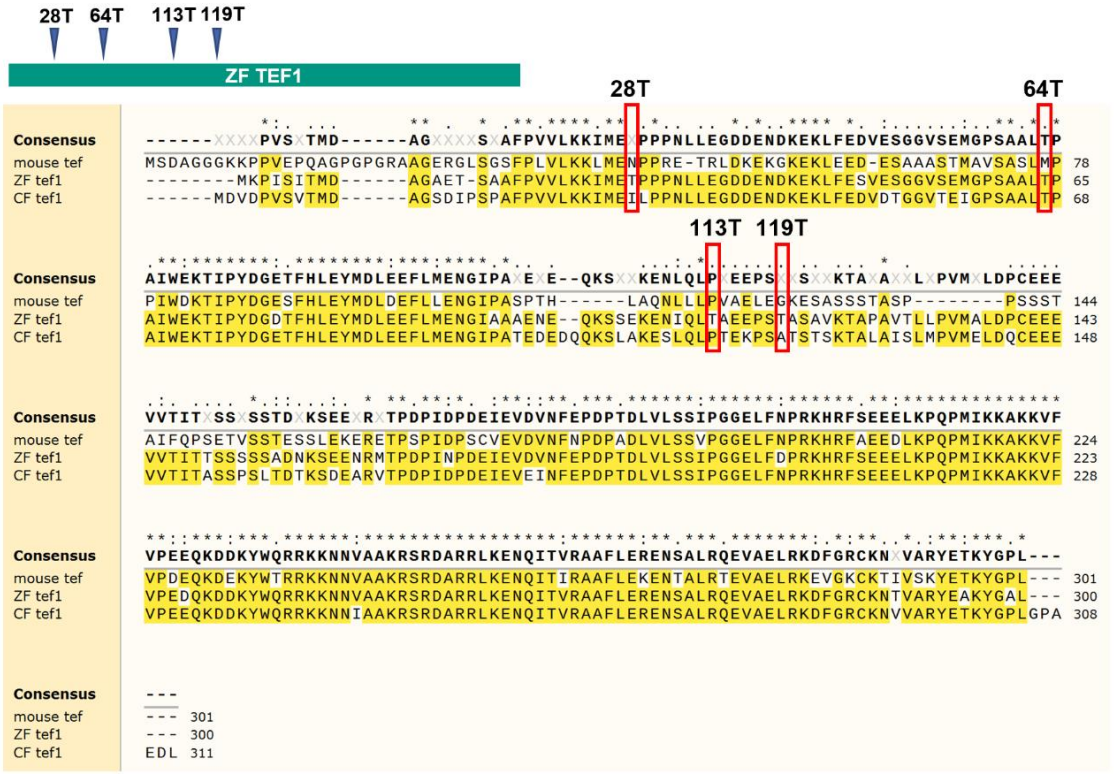

Fig 3.30. Putative MAPK phosphorylation sites of zebrafish TEF1 proteins and amino acid sequence alignment with cavefish and mouse homologs.

To test the functionality of these predicted phosphorylation sites, I prepared several zebrafish TEF1 protein mutants by site-directed mutagenesis. To mimic the non-phosphorylation status, I introduced Thr to Ala mutations at each site. The transcriptional activation function of these mutated TEF1 proteins for the *xpc* promoter reporter construct was then tested by co-transfection in zebrafish PAC-2 cells followed by an *in vitro* luciferase assay. The results showed that all four TEF1 mutants resulted in significant reduction of TEF1-induced activation of the *xpc* reporter (Fig 3.31 A). This indicates that these amino acids might serve as key regulatory sites and together are involved in trans-activation function of the zebrafish TEF1 protein in a ROS-dependent manner. Considering the conservation of Thr64-Pro65 in the cavefish TEF1 protein, I speculate that this site may contribute to the low level of transactivation at the D-box and attenuated ROS responsiveness in cavefish. To further test the importance of these putative phosphorylation sites, I also generated cavefish TEF1 mutant proteins

by converting the Ile31 and Ile31-Leu32 to Thr31 and Thr31-Pro32, respectively. These mutations mimic a normal MAPK phosphorylation motif such as that at Thr28-Pro29 in zebrafish TEF1. Co-transfection assays using these cfTEF1 mutants revealed that both displayed a significant increase of activation of the *xpc* reporter in EPA cells. In addition, upon co-transfecting the catalase expression vector with these various mutant cavefish TEF1 protein expression vectors, I revealed that their activation effects were strongly reduced and so indicating that these mutant proteins are strongly regulated by ROS levels (Fig 3.31 B). Therefore, I conclude that the 28T, 64T, 113A and 119A are potentially important MAPK phosphorylation sites for the regulation of D-box mediated transcription in response to ROS levels in zebrafish. Therefore, the mutation of these sites in cavefish has led to attenuated TEF1 mediated activation in response to ROS and consequently globally influenced target gene expression such as that of *xpc*.

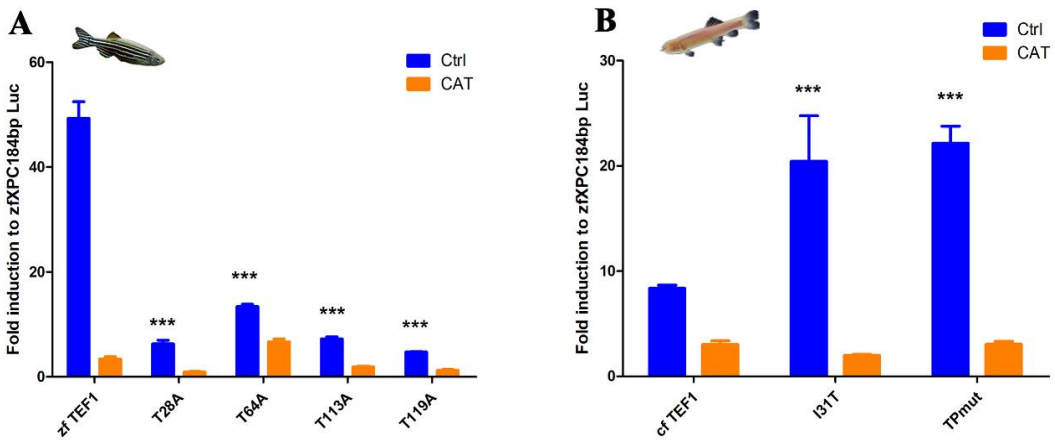

Fig 3.31. In vitro luciferase assay from zebrafish PAC-2 cells (A) or cavefish EPA cells (B) co-transfected with zfXPC184-Luc reporter vector together with different zfTEF1 or cfTEF1 mutant expression constructs (1 ng). Asterisks represent significant difference between wildtype TEF1 (cfTEF1 or zf TEF1) and the mutant (*p <0.05, **p<0.01, *** p<0.001).

3.4.5 Effects of ROS on nuclear translocation of fish TEF1 protein

I next wished to explore precisely how TEF1 protein function might be regulated in

response to MAPK phosphorylation following ROS exposure. One property that has been shown for other transcription factors that are regulated by ROS is regulation of their subcellular localization. Therefore, I initially performed an immunofluorescence staining assay with Myc-tagged zebrafish and cavefish TEF1 proteins following transient transfection into either zebrafish or cavefish cells. To test for any effects of cellular ROS on TEF1 subcellular localization, I treated both cell lines with 300 μM H_2O_2 for 3 hours. In order to test the effects of reducing ROS levels in transfected cells, I co-transfected the Tef1 expression vector together with an expression vector for the zebrafish catalase enzyme to convert endogenous H_2O_2 to H_2O. Both zebrafish and cavefish TEF1 proteins were predominantly localized to the nucleus and addition of H_2O_2 did not influence its subcellular localization. However, catalase co-transfection significantly decreased the nucleic localization in zebrafish cells but not in cavefish cells (Fig 3.32). My results indicate that intracellular ROS levels have a significant effect on TEF1 nuclear localization in zebrafish.

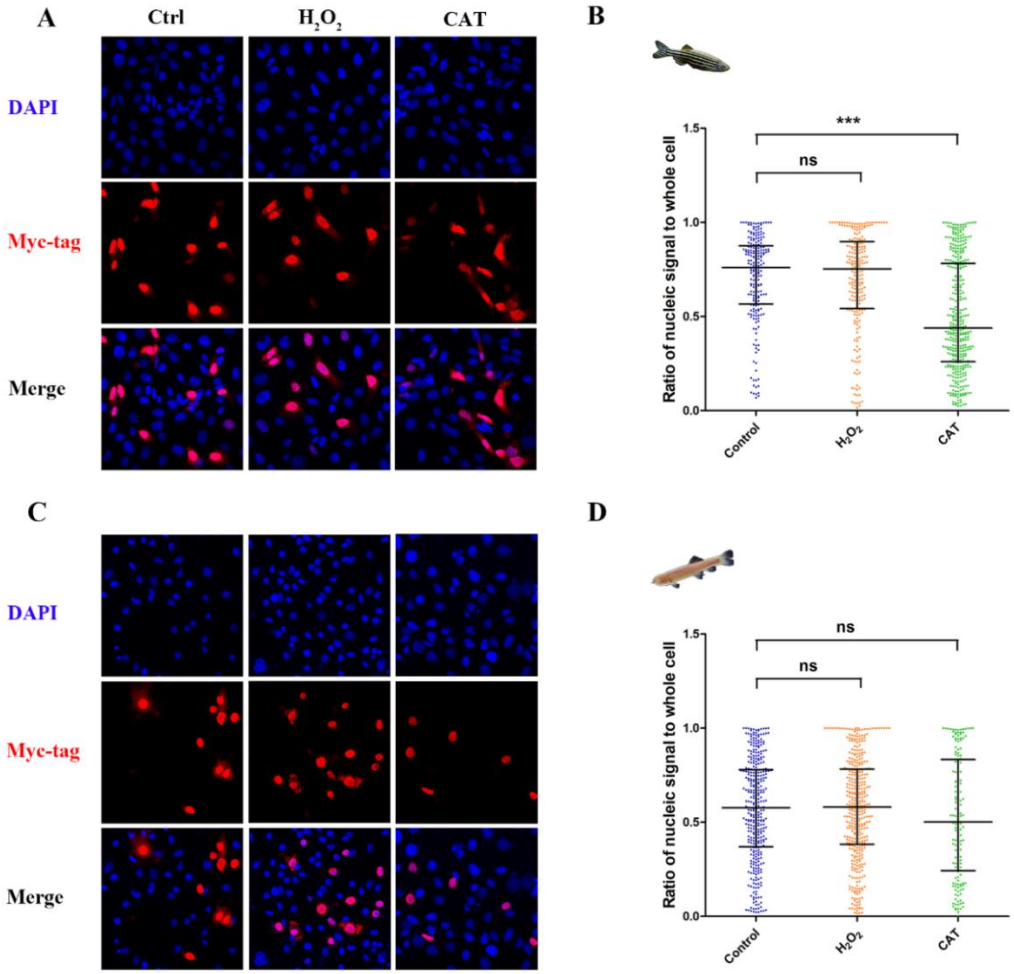

Fig 3.32. Subcellular localization of fish TEF1 proteins. Myc-tagged zebrafish or cavefish TEF1 proteins were transiently transfected into zebrafish PAC-2 and cavefish EPA cells, respectively. For the H_2O_2 group, cells were treated with 300 μM H_2O_2 3 hours before sampling. For H_2O_2 clearance, cells were cotransfected with the zebrafish catalase expression vector as well as the TEF1 expression vector. The localization of TEF1 proteins was visualized by immunofluorescence staining and imaged by Confocal Microscopy. Upper panels are representative images of zebrafish TEF1 protein in PAC-2 cells (A) and the quantitative analysis by the CellProfiler software (B). Lower panels (C and D) are for cavefish cells. At least 150 cells were individually analyzed for the ratio of Myc-tag fluorescence signal in nucleus to the signals in the whole cell. Data was illustrated as scatter plot with median value (central line) and interquartile (upper or lower lines). A Student's t-test (Unpaired, two-tailed) was adopted for the comparison of each groups (*p <0.05, **p<0.01, *** p<0.001 and ns: no significant difference).

3.4.6 Role of TEF in ROS-induced expression in mouse

Is the regulatory effect of TEF on D-box-mediated gene expression in fish also conserved in mammals? In this study, I found that the D-box enhancer is no longer directly responsive to ROS in 3T3 cells by *in vivo* luciferase assay (see Fig 3.21). As a next step I co-transfected 3T3 cells with the zebrafish TEF1 or TEF2 expression vectors together with zfXPC-2×D-box-Luc reporter. As shown in Fig 3.33, ectopic expression of zebrafish TEF1 protein but not TEF2 activates the D-box reporter expression in 3T3 cells and makes it ROS responsive, with an induction of reporter expression by 6 h exposure to H_2O_2 and a reduction of reporter expression upon co-expression with catalase. This indicates that in mouse cells, the upstream signaling elements targeting TEF-regulated D-box-driven transcription are well conserved. Then, how have mammalian cells lost the D-box-mediated ROS inducibility? To tackle this question, I cloned the mouse TEF protein into the pCS2-MTK expression vector and then tested its functionality in co-transfection assays. The mTEF protein displayed a similar regulatory effect compared with zebrafish TEF1 when transfected in zebrafish PAC-2 cells, namely it successfully activated the 15×Dbox-Luc reporter in zebrafish cells in a ROS-dependent manner (Fig 3.34). However, in mouse cells, although mTEF was also able to activate the 15×D-box Luc reporter and be negatively regulated by co-expression with dominant negative forms of p38 and JNK, H_2O_2 treatment did not further increase its transcriptional activation of the *xpc* promoter reporter construct expression and also, catalase co-expression did not inhibit the mTEF activation. Therefore, regulation of D-box-regulated expression by TEF is still conserved in mouse cells with an intact up-stream signaling. However, it has become ROS-independent during evolution from fish to mammals.

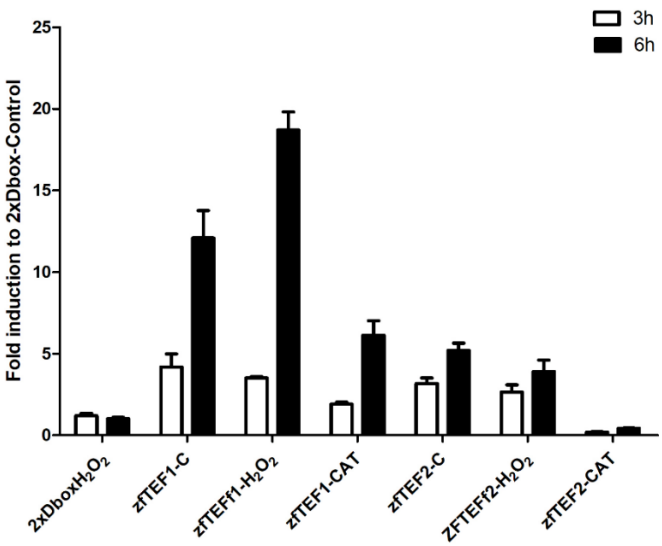

Fig 3.33. *In vitro* luciferase assay from mouse NIH-3T3 cells co-transfected with zfXPC-2×Dbox-Luc reporter vector together with zfTEF1 or zfTEF2 expression constructs (1 ng). For H_2O_2 treatment, transfected Cells were exposed to 300 µM H_2O_2 and sampled after 3 h or 6 h exposure respectively. For H_2O_2 clearance, cells were co-transfected with 100 ng of zfCAT expression vector. Fold induction of relative bioluminescence levels are plotted on the y-axis. Data were standardized for transfection efficiency by using β-gal as an internal control.

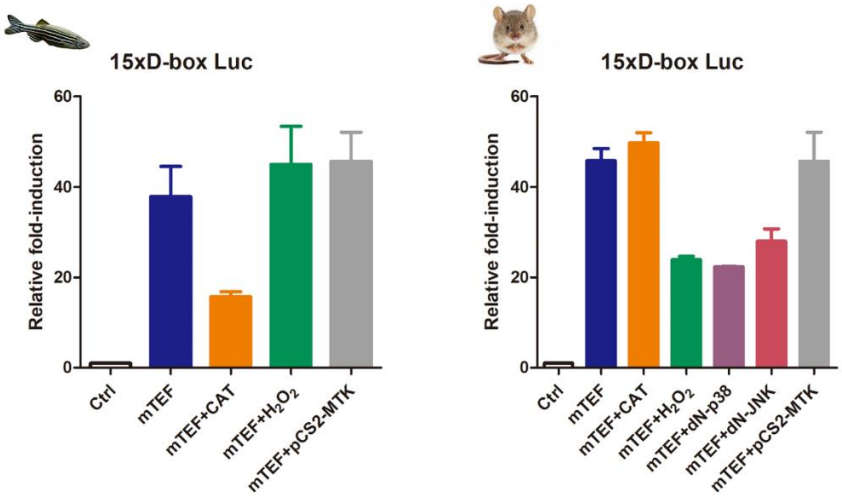

Fig 3.34. In vitro luciferase assay from zebrafish PAC-2 cells (left panel) and mouse NIH-3T3 cells (right panel) co-transfected with 15×D-box-Luc reporter vector together with zfTEF1 or mTEF expression constructs (1 ng). Fold induction of relative bioluminescence levels are plotted on the y-axis. Data were standardized for transfection efficiency by using β-gal as an internal control.

4 Discussion

In this project, I have explored the transcriptional response to ROS in vertebrates and how it has changed over the course of evolution, by using a combination of different cell culture models. My transcriptome analysis revealed a variety of differences in gene expression in response to sublethal doses of H_2O_2 in mouse, zebrafish and cavefish cells. In particular, the group of DNA repair genes exhibits a distinct ROS-induced expression pattern among cell lines derived from the three species. I then reveal that in the zebrafish, the ROS responsiveness of transcription of a key DNA repair gene, *xpc* is driven by the D-box enhancer element. However, the D-box fails to mediate ROS induced transcription of gene expression in other vertebrate cell lines derived from mouse, turtle and frog. Importantly, D-box / ROS regulated transcription is also absent in the Somalian cavefish, *Phreatichthys andruzzii*. Functional analysis of the D-box binding transcription factor, TEF1 reveals that it plays a key role in directing ROS induced transcription in fish cells, and that conserved MAPK phosphorylation target sites in the N-terminal portion of the protein seem to be vital for regulating activation. Amino acid sequence changes in this portion of the cavefish TEF1 protein result in the loss of several of these MAPK phosphorylation sites and thereby confer reduced ROS-induced activation by TEF1 in this species. Furthermore, I present evidence that changes in the subcellular localization of TEF1 are linked with ROS exposure and may contribute to the regulation of this transcription factor.

4.1 ROS as a ‘two-edge sword’ in cell physiology

ROS play a complex role in cell physiology, resembling a 'two-edged sword'. ROS are generated within cells as natural byproducts of various metabolic processes, such as mitochondrial respiration. ROS serves as a major damage source to macromolecules and the excessive accumulation of ROS can lead to oxidative stress and contribute to the development of various diseases [4]. Meanwhile, they are also found to serve as

essential signaling molecules involved in numerous cellular functions, including cell proliferation, immune response, and gene expression regulation [24].

Among all ROS molecules, H_2O_2 is relatively stable and its selective reactivity and diffusibility make it better suited for signaling [1]. Therefore, studies on ROS signaling are predominantly based on H_2O_2. The toxic effects of H_2O_2 have been reported in various species. In zebrafish larvae, 100 mM H_2O_2 exposure for 10 min induces DNA damage and DNA repair gene up-regulation within 6 h [134]. DNA damage was also observed in human peripheral blood lymphocytes upon 200 μM H_2O_2 exposure *in vitro* [135]. Concentrations of H_2O_2 tested in cytotoxic experiments range from 10 μM to over 1000 μM. In mammalian cell lines, a certain pattern of reponse has been demonstrated with growth stimulation at 3-15 μM, permanent growth arrest at intermediate concentrations (250-400 μM) and necrotic cell death at concentrations higher than 1 mM [136]. Furthermore, numerous toxicological studies revealed that xenobiotics such as heavy metals [137], toxins [138] and pesticides [139] induce cytotoxicity and are all linked with elevated intracellular ROS levels.

In this study, I compared H_2O_2 toxicity in different vertebrate cell lines. The results indicate lower H_2O_2 tolerance in frog, turtle and mouse cells compared with two fish lines. Interestingly, oxygen levels are higher on land than in aquatic environments and terrestrial animals experience higher levels of ROS stress due to the development of more efficient aerobic respiration. A recent study demonstrated the molecular evolution of Keap1 protein in vertebrates, may have represented a key step in the adaption to terrestrial life [114]. However, with the important proviso that I examined a small number of cell lines, my results would be consistent with reduced tolerance to ROS in terrestrial animal-derived cell lines compared to fish. Considering the frequent fluctuations in oxygen levels in aquatic habitats, aquatic organisms, such as fish, may have developed a broad range of adaptations to withstand conditions of both low oxygen (hypoxia) and high oxygen (hyperoxia) [140]. This may partially explain why fish cells are able to accomodate higher ROS levels than cells derived from the other major vertebrate groups.

ROS at physiological levels also serve as molecular signals participating in many biological processes, such as cell proliferation, differentiation, gene expression regulation and programmed cell death. For example, ROS has been reported to be essential for tissue regeneration in zebrafish. A study from Han *et al* showed that H_2O_2 generated from Duox/Nox2 promotes heart regeneration in zebrafish through Dusp6 depression [141]. In addition, ROS play pivotal roles in the wound-healing process, for instance, during skin injury and repair [142] as well as in the tails of amphibian tadpoles of *Xenopus laevis* and *Xenopus tropicalis* following amputation [143]. The injury-induced ROS sustained production is essential for complete tail regeneration as well as other well documented types of tissue regeneration in various species. For instance, the Apoptosis signal-regulating kinase 1 (Ask1) acts as an intracellular sensor for elevated ROS levels in injured wing imaginal discs of *Drosophila* and activates the p38 and JNK signaling pathways for regeneration [144]. Sustained ROS production has been observed after adult zebrafish fin amputation, and trigger two parallel pathways, apoptosis and JNK activation, for compensatory proliferation of stump epidermal cells [145]. In the current study, I have documented major differences of the ROS responsiveness at the transcription level between different species, indicating the diversity of ROS signaling networks in advanced vertebrates including the regulation of DNA repair pathways. Furthermore, I have revealed substantial differences in the transcription factor regulatory mechanisms which respond to ROS between different vertebrate groups suggesting significant diversification in the control of transcription by ROS over the course of vertebrate evolution.

4.2 D-box function in ROS-responsive transcription

The D-box enhancer element, characterized by its TTAYGTAA motif in the promoters of mammalian clock and clock controlled genes, represents a crucial component in the circadian clock regulatory loops, specifically in output pathways [146]. Within mammals, CLOCK and BMAL1 proteins engage with the E-box element to stimulate

the expression of numerous target genes, encompassing both their negative regulators, the per and cry genes. Subsequently, these negative regulators inhibit the transcriptional activity of the CLOCK/BMAL1 complex, thereby finalizing the core molecular clock feedback loop [147]. However, a regulatory network of rhythmic gene expression, coordinating circadian transcriptional oscillation, is composed of not only the E-box element but also the REV-ERB/ROR-binding element (RRE), the binding site for retinoic acid-related orphan receptors (RORs) as activators and REV-ERBs as repressors of Nfil3 transcription, and the D-box [147]. The D-box cis-regulatory element is the binding site of three PAR bZip family members, DBP, TEF and HLF. In mammals, the promoters of the genes encoding these transcription factors contain E-box enhancer elements and their transcription is thereby under circadian clock control [148]. Consequently, the protein levels and transcriptional activation function of the PAR bZip factors is strongly time of day dependent and they thereby modulate the rhythmic expression of clock-controlled genes, leading to daily changes in physiological responses and behavior. Transactivation dependent on the D-box is inhibited by another class of bZip transcription factors, specifically the nuclear factor interleukin 3 (Nfil3, also known as E4BP4) [149]. The clock genes including *per1*, *per2*, *per3*, *Nr1d1*, *Nr1d2*, *Rora* and *Rorb* have been shown to contain conserved D-box elements in their promoter regions and so the transcriptional circuits regulated by the D-box show a repressor-antiphasic-to-activator mechanism [146]. However, in mammals the transcription of D-box containing genes does not directly respond to environmental signals such as visible light, UV or ROS [23]. Therefore, the mammalian D-box element appears to be predominantly clock regulated and serves as a downstream component involved in the clock output pathway, for example, the antioxidative gene expression in redox homeostasis [130]. In contrast, D-box-mediated regulation is directly induced by light, UV and ROS exposure in fish. More importantly, the light and UV responsiveness is tightly linked with intracellular ROS production [93]. Therefore, ROS appears to serve as a key intracellular signal which directs transcription of various stress responsive genes via the D-box element. The molecular mechanisms underlying the profound differences between fish and mammalian D-box function

remain poorly understood and for this reason were the subject of more detailed study in my thesis. (Fig 4.1 and see section 4.3).

In the present study, by focusing on the key NER regulatory gene *xpc*, I have shown that different transcriptional control mechanisms activate this gene in response to ROS in zebrafish, cavefish and mouse. In zebrafish, ROS-induced *xpc* expression is regulated by three D-box elements. However, the sequences of these D-boxes do not conform to the typical D-box consensus (TTAYGTAA) identified in previous studies. A recent study indicates that differences in the D-box enhancer sequence result in differential binding of the various PAR bZip and Nfil3 transcription factors in mouse [149]. Furthermore, the D-box sequences identified in the fish *cpd* and *6-4phr* photolyase genes differ from the D-box elements in clock genes like *per2* or *cry1a* in zebrafish [84, 92]. Therefore, a diversity of D-box sequences may confer different transcriptional responses to environmental signals as a result of the binding of different combinations of PAR bZip and Nfil3 transcription factors. In cavefish cells, no *xpc* transcriptional induction was observed in response to ROS exposure. However, highly conserved D-box elements were identified in the cavefish *xpc* gene promoter and also a cavefish *xpc* promoter reporter construct was robustly induced by ROS in zebrafish cells. These results suggest that during evolution in their extreme constant dark cave environment, the cavefish has experienced changes in the ROS-dependent function of mechanisms which lie upstream of the D-box enhancer. While mouse *xpc* is also up-regulated by ROS exposure transcriptionally, I failed to identify consensus D-box sequences in the *xpc* promoter. Furthermore, D-box enhancers fail to induce transcription in response to ROS exposure in mouse cells, consistent with my similar observations in frog and turtle cells. I therefore conclude that ROS-responsive regulation by the D-box enhancer may be specific to fish species and not encountered in the other major vertebrate groups. Certainly, enhancers responsible for regulating gene expression often display a pronounced level of species-specificity, characterized by the faster evolutionary rate of transcription factor binding sites compared to the TFs themselves and the genes under their control [150]. This would be consistent with the

observed differences in transcriptional control of the DNA repair genes in response to ROS in different vertebrate groups. Further efforts are needed to precisely demonstrate key ROS-responsive regulatory elements in different vertebrate species and to explain the evolutionary mechanisms underlying this diversity.

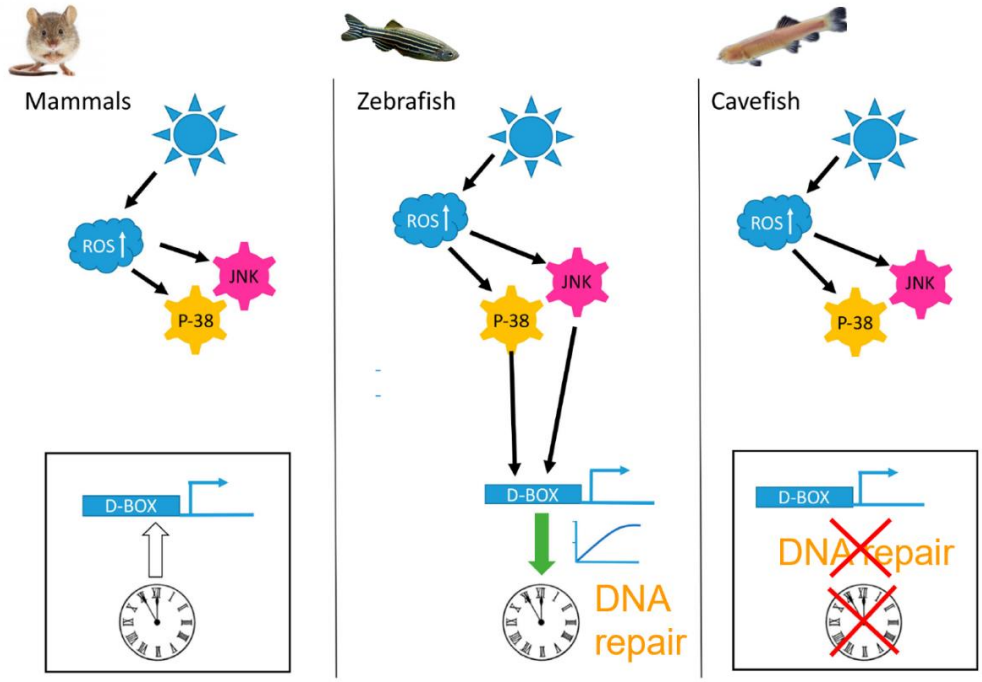

Fig 4.1. Schematic representation of different transcriptional control mechanisms in response to light and ROS in mammals, zebrafish and cavefish. In all three species, light radiation induces intracellular ROS levels, resulting in activation of p38 mitogen-activated protein kinase (MAPK) or c-Jun NH_2 terminal kinase (JNK) pathway. In zebrafish (middle panel), activated p38 or JNK target D-box elements to drive the transcription of a subset of genes, including clock genes and DNA repair genes. In mammals, this signaling pathway does not activate gene expression through the D-box element (as depicted in the left panel). Instead, D-box-mediated gene expression is exclusively regulated by the circadian clock (indicated by a white arrow). Similarly, in cavefish, this signaling pathway is also ineffective in initiating target gene expression through the D-box element (shown in the right panel) [93].

4.3 Regulation of D-box-mediated expression by PAR/E4BP4 factors

PAR factors contribute to D-box-driven expression of the *xpc* DNA repair gene in response to ROS. In my study, a strong induction of D-box-mediated expression in the *xpc* promoter was found by co-transfection of an expression vector for zfTEF1 in zebrafish cells. Furthermore, knockdown of *tef1* mRNA resulted in significant reduction of *xpc* and *ddb2* expression upon H_2O_2 treatment. Similar results were obtained by Gavriouchkina *et al* who showed that knockdown of TEF1 in zebrafish embryos lead to significant reduction of light-induced expression of DNA repair genes, *ddb2* and *neil1* [151]. As I mentioned above, ROS seem to also represent a critical signal in the regulation of both light- and UV-induced gene expression. Therefore, TEF1 appears to serve as a major regulator involved in the ROS responsiveness via the D-box element, at least in these important NER genes.

Interestingly, much lower activation was observed upon cavefish TEF1 co-transfection in both zebrafish and cavefish cells. Replacement of the C-terminal region of cfTEF1 with the corresponding portion of zfTEF1 in a "hybrid" TEF1 expression vector failed to elevate the level of ROS-induced expression. This indicates the important contribution of the N-terminal region of the protein to maintaining transcriptional activation function. How does ROS regulate the transactivation of PAR factors? While treatment of cells with H_2O_2 fails to increase TEF1 transactivation levels compared with untreated control cells, by coexpression of the H_2O_2 scavenger enzyme catalase, I found a remarkable decrease of D-box-driven expression mediated by all the PAR factors in zebrafish. Consistent results were found in previous studies showing that ROS inhibitors such as N-acetylcysteine (NAC) attenuate UV [84] or light-induced gene expression [93] which are also driven by the D-box enhancer in fish cells. The failure to induce TEF1 transactivation further by H_2O_2 treatment could be explained by elevation of intracellular ROS during the transfection procedure and therefore maximal activation been obtained in untreated, transfected cells. In this scenario, only by enzymatically or pharmacologically reducing intracellular ROS levels would I observed an impact on TEF1 activation. Therefore, the ROS-dependent, D-box

mediated gene expression through PAR factors could be a general mechanism involving different biological processes.

From my RNA-seq data, no significant up-regulation of *tef1* mRNA levels was detected in zebrafish, cavefish or mouse cells upon H_2O_2 exposure. A study on the Mexican cavefish *Astyanax mexicanus* also showed no light induction of *tef1* gene expression in surface or any cave populations [109]. Therefore, together with the results of all my cotransfection experiments using ectopically overexpressed TEF1 protein, I speculate that the TEF1 protein rather than its mRNA is modulated by the ROS signal, thereafter, targeting the D-box element for downstream gene regulation. PAR factors under control of the circadian clock have been shown to contribute to the regulation of xenobiotic metabolism, detoxification, antioxidation and apoptosis in mammals [152]. Furthermore, the bZIP factors also frequently function as environmental sensors in mediating the response to oxidative stress and redox homeostasis via protein phosphorylation [153-155].

4.4 D-box regulation by the MAPK pathway

The MAPK cascades represent highly conserved signal transduction pathways across evolution. They are responsible for regulating a wide array of cellular processes including stress responses. Each cascade comprises three fundamental kinases, namely MAPKKK, MAPKK, and MAPK. Within these cascades, signal propagation occurs through kinase phosphorylation and activation events, culminating in the phosphorylation of specific regulatory proteins [25]. Among numerous upstream signaling pathways which may potentially regulate PAR factors, the MAPK pathway is a promising candidate due to its extensive involvement in various stress-related signaling cascades. Indeed, many transcription factors are directly or indirectly regulated by MAPK including bZip factors such as c-Fos, c-Jun, ATF2, etc [25]. One primary nuclear role of MAPKs involves modulating transcription factors through stress-activated cascades via phosphorylation. For example, the activation of c-Jun

requires phosphorylation at animo residues of Ser63 and Ser73 within its transactivation domain, which enables its complete transcriptional activity as part of the AP-1 complex, in conjunction with factors such as c-Jun or ATF [156]. Phosphorylation of E47 by p38 promotes formation of a heterodimer of MyoD and E47 thereby controls muscle-specific gene transcription in skeletal myogenesis [157].

No evidence has been shown to date that MAPKs regulate PAR factors directly in any biological process. However, a previous study from my group demonstrated the tight connection between MAPK activation and D-box-mediated gene expression in zebrafish. H_2O_2 exposure immediately provokes p38 and JNK phosphorylation, followed by induction of D-box reporter expression from *cry1a*, whereas MAPK inhibition blocked the expression induced by H_2O_2 [93]. Thus, in the present study, I speculate that MAPKs also play important roles in TEF activation in D-box-mediated expression. I identified 4 potential MAPK phosphorylation sites in the N-terminal portion of the zebrafish TEF1 protein. By functional tests with both wildtype and mutants, all the 4 putative MAPK phosphorylation sites were demonstrated as being essential for the robust induction by TEF1 in zebrafish. In the cavefish TEF1 sequence, only one of these four putative sites is conserved. The mutation of these key amino acids in zfTEF1 resulted in a significant reduction of D-box mediated activation. Importantly, mutation of the 31Ile to a Ser, or 31I32L to constitute a TP site to mimic the zebrafish protein significantly increased the magnitude of cfTEF1 activated, D-box driven transcription in cavefish cells. The S/T-P motifs are canonical MAPK targets for most phosphorylation reactions [132]. For instance, JNK and p38 were demonstrated to regulate ATF2 function via the 69-TPTP-72 motif which has been termed a 'phosphoswitch' [158]. Considering the significant reduction in transcriptional activation by zfTEF1 when the 64Thr site is mutated to Ala and the conservation of the 64T65P site between zebrafish and cavefish, the TP site is probably one of the key phosphorylation targets for MAPKs for both zebrafish and cavefish. It explains, at least partially, the attenuation, but not the complete loss of cfTEF1 activation in D-box-mediated expression in cavefish. Considering all my data, zebrafish TEF1 may have

multiple phosphorylation sites targeted by MAPKs such as p38 and JNK, which upon phosphorylation, activate the function of these transcription factors. Mutations of these key sites in cavefish TEF1 may account for the observed reduced activation.

One potential mechanism highlighted by my work that may account for how TEF1 is regulated by the MAPK pathways is via the modulation of the subcellular localization. Many factors, for example, the transcription factor hypoxia-inducible factor-1 (HIF-1) is directly phosphorylated by the p42/p44 ERK MAPKs which thereby promotes its nuclear accumulation [159]. In contrast, phosphorylation of β-catenin by JNKs has been observed in *xenopus* embryos which prevents the nuclear localization of β-catenin proteins [160]. In this study, nuclear localization of zebrafish TEF1 was reduced in zebrafish cells by H_2O_2 clearance via catalase action whereas no such effect was found in cavefish cells. p38, JNK and ERK are phosphorylated rapidly by 300 μM H_2O_2 exposure in both zebrafish and cavefish cells, indicating that ROS activates the MAPK signaling cascade in cavefish as well as zebrafish cells [93]. Fig 4.2 illustrates my hypothesis to explain how D-box-mediated gene transcription responds to ROS via MAPK regulation. In zebrafish, the phosphorylation of multiple MAPK sites on the TEF1 protein results in a much stronger activation by MAPKs such as p38, JNK and ERK, which in turn enhances the translocation of TEF1 into the nucleus. However, lower levels of MAPK-induced phosphorylation in cavefish TEF1 as a result of the multiple amino acid substitutions in this protein compared with zebrafish TEF1, lead to a weaker transcriptional response. As well as confirming and quantifying changes in ROS-induced phosphorylation of the zebrafish and cavefish TEF1 proteins, it will also be important to test the nuclear localization of the mutant TEF proteins that I have generated as part of this work, in order to further test this hypothesis.

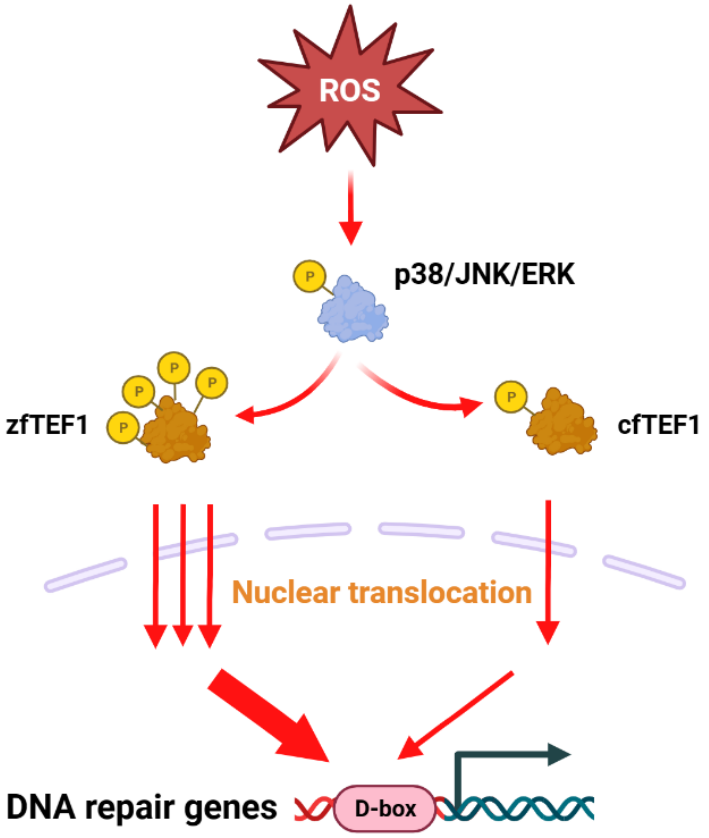

Fig 4.2 Schematic representation of ROS induced DNA repair gene expression regulated by MAPK signaling in zebrafish and cavefish. Elevated ROS levels activate phosphorylation of the p38 and JNK MAPKs in both zebrafish and cavefish cells, then result in phosphorylation of the TEF1 protein. More phosphorylation sites identified in zebrafish TEF1 protein may lead to an increase in nuclear translocation, which accounts for the stronger transcriptional activation of D-box-mediated DNA repair gene expression.

4.5 Conservation and adaptive evolution of ROS signaling

The detoxification mechanisms which counter the damaging effects of ROS are highly conserved from bacteria to higher vertebrates, pointing to them emerging relatively early during evolution. This pattern of conservation is evident for antioxidant enzymes such as superoxide dismutase (SOD) and catalase [161, 162], the thioredoxin (TXR) proteins which facilitate the reduction of disulfide bonds in specific proteins [163], thiol

peroxidases which protect protein thiols from oxidation and the NADPH oxidase family which generates superoxide radicals using NADPH as an electron donor [164].

Major steps in evolution such as the transition from aqueous environments to terrestrial habitats have required significant adaptations to ROS signaling. Land-dwelling organisms encounter higher levels of oxidative stress due to increased exposure to UV radiation and oxygen concentrations and it has been speculated that changes in the functionality of the Nrf2-Keap1 pathway in terrestrial vertebrates compared to their aquatic counterparts has been essential to enable this major habitat shift [114]. Another example is a significant reduction in the NOX gene repertoire in the ctenophore *Mnemiopsis leidyi*. Only NOX5 is retained in this species which undergoes diurnal vertical migrations to avoid exposure to intense sunlight, potentially affecting its cellular redox balance [165, 166]. Possibly to compensate for the limited variety of NOX enzymes, *M. leidyi* possesses an unusually broad array of Cu/ZnSODs, suggesting that this shift in the organization of the antioxidant regulatory networks represents an evolutionary adaptation to a unique set of environmental challenges faced by this organism [166].

In the current study, I have explored D-box enhancer-driven, ROS-induced gene expression in zebrafish, a mechanism which does not operate in cavefish and mouse cells. A TEF1-mediated mechanism regulated by p38 or JNK MAPKs and involving the control of nuclear localization lies upstream of this D-box-driven transcription. In fish cells, ROS may serve as a secondary messenger in response to environmental stress including light or UV radiation, activating MAPK cascades and their downstream targets including PAR factors, such as TEF1, to initiate target gene transcription. Given the coincident loss of ROS-regulated, D-box mediated gene expression in mice and a blind cavefish species which share a distant phylogenetic relationship, it is tempting to speculate that ancestors of both species may have experienced an extreme perpetually dark environment. Specifically, the ‘Nocturnal Bottleneck’ hypothesis has been proposed to account for a number of characteristics of mammals such as the loss of photoreactivation DNA repair as well as the loss of peripheral photoreception [72, 167]

as a result of evolution in darkness. During the late Cretaceous when dinosaurs still dominated the earth, the ancestors of modern mammals are predicted to have lived a subterranean, nocturnal life to avoid predation from diurnal carnivorous dinosaurs. As a result, many basic changes in light dependent physiology occurred. Long term evolution in subterranean caves where there may be a constant hypoxic environment with minimal fluctuation of O_2 levels may also contribute to alterations in the mechanisms of ROS-dependent signaling such as the loss of D-box-mediated gene expression in ROS inducible genes.

In summary, my current study has revealed a diversity of ROS-mediated transcriptional regulation among different vertebrates, whereas the ROS signaling in redox homeostasis in many other important biological events has been highly conserved. Since ROS act as second cellular messengers which are sensitive to environmental stress, the observed diversity of specific ROS signaling pathway in species may form a key part of the adaptive evolution of organisms to a diversity of environmental conditions.

4.6 Perspectives

In this project, I have explored the transcriptional response to ROS in different vertebrate models by multiple molecular biological approaches. My results have revealed different transcriptional profiles in response to ROS and particularly, the D-box-driven gene expression which fundamentally varies during vertebrate evolution. Notwithstanding many gaps in understanding of the precise mechanisms which operate, these discoveries reveal the flexibility of a conserved regulatory element among different species and provide a starting point to understand in depth how the environment shapes the complex mechanism in ROS signaling.

In my transcriptome data, I only focused on a small subset of genes. For example, genes coding proteins with heme binding and synthesis functions, which are ubiquitous in biological systems for diverse biological activities including circadian rhythms and gas

transport, have also lost ROS inducibility in cavefish cells. Are all these genes also regulated by ROS via D-box elements? Similar functional studies of these genes should improve our understanding of the general role of ROS signaling at the level of gene expression. A major limitation of my work is the use of a restricted group of cell lines rather that *in vivo* models. Thus, for example, the differences I have described between zebrafish and mouse may more reflect cell type or cell line-specific differences rather than fundamental species-specific differences. Furthermore, of course based on the analysis of a cell line from a single species it is difficult to extrapolate that these results reflect a general property of all species in that vertebrate group.

While I have implicated putative MAPK phosphorylation sites on the TEF1 PAR bZip transcription factor in conferring regulation by ROS of the D-box enhancer element, more concrete evidence is required. Quantification of phosphorylation at these predicted MAPK target sites will be an important next step. Furthermore, it will be important to explore in more detail the potential links between MAPK phosphorylation and the translocation of the TEF1 protein into the nucleus. Do similar mechanisms operate as have already been described for the other PAR bZip transcription factors?

Finally, from a broader perspective, zebrafish has been widely used as a genetic model system to study various human genetic disorders. An underlying assumption is that given that zebrafish and humans are both vertebrates, then all the main features of the major molecular and genetic regulatory pathways will be highly conserved, Therefore, lessons from zebrafish are directly relevant for studying human biology. However, my current work, combined with previous studies from my group have documented a fundamental difference of one key regulatory mechanism in ROS signaling between zebrafish and mammals. Therefore, I feel that it is vital to consider the existence and importance of fish-specific mechanisms that may differ fundamentally from those observed in mammals such as humans.

References:

[1] B. D'Autréaux, M.B. Toledano, ROS as signalling molecules: mechanisms that generate specificity in ROS homeostasis, Nature Reviews Molecular Cell Biology, 8 (2007) 813-824.

[2] A. Boveris, B. Chance, The mitochondrial generation of hydrogen peroxide. General properties and effect of hyperbaric oxygen, Biochemical Journal, 134 (1973) 707-716.

[3] A.J. Kowaltowski, N.C. de Souza-Pinto, R.F. Castilho, A.E. Vercesi, Mitochondria and reactive oxygen species, Free Radical Biology and Medicine, 47 (2009) 333-343.

[4] Q. Ma, Transcriptional responses to oxidative stress: Pathological and toxicological implications, Pharmacology & Therapeutics, 125 (2010) 376-393.

[5] A.A. Alfadda, R.M. Sallam, Reactive Oxygen Species in Health and Disease, Journal of Biomedicine and Biotechnology, 2012 (2012) 936486.

[6] D.P. Jones, Redefining Oxidative Stress, Antioxidants & Redox Signaling, 8 (2006) 1865-1879.

[7] L.A. del Río, E. López-Huertas, ROS Generation in Peroxisomes and its Role in Cell Signaling, Plant and Cell Physiology, 57 (2016) 1364-1376.

[8] B. Bhandary, A. Marahatta, H.-R. Kim, H.-J. Chae, An Involvement of Oxidative Stress in Endoplasmic Reticulum Stress and Its Associated Diseases, in: International Journal of Molecular Sciences, 2013, pp. 434-456.

[9] F. Magnani, A. Mattevi, Structure and mechanisms of ROS generation by NADPH oxidases, Current Opinion in Structural Biology, 59 (2019) 91-97.

[10] P.D. Ray, B.-W. Huang, Y. Tsuji, Reactive oxygen species (ROS) homeostasis and redox regulation in cellular signaling, Cellular Signalling, 24 (2012) 981-990.

[11] L.-O. Klotz, H. Steinbrenner, Cellular adaptation to xenobiotics: Interplay between xenosensors, reactive oxygen species and FOXO transcription factors, Redox Biology, 13 (2017) 646-654.

[12] M. Schieber, Navdeep S. Chandel, ROS Function in Redox Signaling and Oxidative Stress, Current Biology, 24 (2014) R453-R462.

[13] Y. Hong, A. Boiti, D. Vallone, N.S. Foulkes, Reactive Oxygen Species Signaling and Oxidative Stress: Transcriptional Regulation and Evolution, in: Antioxidants, 2024.
[14] M. Valko, C.J. Rhodes, J. Moncol, M. Izakovic, M. Mazur, Free radicals, metals and antioxidants in oxidative stress-induced cancer, Chemico-Biological Interactions, 160 (2006) 1-40.
[15] A. Okado-Matsumoto, I. Fridovich, Subcellular Distribution of Superoxide Dismutases (SOD) in Rat Liver: Cu,Zn-SOD IN MITOCHONDRIA *, Journal of Biological Chemistry, 276 (2001) 38388-38393.
[16] C. Vives-Bauza, A. Starkov, E. Garcia-Arumi, Measurements of the Antioxidant Enzyme Activities of Superoxide Dismutase, Catalase, and Glutathione Peroxidase, in: Methods in Cell Biology, Academic Press, 2007, pp. 379-393.
[17] K.J.A. Davies, Intracellular proteolytic systems may function as secondary antioxidant defenses: An hypothesis, Journal of Free Radicals in Biology & Medicine, 2 (1986) 155-173.
[18] S. Loft, H.E. Poulsen, Antioxidant intervention studies related to DNA damage, DNA repair and gene expression, Free Radic Res, 33 Suppl (2000) S67-83.
[19] S.J. Padayatty, A. Katz, Y. Wang, P. Eck, O. Kwon, J.-H. Lee, S. Chen, C. Corpe, A. Dutta, S.K. Dutta, M. Levine, Vitamin C as an Antioxidant: Evaluation of Its Role in Disease Prevention, Journal of the American College of Nutrition, 22 (2003) 18-35.
[20] M. Shakeri, E. Oskoueian, H.H. Le, M. Shakeri, Strategies to Combat Heat Stress in Broiler Chickens: Unveiling the Roles of Selenium, Vitamin E and Vitamin C, in: Veterinary Sciences, 2020.
[21] I.F.F. Benzie, M. Devaki, The ferric reducing/antioxidant power (FRAP) assay for non-enzymatic antioxidant capacity: concepts, procedures, limitations and applications, in: Measurement of Antioxidant Activity & Capacity, 2018, pp. 77-106.
[22] J. Zhang, X. Wang, V. Vikash, Q. Ye, D. Wu, Y. Liu, W. Dong, ROS and ROS-Mediated Cellular Signaling, Oxidative Medicine and Cellular Longevity, 2016 (2016) 4350965.

[23] R. Siauciunaite, N.S. Foulkes, V. Calabrò, D. Vallone, Evolution Shapes the Gene Expression Response to Oxidative Stress, in: International Journal of Molecular Sciences, 2019.

[24] R.B. Hamanaka, N.S. Chandel, Mitochondrial reactive oxygen species regulate cellular signaling and dictate biological outcomes, Trends in Biochemical Sciences, 35 (2010) 505-513.

[25] A. Plotnikov, E. Zehorai, S. Procaccia, R. Seger, The MAPK cascades: Signaling components, nuclear roles and mechanisms of nuclear translocation, Biochimica et Biophysica Acta (BBA) - Molecular Cell Research, 1813 (2011) 1619-1633.

[26] Y. Liu, C. He, A review of redox signaling and the control of MAP kinase pathway in plants, Redox Biology, 11 (2017) 192-204.

[27] A. Matsuzawa, H. Ichijo, Redox control of cell fate by MAP kinase: physiological roles of ASK1-MAP kinase pathway in stress signaling, Biochimica et Biophysica Acta (BBA) - General Subjects, 1780 (2008) 1325-1336.

[28] S. Yoon, R. Seger, The extracellular signal-regulated kinase: Multiple substrates regulate diverse cellular functions, Growth Factors, 24 (2006) 21-44.

[29] R.J. Davis, MAPKs: new JNK expands the group, Trends in Biochemical Sciences, 19 (1994) 470-473.

[30] J.M. Kyriakis, J. Avruch, Mammalian Mitogen-Activated Protein Kinase Signal Transduction Pathways Activated by Stress and Inflammation, Physiological Reviews, 81 (2001) 807-869.

[31] T. Takata, S. Araki, Y. Tsuchiya, Y. Watanabe, Oxidative Stress Orchestrates MAPK and Nitric-Oxide Synthase Signal, in: International Journal of Molecular Sciences, 2020.

[32] Y.-R. Chen, A. Shrivastava, T.-H. Tan, Down-regulation of the c-Jun N-terminal kinase (JNK) phosphatase M3/6 and activation of JNK by hydrogen peroxide and pyrrolidine dithiocarbamate, Oncogene, 20 (2001) 367-374.

[33] H. Kamata, S.-i. Honda, S. Maeda, L. Chang, H. Hirata, M. Karin, Reactive Oxygen Species Promote TNFα-Induced Death and Sustained JNK Activation by Inhibiting MAP Kinase Phosphatases, Cell, 120 (2005) 649-661.

[34] S. Park, J.-Y. Ahn, M.-J. Lim, M.-H. Kim, Y.-S. Yun, G. Jeong, J.-Y. Song, Sustained expression of NADPH oxidase 4 by p38 MAPK-Akt signaling potentiates radiation-induced differentiation of lung fibroblasts, Journal of Molecular Medicine, 88 (2010) 807-816.

[35] Y. Filina, A. Gabdoulkhakova, A. Rizvanov, V. Safronova, MAP kinases in regulation of NOX activity stimulated through two types of formyl peptide receptors in murine bone marrow granulocytes, Cellular Signalling, 90 (2022) 110205.

[36] Y. Son, Y.-K. Cheong, N.-H. Kim, H.-T. Chung, D.G. Kang, H.-O.J.J.o.s.t. Pae, Mitogen-activated protein kinases and reactive oxygen species: how can ROS activate MAPK pathways?, Journal of Signal Transduction, 2011 (2011).

[37] M.J. Morgan, Z.-g. Liu, Crosstalk of reactive oxygen species and NF-κB signaling, Cell Research, 21 (2011) 103-115.

[38] K. Lingappan, NF-κB in oxidative stress, Current Opinion in Toxicology, 7 (2018) 81-86.

[39] G. Gloire, S. Legrand-Poels, J. Piette, NF-κB activation by reactive oxygen species: Fifteen years later, Biochemical Pharmacology, 72 (2006) 1493-1505.

[40] E. Turillazzi, M. Neri, D. Cerretani, S. Cantatore, P. Frati, L. Moltoni, F.P. Busardò, C. Pomara, I. Riezzo, V. Fineschi, Lipid peroxidation and apoptotic response in rat brain areas induced by long-term administration of nandrolone: the mutual crosstalk between ROS and NF-kB, Journal of Cellular and Molecular Medicine, 20 (2016) 601-612.

[41] K.H. Vousden, X. Lu, Live or let die: the cell's response to p53, Nature Reviews Cancer, 2 (2002) 594-604.

[42] B. Liu, Y. Chen, D.K. St. Clair, ROS and p53: A versatile partnership, Free Radical Biology and Medicine, 44 (2008) 1529-1535.

[43] H.A. Abbas, D.R. Maccio, S. Coskun, J.G. Jackson, A.L. Hazen, T.M. Sills, M.J. You, K.K. Hirschi, G. Lozano, Mdm2 Is Required for Survival of Hematopoietic Stem Cells/Progenitors via Dampening of ROS-Induced p53 Activity, Cell Stem Cell, 7 (2010) 606-617.

[44] Y. Chen, K. Liu, Y. Shi, C. Shao, The tango of ROS and p53 in tissue stem cells, Cell Death & Differentiation, 25 (2018) 639-641.

[45] S. Matoba, J.-G. Kang, W.D. Patino, A. Wragg, M. Boehm, O. Gavrilova, P.J. Hurley, F. Bunz, P.M. Hwang, p53 Regulates Mitochondrial Respiration, Science, 312 (2006) 1650-1653.

[46] T.W. Kensler, N. Wakabayashi, S. Biswal, Cell Survival Responses to Environmental Stresses Via the Keap1-Nrf2-ARE Pathway, Annual Review of Pharmacology and Toxicology, 47 (2007) 89-116.

[47] S.M. Aaen, T.E. Horsberg, A screening of multiple classes of pharmaceutical compounds for effect on preadult salmon lice Lepeophtheirus salmonis, Journal of Fish Diseases, 39 (2016) 1213-1223.

[48] T. Yamamoto, T. Suzuki, A. Kobayashi, J. Wakabayashi, J. Maher, H. Motohashi, M. Yamamoto, Physiological Significance of Reactive Cysteine Residues of Keap1 in Determining Nrf2 Activity, Molecular and Cellular Biology, 28 (2008) 2758-2770.

[49] P. Rajendran, N. Nandakumar, T. Rengarajan, R. Palaniswami, E.N. Gnanadhas, U. Lakshminarasaiah, J. Gopas, I. Nishigaki, Antioxidants and human diseases, Clinica Chimica Acta, 436 (2014) 332-347.

[50] M. Suzuki, A. Otsuki, N. Keleku-Lukwete, M. Yamamoto, Overview of redox regulation by Keap1–Nrf2 system in toxicology and cancer, Current Opinion in Toxicology, 1 (2016) 29-36.

[51] D.D. Zhang, The Nrf2-Keap1-ARE Signaling Pathway: The Regulation and Dual Function of Nrf2 in Cancer, Antioxidants & Redox Signaling, 13 (2010) 1623-1626.

[52] W. Tu, H. Wang, S. Li, Q. Liu, H. Sha, The Anti-Inflammatory and Anti-Oxidant Mechanisms of the Keap1/Nrf2/ARE Signaling Pathway in Chronic Diseases, Aging and disease, 10 (2019) 637-651.

[53] M. Rosbash, The Implications of Multiple Circadian Clock Origins, PLOS Biology, 7 (2009) e1000062.

[54] A.G. Lai, C.J. Doherty, B. Mueller-Roeber, S.A. Kay, J.H.M. Schippers, P.P. Dijkwel, CIRCADIAN CLOCK-ASSOCIATED 1 regulates ROS homeostasis and

oxidative stress responses, Proceedings of the National Academy of Sciences, 109 (2012) 17129-17134.

[55] T. Tamaru, M. Hattori, Y. Ninomiya, G. Kawamura, G. Varès, K. Honda, D.P. Mishra, B. Wang, I. Benjamin, P. Sassone-Corsi, T. Ozawa, K. Takamatsu, ROS Stress Resets Circadian Clocks to Coordinate Pro-Survival Signals, PLOS ONE, 8 (2013) e82006.

[56] L. Wu, Akhilesh B. Reddy, Rethinking the clockwork: redox cycles and non-transcriptional control of circadian rhythms, Biochemical Society Transactions, 42 (2014) 1-10.

[57] Andrew S.I. Loudon, Circadian Biology: A 2.5 Billion Year Old Clock, Current Biology, 22 (2012) R570-R571.

[58] J.S. Takahashi, Transcriptional architecture of the mammalian circadian clock, Nature Reviews Genetics, 18 (2017) 164-179.

[59] M. Wilking, M. Ndiaye, H. Mukhtar, N. Ahmad, Circadian Rhythm Connections to Oxidative Stress: Implications for Human Health, Antioxidants & Redox Signaling, 19 (2012) 192-208.

[60] J.-F. Pei, X.-K. Li, W.-Q. Li, Q. Gao, Y. Zhang, X.-M. Wang, J.-Q. Fu, S.-S. Cui, J.-H. Qu, X. Zhao, D.-L. Hao, D. Ju, N. Liu, K.S. Carroll, J. Yang, E.E. Zhang, J.-M. Cao, H.-Z. Chen, D.-P. Liu, Diurnal oscillations of endogenous H2O2 sustained by p66Shc regulate circadian clocks, Nature Cell Biology, 21 (2019) 1553-1564.

[61] T.B. Kryston, A.B. Georgiev, P. Pissis, A.G. Georgakilas, Role of oxidative stress and DNA damage in human carcinogenesis, Mutation Research/Fundamental and Molecular Mechanisms of Mutagenesis, 711 (2011) 193-201.

[62] M. Yousefzadeh, C. Henpita, R. Vyas, C. Soto-Palma, P. Robbins, L. Niedernhofer, DNA damage—how and why we age?, eLife, 10 (2021) e62852.

[63] R.P. Sinha, D.-P. Häder, UV-induced DNA damage and repair: a review, Photochemical & Photobiological Sciences, 1 (2002) 225-236.

[64] A. Yasui, A.P. Eker, S. Yasuhira, H. Yajima, T. Kobayashi, M. Takao, A. Oikawa, A new class of DNA photolyases present in various organisms including aplacental mammals, The EMBO Journal, 13 (1994) 6143-6151.

[65] Y. Kobayashi, T. Ishikawa, J. Hirayama, H. Daiyasu, S. Kanai, H. Toh, I. Fukuda, T. Tsujimura, N. Terada, Y. Kamei, S. Yuba, S. Iwai, T. Todo, Molecular analysis of zebrafish photolyase/cryptochrome family: two types of cryptochromes present in zebrafish, Genes to Cells, 5 (2000) 725-738.

[66] M. Ahmad, J.A. Jarillo, L.J. Klimczak, L.G. Landry, T. Peng, R.L. Last, A.R. Cashmore, An enzyme similar to animal type II photolyases mediates photoreactivation in Arabidopsis, The Plant Cell, 9 (1997) 199-207.

[67] S. Weber, Light-driven enzymatic catalysis of DNA repair: a review of recent biophysical studies on photolyase, Biochimica et Biophysica Acta (BBA) - Bioenergetics, 1707 (2005) 1-23.

[68] S.D. Cline, P.C. Hanawalt, Who's on first in the cellular response to DNA damage?, Nature Reviews Molecular Cell Biology, 4 (2003) 361-373.

[69] A. Sancar, L.A. Lindsey-Boltz, K. Ünsal-Kaçmaz, S. Linn, Molecular Mechanisms of Mammalian DNA Repair and the DNA Damage Checkpoints, Annual Review of Biochemistry, 73 (2004) 39-85.

[70] G.T.J.v.d. Horst, M. Muijtjens, K. Kobayashi, R. Takano, S.-i. Kanno, M. Takao, J.d. Wit, A. Verkerk, A.P.M. Eker, D.v. Leenen, R. Buijs, D. Bootsma, J.H.J. Hoeijmakers, A. Yasui, Mammalian Cry1 and Cry2 are essential for maintenance of circadian rhythms, Nature, 398 (1999) 627-630.

[71] A.P.M. Eker, C. Quayle, I. Chaves, G.T.J. van der Horst, DNA Repair in Mammalian Cells, Cellular and Molecular Life Sciences, 66 (2009) 968-980.

[72] M.P. Gerkema, W.I.L. Davies, R.G. Foster, M. Menaker, R.A. Hut, The nocturnal bottleneck and the evolution of activity patterns in mammals, Proceedings of the Royal Society B: Biological Sciences, 280 (2013) 20130508.

[73] T.S. Dexheimer, DNA Repair Pathways and Mechanisms, in: L.A. Mathews, S.M. Cabarcas, E.M. Hurt (Eds.) DNA Repair of Cancer Stem Cells, Springer Netherlands, Dordrecht, 2013, pp. 19-32.

[74] M. Christmann, M.T. Tomicic, W.P. Roos, B. Kaina, Mechanisms of human DNA repair: an update, Toxicology, 193 (2003) 3-34.

[75] N.C. Bauer, A.H. Corbett, P.W. Doetsch, The current state of eukaryotic DNA base damage and repair, Nucleic Acids Research, 43 (2015) 10083-10101.

[76] J.A. Marteijn, H. Lans, W. Vermeulen, J.H.J. Hoeijmakers, Understanding nucleotide excision repair and its roles in cancer and ageing, Nature Reviews Molecular Cell Biology, 15 (2014) 465-481.

[77] A. Sancar, Mechanisms of DNA Repair by Photolyase and Excision Nuclease (Nobel Lecture), Angew. Chem. Int. Ed, 55 (2016) 8502-8527.

[78] F. Chavanne, B.C. Broughton, D. Pietra, T. Nardo, A. Browitt, A.R. Lehmann, M. Stefanini, Mutations in the XPC Gene in Families with Xeroderma Pigmentosum and Consequences at the Cell, Protein, and Transcript Levels1, Cancer Research, 60 (2000) 1974-1982.

[79] T.A. Kunkel, D.A. Erie, DNA MISMATCH REPAIR, Annual Review of Biochemistry, 74 (2005) 681-710.

[80] L. Stojic, R. Brun, J. Jiricny, Mismatch repair and DNA damage signalling, DNA Repair, 3 (2004) 1091-1101.

[81] L. Krejci, V. Altmannova, M. Spirek, X. Zhao, Homologous recombination and its regulation, Nucleic Acids Research, 40 (2012) 5795-5818.

[82] E. Weterings, D.C. van Gent, The mechanism of non-homologous end-joining: a synopsis of synapsis, DNA Repair, 3 (2004) 1425-1435.

[83] A. Balmain, J. Gray, B. Ponder, The genetics and genomics of cancer, Nature Genetics, 33 (2003) 238-244.

[84] H. Zhao, G. Di Mauro, S. Lungu-Mitea, P. Negrini, A.M. Guarino, E. Frigato, T. Braunbeck, H. Ma, T. Lamparter, D. Vallone, C. Bertolucci, N.S. Foulkes, Modulation of DNA Repair Systems in Blind Cavefish during Evolution in Constant Darkness, Current Biology, 28 (2018) 3229-3243.e3224.

[85] U.S. Srinivas, B.W.Q. Tan, B.A. Vellayappan, A.D. Jeyasekharan, ROS and the DNA damage response in cancer, Redox Biology, 25 (2019) 101084.

[86] S. Jayakumar, D. Pal, S.K. Sandur, Nrf2 facilitates repair of radiation induced DNA damage through homologous recombination repair pathway in a ROS

independent manner in cancer cells, Mutation Research/Fundamental and Molecular Mechanisms of Mutagenesis, 779 (2015) 33-45.

[87] G. Achanta, P. Huang, Role of p53 in Sensing Oxidative DNA Damage in Response to Reactive Oxygen Species-Generating Agents, Cancer Research, 64 (2004) 6233-6239.

[88] T.S. Lisse, B.L. King, S. Rieger, Comparative transcriptomic profiling of hydrogen peroxide signaling networks in zebrafish and human keratinocytes: Implications toward conservation, migration and wound healing, Scientific Reports, 6 (2016) 20328.

[89] S. Saleem, R.R. Kannan, Zebrafish: an emerging real-time model system to study Alzheimer's disease and neurospecific drug discovery, Cell Death Discovery, 4 (2018) 45.

[90] G. Vatine, D. Vallone, Y. Gothilf, N.S. Foulkes, It's time to swim! Zebrafish and the circadian clock, FEBS Letters, 585 (2011) 1485-1494.

[91] D. Whitmore, N.S. Foulkes, P. Sassone-Corsi, Light acts directly on organs and cells in culture to set the vertebrate circadian clock, Nature, 404 (2000) 87-91.

[92] G. Vatine, D. Vallone, L. Appelbaum, P. Mracek, Z. Ben-Moshe, K. Lahiri, Y. Gothilf, N.S. Foulkes, Light Directs Zebrafish period2 Expression via Conserved D and E Boxes, PLOS Biology, 7 (2009) e1000223.

[93] C. Pagano, R. Siauciunaite, M.L. Idda, G. Ruggiero, R.M. Ceinos, M. Pagano, E. Frigato, C. Bertolucci, N.S. Foulkes, D. Vallone, Evolution shapes the responsiveness of the D-box enhancer element to light and reactive oxygen species in vertebrates, Scientific Reports, 8 (2018) 13180.

[94] C. Pagano, R.M. Ceinos, D. Vallone, N.S. Foulkes, The Fish Circadian Timing System: The Illuminating Case of Light-Responsive Peripheral Clocks, in: V. Kumar (Ed.) Biological Timekeeping: Clocks, Rhythms and Behaviour, Springer India, New Delhi, 2017, pp. 177-192.

[95] M.W. Hankins, W.I.L. Davies, R.G. Foster, The Evolution of Non-visual Photopigments in the Central Nervous System of Vertebrates, in: D.M. Hunt, M.W. Hankins, S.P. Collin, N.J. Marshall (Eds.) Evolution of Visual and Non-visual Pigments, Springer US, Boston, MA, 2014, pp. 65-103.

[96] I.A. Frøland Steindal, D. Whitmore, Circadian Clocks in Fish—What Have We Learned so far?, in: Biology, 2019.

[97] B. Razaghi, S.L. Steele, S.V. Prykhozhij, M.R. Stoyek, J.A. Hill, M.D. Cooper, L. McDonald, W. Lin, M. Daugaard, N. Crapoulet, S. Chacko, S.M. Lewis, I.C. Scott, P.H.B. Sorensen, J.N. Berman, hace1 Influences zebrafish cardiac development via ROS-dependent mechanisms, Developmental Dynamics, 247 (2018) 289-303.

[98] S. Rieger, A. Sagasti, Hydrogen Peroxide Promotes Injury-Induced Peripheral Sensory Axon Regeneration in the Zebrafish Skin, PLOS Biology, 9 (2011) e1000621.

[99] F. Meda, C. Gauron, C. Rampon, J. Teillon, M. Volovitch, S. Vriz, Nerves Control Redox Levels in Mature Tissues Through Schwann Cells and Hedgehog Signaling, Antioxidants & Redox Signaling, 24 (2015) 299-311.

[100] D. Yamajuku, Y. Shibata, M. Kitazawa, T. Katakura, H. Urata, T. Kojima, S. Takayasu, O. Nakata, S. Hashimoto, Cellular DBP and E4BP4 proteins are critical for determining the period length of the circadian oscillator, FEBS Letters, 585 (2011) 2217-2222.

[101] Z. Ben-Moshe, G. Vatine, S. Alon, A. Tovin, P. Mracek, N.S. Foulkes, Y. Gothilf, MULTIPLE PAR AND E4BP4 bZIP TRANSCRIPTION FACTORS IN ZEBRAFISH: DIVERSE SPATIAL AND TEMPORAL EXPRESSION PATTERNS, Chronobiology International, 27 (2010) 1509-1531.

[102] J.A. Ripperger, L.P. Shearman, S.M. Reppert, U. Schibler, CLOCK, an essential pacemaker component, controls expression of the circadian transcription factor DBP, Genes Dev, 14 (2000) 679-689.

[103] F.G. Howarth, O.T. Moldovan, The Ecological Classification of Cave Animals and Their Adaptations, in: O.T. Moldovan, Ľ. Kováč, S. Halse (Eds.) Cave Ecology, Springer International Publishing, Cham, 2018, pp. 41-67.

[104] M. Stemmer, L.-N. Schuhmacher, N.S. Foulkes, C. Bertolucci, J. Wittbrodt, Cavefish eye loss in response to an early block in retinal differentiation progression, Development, 142 (2015) 743-752.

[105] F.A. Lagunas-Rangel, V. Chávez-Valencia, Learning of nature: The curious case of the naked mole rat, Mechanisms of Ageing and Development, 164 (2017) 76-81.

[106] M. Yoshizawa, Y. Yamamoto, K.E. O'Quin, W.R. Jeffery, Evolution of an adaptive behavior and its sensory receptors promotes eye regression in blind cavefish, BMC Biology, 10 (2012) 108.

[107] D. Soares, M.L. Niemiller, Sensory Adaptations of Fishes to Subterranean Environments, BioScience, 63 (2013) 274-283.

[108] W.R. Jeffery, Cavefish as a Model System in Evolutionary Developmental Biology, Developmental Biology, 231 (2001) 1-12.

[109] A. Beale, C. Guibal, T.K. Tamai, L. Klotz, S. Cowen, E. Peyric, V.H. Reynoso, Y. Yamamoto, D. Whitmore, Circadian rhythms in Mexican blind cavefish Astyanax mexicanus in the lab and in the field, Nature Communications, 4 (2013) 2769.

[110] A. Ercolini, R. Berti, L. Chelazzi, G. Messana, RESEARCHES ON THE PHREATOBIC FISHES OF SOMALIA: ACHIEVEMENTS AND PROSPECTS, Monitore Zoologico Italiano. Supplemento, 17 (1982) 219-241.

[111] N. Cavallari, E. Frigato, D. Vallone, N. Fröhlich, J.F. Lopez-Olmeda, A. Foà, R. Berti, F.J. Sánchez-Vázquez, C. Bertolucci, N.S. Foulkes, A Blind Circadian Clock in Cavefish Reveals that Opsins Mediate Peripheral Clock Photoreception, PLOS Biology, 9 (2011) e1001142.

[112] C. Selman, J.D. Blount, D.H. Nussey, J.R. Speakman, Oxidative damage, ageing, and life-history evolution: where now?, Trends in Ecology & Evolution, 27 (2012) 570-577.

[113] M.A. Inupakutika, S. Sengupta, A.R. Devireddy, R.K. Azad, R. Mittler, The evolution of reactive oxygen species metabolism, Journal of Experimental Botany, 67 (2016) 5933-5943.

[114] K. Yumimoto, S. Sugiyama, S. Motomura, D. Takahashi, K.I. Nakayama, Molecular evolution of Keap1 was essential for adaptation of vertebrates to terrestrial life, Science Advances, 9 eadg2379.

[115] S. Lin, N. Gaiano, P. Culp, J.C. Burns, T. Friedmann, J.-K. Yee, N. Hopkins, Integration and Germ-Line Transmission of a Pseudotyped Retroviral Vector in Zebrafish, Science, 265 (1994) 666-669.

[116] O. Bartholomé, C. Franck, P. Piscicelli, N. Lalun, J. Defourny, J. Renauld, N. Thelen, F. Lamaye, D. Ploton, M. Thiry, Relationships between the structural and functional organization of the turtle cell nucleolus, Journal of Structural Biology, 208 (2019) 107398.

[117] L. Sinzelle, R. Thuret, H.-Y. Hwang, B. Herszberg, E. Paillard, O.J. Bronchain, D.L. Stemple, S. Dhorne-Pollet, N. Pollet, Characterization of a novel Xenopus tropicalis cell line as a model for in vitro studies, genesis, 50 (2012) 316-324.

[118] K.K. P. Senthilraja, In vitro cytotoxicity MTT assay in Vero, HepG2 and MCF - 7 cell lines study of Marine Yeast, Journal of Applied Pharmaceutical Science, 5 (2015) 080-084.

[119] J. van Meerloo, G.J.L. Kaspers, J. Cloos, Cell Sensitivity Assays: The MTT Assay, in: I.A. Cree (Ed.) Cancer Cell Culture: Methods and Protocols, Humana Press, Totowa, NJ, 2011, pp. 237-245.

[120] L. Nemzow, A. Lubin, L. Zhang, F. Gong, XPC: Going where no DNA damage sensor has gone before, DNA Repair, 36 (2015) 19-27.

[121] H. Zhao, H. Li, J. Du, G. Di Mauro, S. Lungu-Mitea, N. Geyer, D. Vallone, C. Bertolucci, N.S. Foulkes, Regulation of ddb2 expression in blind cavefish and zebrafish reveals plasticity in the control of sunlight-induced DNA damage repair, PLOS Genetics, 17 (2021) e1009356.

[122] P. Mracek, C. Santoriello, M.L. Idda, C. Pagano, Z. Ben-Moshe, Y. Gothilf, D. Vallone, N.S. Foulkes, Regulation of per and cry Genes Reveals a Central Role for the D-Box Enhancer in Light-Dependent Gene Expression, PLOS ONE, 7 (2012) e51278.

[123] D. Gau, T. Lemberger, C. von Gall, O. Kretz, N. Le Minh, P. Gass, W. Schmid, U. Schibler, H.W. Korf, G. Schütz, Phosphorylation of CREB Ser142 Regulates Light-Induced Phase Shifts of the Circadian Clock, Neuron, 34 (2002) 245-253.

[124] B.E. Lonze, D.D. Ginty, Function and Regulation of CREB Family Transcription Factors in the Nervous System, Neuron, 35 (2002) 605-623.

[125] D.P. Singh, E. Kubo, B. Chhunchha, Core Clock Protein Bmal 1 Controls Reactive Oxygen Species Homeostasis And Oxidative Responses By Transregulating

Prdx6 Expression, Investigative Ophthalmology & Visual Science, 60 (2019) 1127-1127.

[126] W. Zhang, H.T. Liu, MAPK signal pathways in the regulation of cell proliferation in mammalian cells, Cell Research, 12 (2002) 9-18.

[127] S.-H. Yang, A.D. Sharrocks, A.J. Whitmarsh, Transcriptional regulation by the MAP kinase signaling cascades, Gene, 320 (2003) 3-21.

[128] P. Mracek, Regulation of Vertebrate Clock Gene Expression by Light, in, Heidelburg University, 2012.

[129] S. Rezatabar, A. Karimian, V. Rameshknia, H. Parsian, M. Majidinia, T.A. Kopi, A. Bishayee, A. Sadeghinia, M. Yousefi, M. Monirialamdari, B. Yousefi, RAS/MAPK signaling functions in oxidative stress, DNA damage response and cancer progression, Journal of Cellular Physiology, 234 (2019) 14951-14965.

[130] F. Gachon, F.F. Olela, O. Schaad, P. Descombes, U. Schibler, The circadian PAR-domain basic leucine zipper transcription factors DBP, TEF, and HLF modulate basal and inducible xenobiotic detoxification, Cell Metabolism, 4 (2006) 25-36.

[131] P. Fonjallaz, V. Ossipow, G. Wanner, U. Schibler, The two PAR leucine zipper proteins, TEF and DBP, display similar circadian and tissue-specific expression, but have different target promoter preferences, The EMBO Journal, 15 (1996) 351-362.

[132] G. Pimienta, J. Pascual, Canonical and Alternative MAPK Signaling, Cell Cycle, 6 (2007) 2628-2632.

[133] L. Bardwell, Mechanisms of MAPK signalling specificity, Biochemical Society Transactions, 34 (2006) 837-841.

[134] H.C. Reinardy, J. Dharamshi, A.N. Jha, T.B. Henry, Changes in expression profiles of genes associated with DNA repair following induction of DNA damage in larval zebrafish Danio rerio, Mutagenesis, 28 (2013) 601-608.

[135] L.A. Brennan, G.M. Morris, G.R. Wasson, B.M. Hannigan, Y.A. Barnett, The effect of vitamin C or vitamin E supplementation on basal and H2O2-induced DNA damage in human lymphocytes, British Journal of Nutrition, 84 (2000) 195-202.

[136] M. Gülden, A. Jess, J. Kammann, E. Maser, H. Seibert, Cytotoxic potency of H2O2 in cell cultures: Impact of cell concentration and exposure time, Free Radical Biology and Medicine, 49 (2010) 1298-1305.
[137] J. Liu, W. Qu, M.B. Kadiiska, Role of oxidative stress in cadmium toxicity and carcinogenesis, Toxicology and Applied Pharmacology, 238 (2009) 209-214.
[138] J.M. Matés, J.A. Segura, F.J. Alonso, J. Márquez, Roles of dioxins and heavy metals in cancer and neurological diseases using ROS-mediated mechanisms, Free Radical Biology and Medicine, 49 (2010) 1328-1341.
[139] Y. Liang, B. Dong, N. Pang, J. Hu, ROS generation and DNA damage contribute to abamectin-induced cytotoxicity in mouse macrophage cells, Chemosphere, 234 (2019) 328-337.
[140] V.I. Lushchak, T.V. Bagnyukova, Effects of different environmental oxygen levels on free radical processes in fish, Comparative Biochemistry and Physiology Part B: Biochemistry and Molecular Biology, 144 (2006) 283-289.
[141] P. Han, X.-H. Zhou, N. Chang, C.-L. Xiao, S. Yan, H. Ren, X.-Z. Yang, M.-L. Zhang, Q. Wu, B. Tang, J.-P. Diao, X. Zhu, C. Zhang, C.-Y. Li, H. Cheng, J.-W. Xiong, Hydrogen peroxide primes heart regeneration with a derepression mechanism, Cell Research, 24 (2014) 1091-1107.
[142] X. Hui, Z. Yun-Wen, L. Qi, L. Li-Ping, L. Feng-Lin, Z. Hu-Chen, I. Hiroko, O. Nobuhiro, L. Yu-Mei, Reactive Oxygen Species in Skin Repair, Regeneration, Aging, and Inflammation, in: F. Cristiana, A. Elena (Eds.) Reactive Oxygen Species (ROS) in Living Cells, IntechOpen, Rijeka, 2017, pp. Ch. 5.
[143] N.R. Love, Y. Chen, S. Ishibashi, P. Kritsiligkou, R. Lea, Y. Koh, J.L. Gallop, K. Dorey, E. Amaya, Amputation-induced reactive oxygen species are required for successful Xenopus tadpole tail regeneration, Nature Cell Biology, 15 (2013) 222-228.
[144] P. Santabárbara-Ruiz, J. Esteban-Collado, L. Pérez, G. Viola, J.F. Abril, M. Milán, M. Corominas, F. Serras, Ask1 and Akt act synergistically to promote ROS-dependent regeneration in Drosophila, PLOS Genetics, 15 (2019) e1007926.

[145] C. Gauron, C. Rampon, M. Bouzaffour, E. Ipendey, J. Teillon, M. Volovitch, S. Vriz, Sustained production of ROS triggers compensatory proliferation and is required for regeneration to proceed, Scientific Reports, 3 (2013) 2084.

[146] H.R. Ueda, S. Hayashi, W. Chen, M. Sano, M. Machida, Y. Shigeyoshi, M. Iino, S. Hashimoto, System-level identification of transcriptional circuits underlying mammalian circadian clocks, Nature Genetics, 37 (2005) 187-192.

[147] E.A. Susaki, J. Stelling, H.R. Ueda, Challenges in synthetically designing mammalian circadian clocks, Current Opinion in Biotechnology, 21 (2010) 556-565.

[148] F. Gachon, Physiological function of PARbZip circadian clock‐controlled transcription factors, Annals of Medicine, 39 (2007) 562-571.

[149] H. Yoshitane, Y. Asano, A. Sagami, S. Sakai, Y. Suzuki, H. Okamura, W. Iwasaki, H. Ozaki, Y. Fukada, Functional D-box sequences reset the circadian clock and drive mRNA rhythms, Communications Biology, 2 (2019) 300.

[150] E.S. Wong, D. Zheng, S.Z. Tan, N.I. Bower, V. Garside, G. Vanwalleghem, F. Gaiti, E. Scott, B.M. Hogan, K. Kikuchi, E. McGlinn, M. Francois, B.M. Degnan, Deep conservation of the enhancer regulatory code in animals, Science, 370 (2020) eaax8137.

[151] D. Gavriouchkina, S. Fischer, T. Ivacevic, J. Stolte, V. Benes, M.P.S. Dekens, Thyrotroph Embryonic Factor Regulates Light-Induced Transcription of Repair Genes in Zebrafish Embryonic Cells, PLOS ONE, 5 (2010) e12542.

[152] A. Ritchie, O. Gutierrez, J.L. Fernandez-Luna, PAR bZIP-bik is a novel transcriptional pathway that mediates oxidative stress-induced apoptosis in fibroblasts, Cell Death & Differentiation, 16 (2009) 838-846.

[153] C. Abate, L. Patel, F.J. Rauscher, T. Curran, Redox Regulation of Fos and Jun DNA-Binding Activity in Vitro, Science, 249 (1990) 1157-1161.

[154] C.D. Deppmann, T.M. Thornton, F.E. Utama, E.J. Taparowsky, Phosphorylation of BATF regulates DNA binding: a novel mechanism for AP-1 (activator protein-1) regulation, Biochemical Journal, 374 (2003) 423-431.

[155] G.D. Amoutzias, E. Bornberg-Bauer, S.G. Oliver, D.L. Robertson, Reduction/oxidation-phosphorylation control of DNA binding in the bZIP dimerization network, BMC Genomics, 7 (2006) 107.

[156] B. Dérijard, M. Hibi, I.H. Wu, T. Barrett, B. Su, T. Deng, M. Karin, R.J. Davis, JNK1: A protein kinase stimulated by UV light and Ha-Ras that binds and phosphorylates the c-Jun activation domain, Cell, 76 (1994) 1025-1037.

[157] F. Lluís, E. Ballestar, M. Suelves, M. Esteller, P. Muñoz-Cánoves, E47 phosphorylation by p38 MAPK promotes MyoD/E47 association and muscle-specific gene transcription, The EMBO Journal, 24 (2005) 974-984.

[158] K. Kirsch, A. Zeke, O. Tőke, P. Sok, A. Sethi, A. Sebő, G.S. Kumar, P. Egri, Á.L. Póti, P. Gooley, W. Peti, I. Bento, A. Alexa, A. Reményi, Co-regulation of the transcription controlling ATF2 phosphoswitch by JNK and p38, Nature Communications, 11 (2020) 5769.

[159] I. Mylonis, G. Chachami, M. Samiotaki, G. Panayotou, E. Paraskeva, A. Kalousi, E. Georgatsou, S. Bonanou, G. Simos, Identification of MAPK Phosphorylation Sites and Their Role in the Localization and Activity of Hypoxia-inducible Factor-1α*, Journal of Biological Chemistry, 281 (2006) 33095-33106.

[160] G. Liao, Q. Tao, M. Kofron, J.-S. Chen, A. Schloemer, R.J. Davis, J.-C. Hsieh, C. Wylie, J. Heasman, C.-Y. Kuan, Jun NH2-terminal kinase (JNK) prevents nuclear β-catenin accumulation and regulates axis formation in Xenopus embryos, Proceedings of the National Academy of Sciences, 103 (2006) 16313-16318.

[161] S.M. Chiang, H.E. Schellhorn, Regulators of oxidative stress response genes in Escherichia coli and their functional conservation in bacteria, Archives of Biochemistry and Biophysics, 525 (2012) 161-169.

[162] G.N. Landis, J. Tower, Superoxide dismutase evolution and life span regulation, Mechanisms of Ageing and Development, 126 (2005) 365-379.

[163] Y. Meyer, C. Belin, V. Delorme-Hinoux, J.-P. Reichheld, C. Riondet, Thioredoxin and Glutaredoxin Systems in Plants: Molecular Mechanisms, Crosstalks, and Functional Significance, Antioxidants & Redox Signaling, 17 (2012) 1124-1160.

[164] J.H.M. Schippers, H.M. Nguyen, D. Lu, R. Schmidt, B. Mueller-Roeber, ROS homeostasis during development: an evolutionary conserved strategy, Cellular and Molecular Life Sciences, 69 (2012) 3245-3257.

[165] A.F. Galina, E.K. Ahmet, E.A. Boris, A.S. Tamara, R. Abolghaseem, R.T. Mojgan, R. Hosseinali, B. Siamak, Invasive ctenophore Mnemiopsis leidyi in the Caspian Sea: feeding, respiration, reproduction and predatory impact on the zooplankton community, Marine Ecology Progress Series, 314 (2006) 171-185.

[166] O.H. Hewitt, S.M. Degnan, Distribution and diversity of ROS-generating enzymes across the animal kingdom, with a focus on sponges (Porifera), BMC Biology, 20 (2022) 212.

[167] R. Maor, T. Dayan, H. Ferguson-Gow, K.E. Jones, Temporal niche expansion in mammals from a nocturnal ancestor after dinosaur extinction, Nature Ecology & Evolution, 1 (2017) 1889-1895.